Theoretical Study of the Effects of Media on the Properties of Finite Systems: Molecules and Clusters

Dissertation

zur Erlangung des Grades des Doktors der Naturwissenschaften

der Naturwissenschaftlich-Technischen Fakultät III

Chemie, Pharmazie, Bio- und Werkstoffwissenschaften

der Universität des Saarlandes

von

Sahar Abdalla

Saarbrücken

2012

Tag des Kolloquiums:	Donnerstag, 21. June 2012
Dekan:	Prof. Dr. W. F. Maier
Berichterstatter:	Prof. Dr. M. Springborg
	Prof. Dr. A. Speicher
Vorsitz:	Prof. Dr. U. Kazmaier
Akad. Mitarbeiter:	Dr. H. Natter

Dedication

I am sure if they were here they would be proud of me. This thesis is dedicated to the loving memory of my dear parents, for a lifetime of love and support.

Acknowledgments

I cannot express enough thanks to my supervisor Prof. Dr. Michael Springborg, not only for offering me the opportunity to work in his group but also for his endless patience, support, guidance, and consulting with me on all the problems I have encountered. It has been an honor and a privilege to work with him, and above all I am deeply indebted to him for his kind character. I hope that one day I will become as good an advisor to my students as Michael has been to me.

Words fail to express my appreciation to Dr. Yi Dong not only for the useful conversations relating to my work, but also for her friendship, support, generous care, and for making me feel at home in Saarbrücken. She was always beside me during the happy and difficult moments to push me and motivate me.

Collective and individual acknowledgments are also owed to my present and former colleagues: Dr. Valeri G. Grigoryan, Dr. Michael Bauer, Dr. Max Ramirez, Jorge Vargas, Yong Pang, Nathalie Atif, Nicolas Louis, Stephan Kohaut, Dr. Mohammed Molayem, Dr. Violina Spurk, and Dr. Elisaveta Hristova for their readiness to help me.

My sincere thanks also go to our current and past secretaries Silvia Nagel and Ingelore Weidenfeld, for their help in facilitating the administrative affairs.

This work would not have been possible without the unconditional support of my family and friends, and I am not exaggerating when I say that surviving the last four years would have been quite a challenge, and it would have been impossible for me to stay in Germany without their support; I deeply appreciate their belief in me. My special gratitude and thanks go to my brother, Mohammed, for his faith in me, allowing me to be as ambitious as I wanted and providing me with unending encouragement and support.

Finally, I would like to thank the DAAD for the financial support that allowed me to carry on the study presented here.

Contents

Abstract

In the first part, the B3LYP/6-31+G(d,p) method was used to study the properties of tautomers and isomers of substituted pyrrolidines and phospholanes in the gas phase and aqueous phase. For the aqueous phase, we used two different models: (1) the pure PCM and (2) Discrete/PCM. We were particularly interested in the relative energies, molecular geometries in gas phase, and how these properties change when the molecule undergoes solvation. Solvation influences both relative energies and the order of stability of tautomers and isomers. Moreover, moderate change in the molecular geometry parameters was found when the results from the gas phase were compared to solution results.

In the second part, we investigated the energetic and structural properties of isolated and deposited potassium clusters. The global minima of potassium clusters were studied by using the density functional tight binding method combined with the genetic algorithm. The most stable clusters correspond to sizes 8, 18, and 20, in agreement with results obtained from experiments and jellium model. Moreover, we studied the structural similarity. The overall shape of clusters and the radial distribution of atoms were also investigated.

As a result of deposition both the energetic and structural properties changed. The similarity function was used to compare the isolated and deposited clusters. The difference in energies between the deposited and isolated clusters was calculated.

Zusammenfassung

Im ersten Teil die B3LYP/6-31+G(d,p) Methode, um die Eigenschaften Tautomere und Isomere von Pyrrolidin- und Phospholanderivaten in Gas-und wässriger Phase zu untersuchen. Das Lösungsmittel Wasser wurde zum einen implizitüber ein polarisierbares Kontinuumsmodell und zum anderen über die explizite Beschreibung von Wassermolekülen mit einem zusätzlichen Kontinuumsmodell beschrieben. Ziel dieser Studien waren ein Vergleich der relativen Energien und Molekülgeometrien der Derivate in der Gasphase und im Solvens Wasser. In dieser Arbeit konnte gezeigt werden, dass die Solvatisierung nicht nur die relative Stabilität der Isomere beeinflusst, sondern auch zuÄnderungenen in der molekularen Geometrie führt.

Der zweite Teil beschäftigt sich mit den elektronischen und strukturellen Eigenschaften von Kaliumclustern in der Gasphase und unter Wechselwirkung mit Kaliumoberflächen. Mithilfe eines genetischen Algorithmus und der DFTB Methode wurden die jeweiligen globalen Minimumsstrukturen ermittelt, das Cluster mit einer Grösse von 8, 18 und 20 Atomen die grösste Stabilität besitzen, was sich ebenfalls mit Beobachtungen aus Experimenten und mittels Vergleich mit dem Jellium Modell bestätigt hat. In dieser Arbeit wurden nicht nur die Änderungen in der Geometrie beim Uebergang von Clustern in der Gasphase, zu auf der Oberfläche adsorbierten Clustern mithilfe von Ähnlichkeitsfunktionen gezeigt, sondern auch Veränderungen in der elektronischen Struktur berechnet und interpretiert.

Summary of Work

Although most theoretical modeling methods investigate the behavior of systems in gas phase, in which it is assumed that the system is isolated and there is no interaction with surroundings, chemistry laboratories have to consider the effects of the surrounding media. For instance, a wide variety of chemical processes including chemical synthesis, solvent extraction, and measurement of physical properties take place in solution.

The importance of the chemical surrounding has led to increasing research efforts to gain insight into the behavior and properties of chemical systems including the effects of the surrounding media. Therefore there is no doubt that the surrounding medium plays an important role in influencing the properties of chemical materials and biochemical systems due to the interactions between the surroundings and the system.

The first part of the present work investigates the properties of substituted pyrrolidines and phospholanes in both gas phase and aqueous phase. It is worth mentioning that the passage from the theoretical study of molecules within the gas phase to molecules interacting with solvent represents a significant step in the development of theoretical chemistry. Furthermore, there is a variety of theoretical methods developed to study the effect of solvent on the properties and behavior of molecules. To this end, in this thesis we studied the properties of all possible tautomers and isomers of substituted pyrrolidines and phospholanes in gas phase and aqueous phase by using the DFT method. For the sake of simplicity, we classified our systems into four main groups.

In Group[1], we investigated the methylamino and phenylamino-substituted cyclic imdazolines, oxazolines, and thiazolines. Group[2] contains all possible tautomers and isomers of methylphosphino and phenylphosphino-substituted cyclic imdazolines, oxazolines, and thiazolines. Group[3] includes the methylamino and phenylamino-substituted cyclic azaphospholines, oxaphospholines, and thiaphospholines. Finally Group[4] contains the methylphosphino and phenylphosphino-

substituted cyclic azaphospholines, oxaphospholines, and thiaphospholines. We labeled our systems according to substitutions regardless of which group they belonged to; thus there are six molecules: Me-NH, Me-O, Me-S, Ph-NH, Ph-O, and Ph-S in each group. For each molecule we considered four iso- and tautomers, two structures possessing indocyclic double bonds (i.e., the A and B conformers), and two structures with exocyclic double bonds (i.e., the E and Z isomers). All calculations were performed with the Gaussian 03 program package and with the Becke three parameter Lee-Yang-Parr (B3LYP) functional and the 6-31+G(d,p) basis set. In both gas phase and aqueous phase calculations, all stationary points were characterized as minima with no imaginary frequency.

The solute-solvent interactions were described using two different approaches, the pure Polarized Continuum and the Discrete/Continuum models. Two expressions were used to describe such a model, Microsolvated/SCRF or Discrete/SCRF. In the polarized continuum model (PCM), the solute was immersed into a cavity, that had a shape related to that of the solute molecule, whereas the solvent was treated as a continuous dielectric that became polarized due to the presence of the solute molecule. We used water as solvent with a dielectric constant of 78.39. In the Discrete/Continuum (explicit/implicit) model, three water molecules were distributed and placed near the hydrophilic regions of solute as the first solvation shell; those water molecules were treated quantum mechanically as the solute molecule, whereas the rest of the solvent molecules were represented through the continuum model. In both solvation models, the Integral Equation Formalism (IEF) version of the Polarized Continuum Model (PCM) of Self Consistent Reaction Field (SCRF) was used. The molecular cavity was created by using the united atomic topological model (UAO). By using such a model, the molecular cavity was constructed using interlocking spheres centered on heavy (that is, non-hydrogen) atoms. The radius of each sphere was obtained by scaling the corresponding van der Waals radius by a factor of 1.2. In the case of Discrete/Continuum calculations the values of OFac and RMin parameters of the GEPOL algorithm were changed to 0.8 and 0.5 from 0.89 and 0.2 respectively.

We particularly focused on the relative energies, molecular geometries, and dipole moment in gas phase and how these properties change when the molecule is being solvated in water. Moreover, we also studied solvation energies.

The stability of Group[1] in gas phase and PCM can be explained as being due to the intramolecular hydrogen bonds. In the gas phase, the amino forms

are more stable except in the case of Ph-NH, where the imino tautomer of form E is more stable relative to the other isomers. The PCM calculations showed that amino forms are more soluble, the exception being Ph-S, where the imino tautomer is more soluble. In the Discrete/Continuum, stability is attributed to the intermolecular hydrogen bonds between the water molecules and the solute molecule. According to this model, the amino tautomers are more stable in the cases of Me-NH and Ph-NH; however, for Me-O, Me-S, Ph-O, and Ph-S, the imino forms are more stable species.

The calculations for the isomers and tautomers of compounds belonging to Group[2] showed a large preference for the phosphino tautomers of methyl substitution in gas phase, pure PCM, and Discrete/PCM calculations. For the phenyl substitutions, the phosphino forms were more stable in gas phase relative to phosphinidene ones. In the PCM calculations, the phosphinidene form is more stable for Ph-NH, whereas the phosphino forms are more preferred for Ph-O, and Ph-S. The most stable isomers are characterized by the presence of intramolecular hydrogen bonds, which are less than the sum of the van der Waals radii of atoms. The calculations including the three water molecules showed that the Ph-NH and Ph-S are more stable in the phosphinidene forms, whereas the phosphino form is preferred for the Ph-O.

For Group[3], we found a strong preference for the imino tautomers in gas phase relative to the amino ones, with the exception of Me-O and Ph-O for which the amino forms are more stable. In the aqueous phase, the amino forms are more soluble species except for Me-S and Ph-NH for which the imino forms are more stable according to the pure PCM. In the explicit/implicit calculations, the only exception found was for Me-NH and Ph-NH.

The gas phase and pure PCM calculations of Group[4] showed that the phosphino forms of the methyl substitutions are more stable except for Me-NH, where the phosphinidene is more stable. On the other hand, in the explicit/implicit model, the phosphino forms are more preferred than the phosphinidenes. For the phenyl substitutions, the phosphino forms are the preferred species for Ph-NH and Ph-O, whereas the phosphinidene are more preferred for Ph-S independent of the model adopted.

For all molecules, we found without expection that the relative energies and the order of stability of isomers and tautomers of the studied species change in the presence of aqueous media. The dipole moment of the studied species in-

crease when the molecule is being solvated, and this is due to an increase in the stabilizing electrostatic interaction between the solvent and solute. For all the optimized structures, the symmetry is low, i.e. C_1, and the rings adopt a non-planar configuration. Only moderate changes in the geometric parameters were found when comparing gas phase and solution results. We defined two solvation energies, i.e. $\triangle E_{sol,1}$ and $\triangle E_{sol,2}$ corresponding to each solvation model. In general we found that there is hardly correlation between the relative energies and the dipole moment in gas phase and in the PCM approach; nevertheless there is a clear correlation between the solvation energy and the dipole moment.

Furthermore, we compared the properties of nitrogen-containing molecules and their phosphorus analogs in both gas phase and aqueous phase in order to obtain systematic understanding of the effects of substituting the nitrogen atoms in compound containing the amidine group -NH-C(R)=N- by phosphorus atoms -PH-C(R)=N-, -NH-C(R)=P-, -PH-C(R)=P- irrespective of being in gas phase or in solution. We focused on the change in bond length, relative energies, dipole moment, and solvation energies due to the substitutions. We found in both gas phase and pure PCM that the intramolecular hydrogen bonds are responsible for the stability of isomers. The formation of hydrogen bonds were affected by the presence of phosphorus atoms so that compounds containing nitrogen atoms become more stable compared to their phosphorus analogs. The $N \rightarrow P$ substitution also affects the relative stability and the order of stability of the tautomers and isomers. When the explicit treatment of water molecules was considered, we found strong intermolecular hydrogen bonds between the nitrogen-containing compounds and the water molecules; such an effect is less pronounced for the phosphorus-containing compounds. In all cases the inclusion of water molecules led to larger changes in the energy of the compounds compared to the pure PCM approach. Moreover, the changes due to the replacement of both N atoms with P atoms are not simply the superposition of changes of individual substitutions. Finally the solvation energies suggest that the P-containing systems sometimes are not soluble in water.

In the second part of this thesis we studied the energetic and structural properties of isolated potassium clusters up to 20 atoms as well as such clusters deposited on the surface of potassium crystal.

The bottleneck and the challenge in investigating clusters is to find the global minima structures of the clusters due to the complexity of their energy landscape. The global minima structures of potassium clusters were determined by combining

the Density Functional Tight Binding method with the genetic algorithm.

To include the effect of surface, we considered the clusters when being deposited on K(100) and K(110) surfaces. We were interested in the changes of both energetic and structural properties due to the adsorption of potassium clusters on potassium surfaces. For the deposited clusters, the structures were optimized by using the Density Functional Tight Binding method (DFTB). From the stability function of isolated clusters, we found that potassium clusters have an even-odd oscillatory pattern, and the more pronounced peaks correspond to sizes 8, 18, and 20, which is in agreement with the results obtained from the spherical jellium model and experiments of mass spectra of potassium clusters beams. For the structural properties of isolated potassium clusters, we considered the similarity function, radial distance, and the overall shape of the clusters. The similarity function showed that there is a tendency for the smaller clusters to pairwise possess similar structures. This is the case for the clusters with 4 and 5 atoms, with 6 and 7 atoms, with 8 and 9 atoms, etc.

When the potassium clusters are deposited on a potassium surface, both the energetic and the structural properties change. The deposition energy separates into two structural reorganization energies (for the surface and the cluster, respectively), and an interaction energies, we found that the interaction energy is the dominating one, although the restructuring energy of the clusters occasionally is fairly large. We have compared the structures of clusters before and after deposition as well as the structures of the clusters on two different surfaces by using the similarity function, and we found that the structures are changed significantly from the gas phase structures. Moreover, the clusters with the same size have different structures on the two surfaces. From the analysis of the index of epitaxy as a function of cluster size, we found that the cluster atoms did not show any tendency toward an epitaxial growth of the crystal and the surface structures relax significantly compared to the crystal structure.

This thesis is organized as follows: in Chapter 1 we give a short introduction of substituted pyrrolidines and phospholanes and illustrate the theoretical method and solvation models we used in our calculations; Chapter 2 is devoted to the clusters, clusters on surfaces, the DFTB method, and the genetic algorithm; Paper I describes the effect of solvation, substitution, and structure on the properties of imidazolines, oxazolines, and thiazolines; Paper II contains the results from the study of tautomerization and isomerization of methylamino and phenylamino-

substituted cyclic azaphospholines, oxaphospholines, and thiaphospholines in gas phase and aqueous phase; Paper III represents the results of the properties of substituted pyrrolidines and phospholanes in gas and in aqueous phase; and finally Paper IV includes the results of the energetic and structural properties of isolated and deposited potassium clusters.

Preface

This thesis consists of the following papers:

I. S. Abdalla and M. Springborg: *Theoretical Study of the Effect of Solvation, Substitution, and Structure on the Properties of Imidazolines, Oxazolines, and Thiazolines.* J. Phys. Chem. A **114** (2010) 5823-5829. Reprinted with the permission from J. Phys. Chem. A. Copyright 2010, American Chemical Society.

II. S. Abdalla and M. Springborg: *Theoretical Study of Tautomerization and Isomerization of Methylamino and Phenylamino Substituted Cyclic Aazaphospholine, Oxaphospholine, and Thiaphospholines in Gas Phase and Aqueous Phase.* J. Mol. Struct. THEOCHEM **962** (2010) 101-107. Reprinted with the permission from J. Mol. Struct (THEOCHEM). Copyright 2010, Elsevier. License Number: 287415083545.

III. S. Abdalla and M. Springborg: *A DFT Study of the Properties of Substituted Pyrrolidines and Phospholanes in Gas and in Aqueous Phase.* Compu. Theor. Chem. **978** (2011) 143-151. Reprinted with the permission from Compu. Theor. Chem. Copyright 2011, Elsevier. License Number: 2874151201110.

IV. S. Abdalla, M. Springborg, and Yi Dong: *Isolated and Deposited Potassium Clusters: Energetic and Structural Properties.* Submitted.

The first three papers contain the studies of the properties of substituted pyrrolidines and phospholanes in both gas phase and aqueous phase. The last paper investigates the change in the energetics and structural properties due to the deposition of potassium clusters on both K(100) and K(110) surfaces.

The code for the genetic algorithm used in the last paper has been provided by Dr. Yi Dong. The ASE, similarity, and epitaxy codes used to analysis the structures of potassium clusters has been provided by Prof. Dr. Michael Springborg.

1 Pyrrolidines and Phospholanes

1.1 Introduction

The compounds contained in the amidine group -NH-C(R)=N- are strong monoacid bases and can be created through the treatment of the imidic ester hydrochlorides with an ethanolic solution of ammonia.

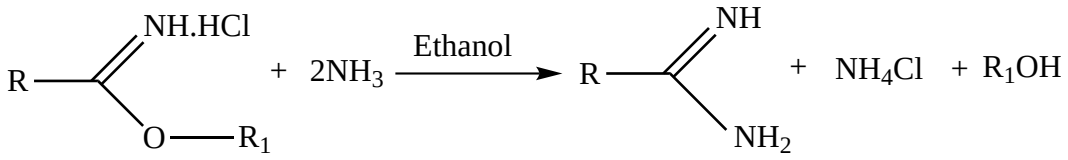

Figure 1.1: Formation of amidine compounds from the imidic esters.

The strength of amidine compounds may be explained through resonance. Since resonance structures are equivalent, the ions will also be stable [1]. Figure 1.2 shows the canonical forms of the amidine compounds. The special conjugation, tautomerism in compounds containing the amidine group, is difficult to study using the current physicochemical methods, because the proton transfer from the amino to the imino nitrogen is very fast, and the separation of the individual tautomers is impossible [2, 3]. In several recent studies, the tautomerism and isomerism of systems containing the amidine group -NH-C(R)=N- were examined [4, 5, 6, 7, 8, 9, 10, 11].

As a natural extension of those we investigated the isoelectronic systems containing the phosphorus atoms; those groups are -PH-C(R)=N-, -NH-C(R)=P-, and -PH-C(R)=P-. Phosphorus compounds have been investigated as relevant materials for a large number of different applications, including lubricants, oil additives, water treatment cleaners, flame-retardants, fertilizers, plasticizers, and pesticides [12, 13]. Phosphorus and organo-phosphorus compounds were also recognized to have important biological functions; e.g. that they are essential constituents of the

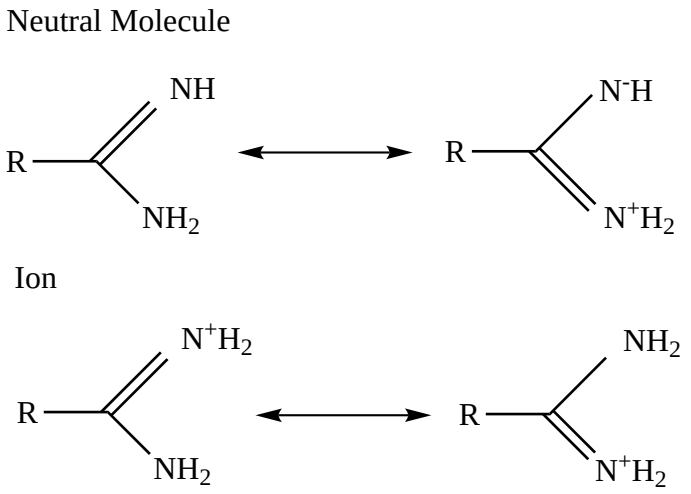

Figure 1.2: The canonical forms of the amidines.

protoplasm [14].

The proton transfer between nitrogen and phosphorus, which is related to this work, was investigated by Kolodiazhnyi *et al.* [15], who concluded that tautomeric equilibrium depends both on the nature of the solvent and the substituents at these atoms.

The tautomeric equilibrium in heterocyclic systems has for a long time been of significant interest and importance [16], and accordingly it has also been studied theoretically, using many different theoretical methods ranging from semiempirical methods [17, 18] to more sophisticated calculations that may include electron correlation [19, 20].

In this work, we report a systematic theoretical examination of all possible tautomers and isomers of five-membered ring heterocyclic compounds containing -NH-C(R)=N-, -PH-C(R)=N-, -NH-C(R)=P-, and -PH-C(R)=P- groups in both gas phase and aqueous phase. It is worth mentioning that compounds containing -NH-C(R)=N- group have been studied in gas phase by Remko *et al.* [11]. Due to the absence of theoretical and experimental data for compounds containing phosphorus atoms, we shall compare them to their nitrogen analogs (-NH-C(R)=N-) [4, 5, 6, 7, 8, 9, 10, 11]. In order to simplify the distinctions between studied molecules, we divided our systems into four groups: Group[1], Group[2], Group[3], and Group[4], corresponding to molecules containing -NH-C(R)=N-, -PH-C(R)=N-, -NH-C(R)=P-, and -PH-C(R)=P-, respectively. For all groups the

substitution at position 1 is either NH, O, or S; and at position 6 it is either methyl or phenyl; therefore we can simply label our systems according to the substitutions at positions 1 and 6, regardless of which group they belong to, since each group has six different molecules: Me-NH, Me-O, Me-S, Ph-NH, Ph-O, and Ph-S. For each molecule, we considered two conformers (i.e., the A and B conformers) with indocyclic double bonds and two geometrical isomers (i.e., the E and Z isomers) with exocyclic double bonds. The molecular structures of our molecules of interest are depicted in detail in Figure 2.3, 2.4, 2.5, and 2.6. We were particularly interested in relative energies, molecular geometries, and dipole moment of tautomers and isomers in gas phase and how these properties change upon solvation.

The effect of solvation on the tautomeric equilibrium of five-membered ring heterocyclic systems has been the subject of many studies [17, 21, 22, 23]. Through studies of tautomerism in different environments, it has been found that the environment is important for the relative stability of various tautomers.

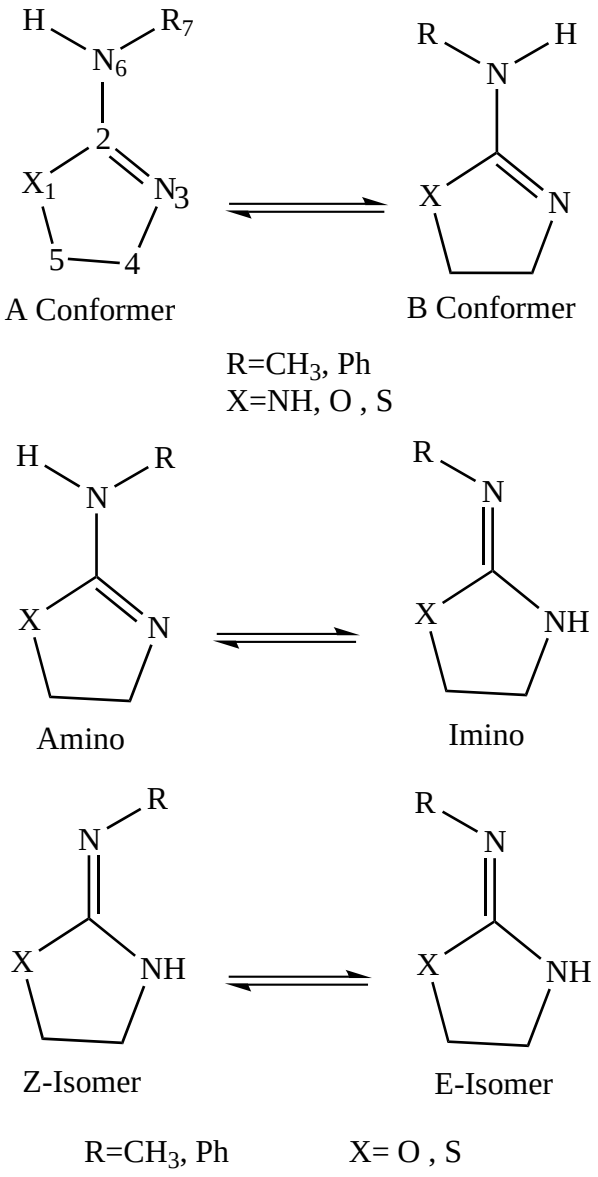

Figure 1.3: Group[1]: Structure and atom numbering of the tautomers and isomers of methylamino and phenylamino-substituted cyclic imidazolines, oxazolines, and thiazolines.

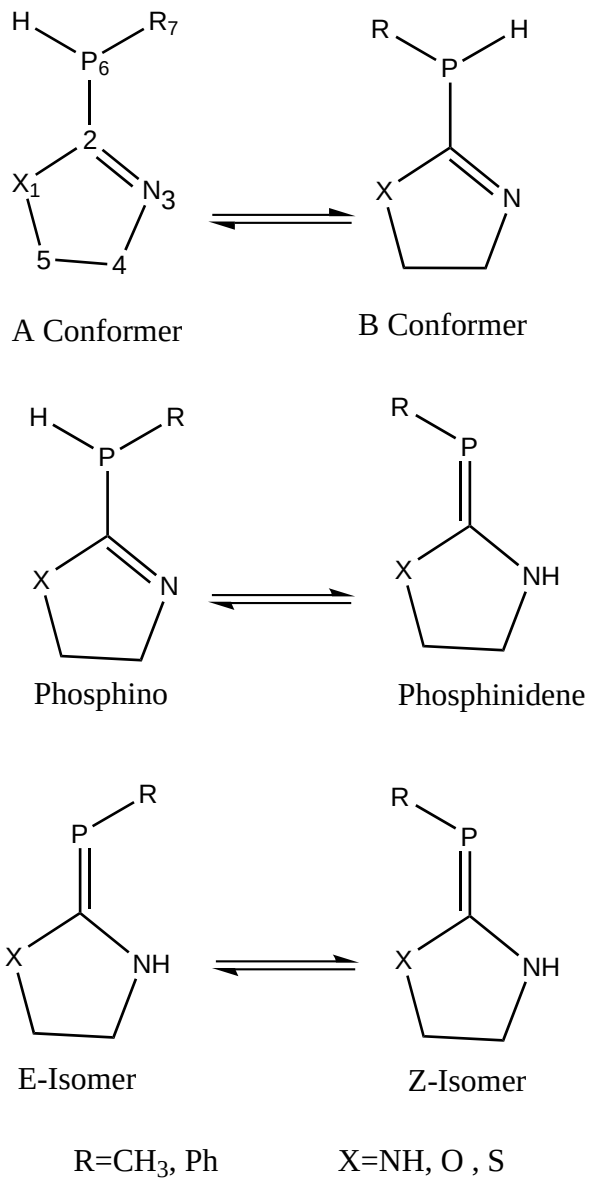

Figure 1.4: Group[2]: Structure and atom numbering of the tautomers and isomers of methylphosphino and phenylphosphino-substituted cyclic imidazolines, oxazolines, and thiazolines.

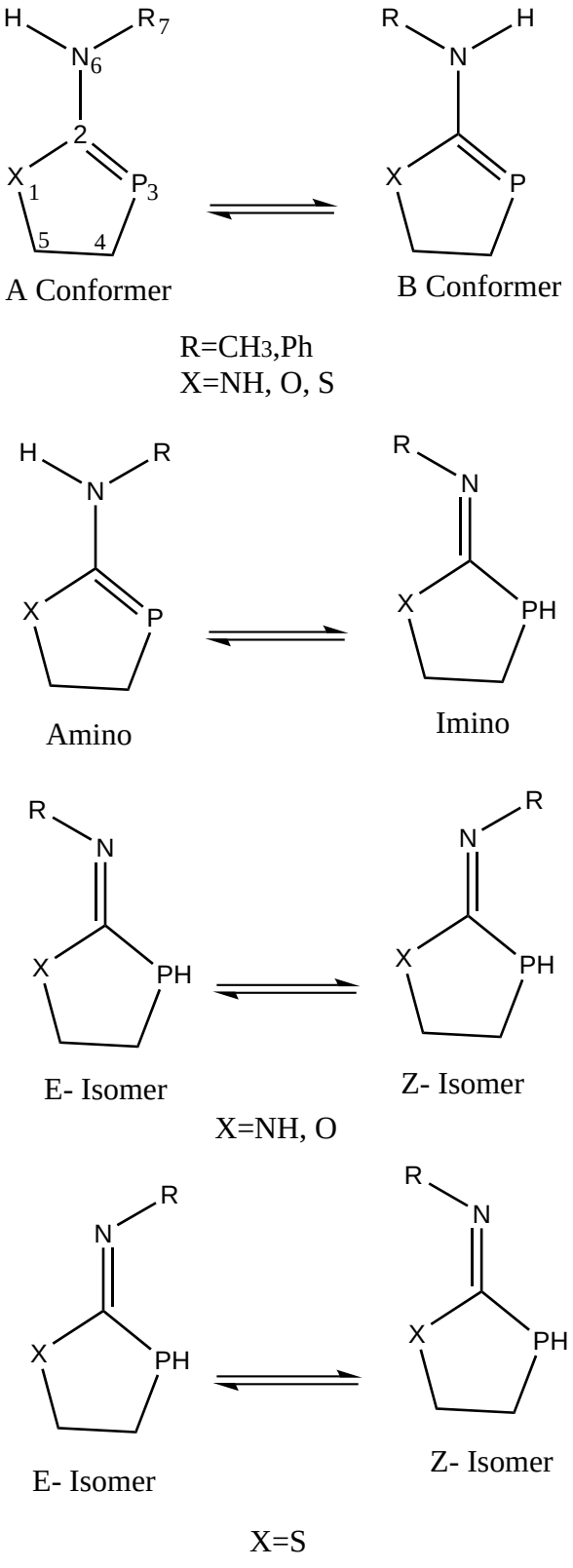

Figure 1.5: Group[3]: Structure and atom numbering of the tautomers and isomers of methylamino and phenylamino-substituted cyclic azaphospholines, oxaphospholines, and thiaphospholines.

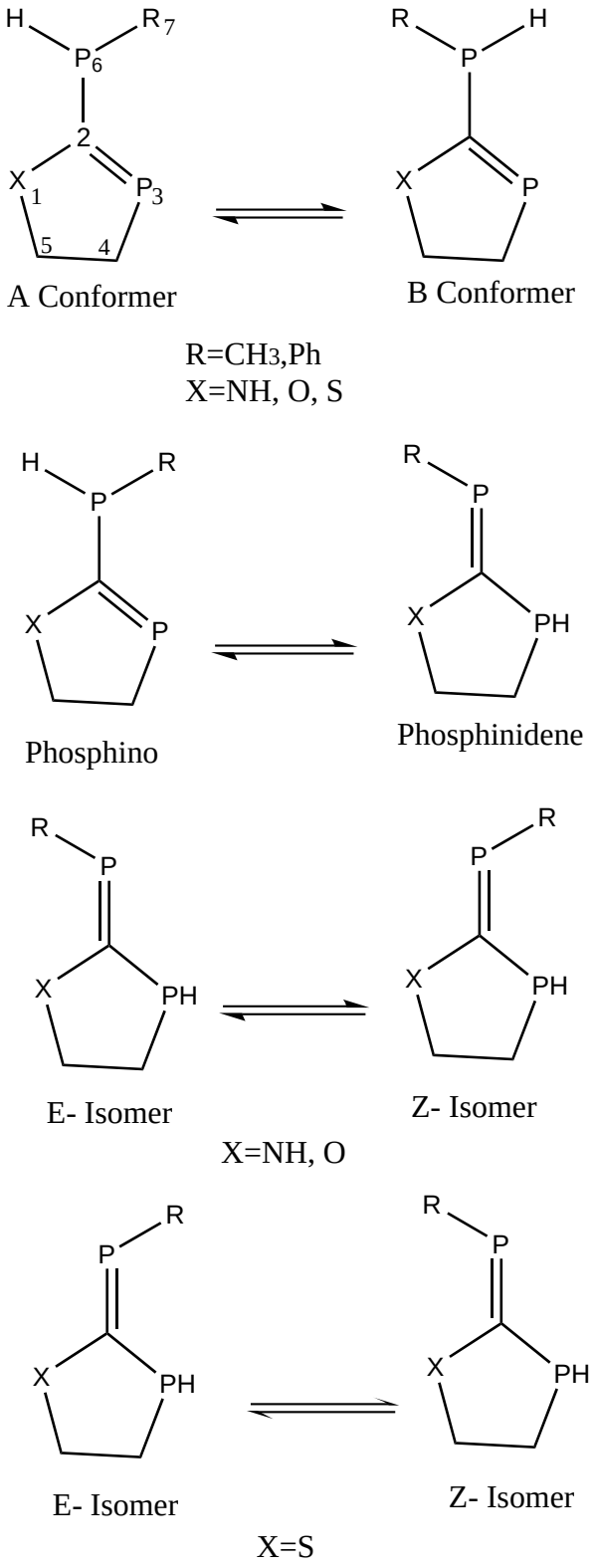

Figure 1.6: Group[4]: Structure and atom numbering of the tautomers and isomers of methylphosphino and phenylphosphino-substituted cyclic azaphospholines, oxaphospholines, and thiaphospholines.

1.2 Theory

1.2.1 Density Functional Theory (DFT)

The main problem in quantum chemistry is to find an approximate solution to the time-independent, non-relativistic Schrödinger equation, which cannot be solved exactly except for hydrogen atom. The Schrödinger equation including coordinates of electrons and nuclei of the system can be written as below.

$$\hat{H}\psi_i = E_i\psi_i(\vec{X_1}, \vec{X_2}....\vec{X_N}, \vec{R_1}, \vec{R_2}, ...\vec{R_M}) \tag{1.1}$$

$$E_i = \frac{\int \psi_i^* \hat{H}\psi_i \delta\tau}{\int \psi_i^* \psi_i \delta\tau} \tag{1.2}$$

The Hamiltonian operater is divided into two parts: the first is the kinetic part of both electrons and nuclei, and the second part refers to the potential interaction. The potential includes the nucleus-electron potential, the electron-electron potential, and the nucleus-nucleus potential. When considering a system that is composed of N electrons and M nuclei, the Hamiltonian (in atomic units) can be represented in the following form.

$$\hat{H} = -\frac{1}{2}\sum_{i=1}^{N}\nabla_i^2 - \frac{1}{2}\sum_{A=1}^{M}\frac{1}{M_A}\nabla_i^2 - \sum_{i=1}^{N}\sum_{A=1}^{M}\frac{Z_A}{r_{iA}} + \sum_{i=1}^{N}\sum_{j>i}^{N}\frac{1}{r_{ij}} + \sum_{A=1}^{M}\sum_{B>A}^{M}\frac{Z_A Z_B}{R_{AB}} \tag{1.3}$$

It is impossible to find an exact solution for multi-electron systems without approximations. In 1927, Born and Oppenheimer argued that the nuclei in the system move much more slowly than the electrons because they are more massive. From this, they assumed that the nuclei in the system are fixed, allowing their kinetic energy to be disregarded and the nuclear-nuclear repulsion term to be constant and therefore added later. After applying the Born-Oppenheimer approximation, the resulting equation is referred to the electronic Schrödinger equation.

$$\hat{H_{ele}}\psi_e = \varepsilon_e\psi_e \tag{1.4}$$

$$\psi_e = \psi_e(\chi_1, \chi_2, \chi_3, ...\chi_N) \tag{1.5}$$

where ψ_e represent the electronic wave function, depending on all electronic degrees of freedom, e.g., three position-space ($r_i = x_i, y_i, z_i$), and one spin coordinate

σ_i for each electron i $[\chi_i = (r_i, \sigma_i) = (x_i, y_i, z_i, \sigma_i)]$.

$$\hat{H}_{elec} = -\frac{1}{2}\sum_{i=1}^{N} \bigtriangledown_i^2 - \sum_{i=1}^{N}\sum_{A=1}^{M} \frac{Z_A}{r_{iA}} + \sum_{i=1}^{N}\sum_{j>i}^{N} \frac{1}{r_{ij}} = T + \hat{V_{Ne}} + \hat{V_{ee}} \tag{1.6}$$

In 1964, Hohenberg and Kohn [24] developed a new theory for calculating the ground state properties of the systems by the knowledge of electron density $\rho(r)$ only, which is called the Density Functional Theory (DFT). Kohn received the Nobel prize in chemistry in 1998 for his development of the density functional theory, shared with John A. Pople. The DFT is based on determining the electron density rather than the wave function. According to the density functional method, the energy is given as a unique functional of the electron density, E[ρ]. The kinetic energy T, the potential energies corresponding to nucleus-electron interaction E_{Ne}, and electron-electron interaction E_{ee} are directly transformed into a functional of the density.

$$E[\rho] = T[\rho] + E_{Ne}[\rho] + E_{ee}[\rho] \tag{1.7}$$

In DFT methods, the kinetic energy T is replaced by the kinetic energy of a non-interacting reference system $T_s[\rho]$, which is a functional of the electron density, introduced by Kohn and Sham [25]. It has the same density as the real interacting system. The potential energy of electron-electron interaction $E_{ee}[\rho]$ is divided into the Coulomb interaction of electron-electron $J[\rho]$ and the exchange-correlation energy $E_{xc}[\rho]$.

$$E_{DFT}[\rho] = T_s[\rho] + E_{Ne}[\rho] + J[\rho] + E_{xc}[\rho] \tag{1.8}$$

By equating $E_{DFT}[\rho]$ to the exact energy, this expression is taken as a definition of $E_{xc}[\rho]$; it is the part that remains after substraction of the non-interacting kinetic energy and $E_{Ne}[\rho]$ and $J[\rho]$ potential energy terms.

$$E_{xc}[\rho] = (T[\rho] - T_s[\rho]) + (E_{ee}[\rho] - J[\rho]) \tag{1.9}$$

The first parenthesis in equation (1.9) is the kinetic correlation energy, while the second contains both exchange and potential correlation energy.

1.2.2 The Local Density Approximation

The exchange-correlation functional is generally written as the sum of two components, an exchange part and a correlation part.

$$E_{xc}[\rho] = E_x[\rho] + E_c[\rho] = \int \rho(r)\varepsilon_x[\rho]dr + \int \rho(r)\varepsilon_c[\rho]dr \tag{1.10}$$

The exchange energy is the sum of contribution from α and β spin densities.

$$E_x[\rho] = E_x^{\alpha}[\rho_\alpha] + E_x^{\beta}[\rho_\beta] \tag{1.11}$$

The Local Density Approximation (LDA) assumes that the density can be treated as uniform electron gas. The exchange energy for uniform electron gas is given by the Dirac formula.

$$E_x^{LDA}[\rho] = -C_x \int \rho^{\frac{4}{3}}(r)dr \tag{1.12}$$

$$\varepsilon_x^{LDA}[\rho] = -C_x\rho^{\frac{1}{3}} \tag{1.13}$$

In case that electron densities for α and β are not equal, the LDA is extended and replaced by the Local Spin-Density Approximation (LSDA). In the LSDA, the density is written as a sum of α and β densities.

$$E_x^{LSDA}[\rho] = -2^{\frac{1}{3}}C_x \int [\rho_\alpha^{\frac{4}{3}} + \rho_\beta^{\frac{4}{3}}(r)]dr \tag{1.14}$$

The local correlation functionals were developed by Vosko, Wilk, and Nusair and involve numbers of terms and empirical factors [26]. The most popular versions are VWN and VWN5. An example of the local exchange functional is the Slater-Dirac exchange energy (S). One of the most popular combination of the local exchange and correlation functionals is the SVWN method.

1.2.3 Generalized Gradient Approximation (GGA)

To make improvement over the LSDA, one assumes that the density is not uniform. Such methods are known as Generalized Gradient Approximation (GGA). GGA methods are sometimes refer to as non-local methods. The exchange correlation functional in the GGA is usually divided into exchange and correlation terms. In

this way one can treats each functional individually.

$$E_{xc}^{GGA} = E_{x}^{GGA} + E_{c}^{GGA} \tag{1.15}$$

Examples of some of the most efficient GGA functionals commonly used in computational chemistry are the following: B is an exchange functional developed by Becke [27]; P86 is a correlation functional developed by Perdew [28]; PW91 is a modification of the P86 functional developed by Perdew and coworkers [29, 30]; B95 is a correlation functional developed by Becke [31]; PBE is an exchange-correlation functional developed by Perdew, Burke, and Ernzerhof [32]; and LYP is a correlation functional developed by Lee, Yang, and Parr [33]. From the previous GGA functionals, a combination between exchange and correlation functionals is made in order to try to describe the system completely. Some of the most common combinations are: BLYP, BP86, and BPW91.

1.2.4 Hybrid Functionals

The exchange part is poorly described by the functional, in contrast to Hartree-Fock (HF), where the exchange part is defined exactly. Hybrid functionals combine exact HF exchange energy (expressed in terms of the Kohn-Sham orbitals rather than the density functional) with exchange and correlation from LSDA. One of the most commonly used versions is B3LYP.

In the present work we used B3LYP functional, which includes Becke's exchange functional [34] along with the non-local correlation functional developed by Lee, Yang, and Parr [33]. The exchange energy actually includes LSDA exchange, the exact exchange, and Becke's 1988 exchange. The correlation energy includes the LYP correlation plus the LSDA correlation.

$$E_{xc}^{B3LYP} = (1-a)E_{x}^{LSDA} + aE_{xc}^{HF} + b\Delta E_{x}^{B88} + cE_{c}^{LYP} + (1-c)E_{c}^{LSDA} \tag{1.16}$$

where a=0.20, b=0.72, and c=0.81 are the three empirical parameters determined by fitting the predicted values to a set of atomization energies, ionization potentials, proton affinities, and total atomic energies.

1.2.5 Basis Set

To carry out calculations we need to specify the basis set. Basis set is a set of functions used to create the molecular orbitals (MO), which are expanded in a linear combination of such functions with the coefficients to be determined. Usually these functions are atomic orbitals (AO) (LCAO-MO approximation). These basis functions can be classified into two main types:

[1] Slater Type Orbitals (STOs).

[2] Gaussian Type Orbitals (GTOs).

The Gaussian Type Orbitals are computationally preferred compared to Slater Type Orbitals, because the product of two GTOs centred on two different atoms is a third one situated between them; therefore GTOs are preferred and used mostly in electronic structure calculations.

There are hundreds of basis sets composed of GTOs. The smallest of these are called minimal basis sets, and they are typically composed of the minimum number of basis functions required to represent all of the electrons on each atom. The most common minimal basis set is STO-nG, where n is an integer. This n value represents the number of Gaussian primitive functions comprising a single basis function. The next improvement of the basis set is the split valence basis set, in which there are multiple basis functions corresponding to each valence atomic orbital, called valence double-, triple-, quadruple-zeta, and so on, basis sets. The split valence basis set is typically x-yzG. Here, x represents the number of primitive Gaussian functions comprising each core atomic orbital basis function. The y and z indicate that the valence orbitals are composed of two basis functions: the first one composed of a linear combination of y primitive Gaussian functions, the other composed of a linear combination of z primitive Gaussian functions. Further improvement of basis functions is achieved by adding d-orbitals to all heavy (non-hydrogen) atoms and the p-orbital to hydrogen atoms. The resulting functions are called polarized functions, and they can be written as x-yzG(d,p) or x-yzG**. The presence of diffuse functions is symbolized by the addition of a plus sign, +, to the basis set.

1.3 Solvation Models

Most of the theoretical methods investigate the behavior of systems in gas phase, in which it is assumed that the system is isolated and there is no interaction with surroundings. In contrast most practical chemistry takes place in solution.

Including the solvent effects is not an easy task; therefore over the years, much effort has been devoted to the theoretical development and inclusion of solvent effects into quantum mechanical calculations. The methods used to treat the solvent effect can be divided to:

[1] Supermolecule model.

[2] Classical (force-field-derived) models.

[3] The hybrid QM-classical models.

[4] The Polarized Continuum Model-Self-Consistent Reaction Field (PCM-SCRF) methods.

The most accurate method would be to treat the complete system (solute+solvent) by using QM methods, but due to the computational demanding such method cannot be applicable. Instead, one may applies a simple model by considering only the closest solvation shells. This is the supermolecule approach. The advantage of this approach is that weak interactions such as hydrogen bonds can be treated accurately. On the other hand, including more than the solvent molecules that are closest to the solute, the size of the system increase and the computational resources put limitations on the applicability of the model [35].

In the classical models, both the solvent and solute are represented by classic Hamiltonian. This can be done through using molecular dynamics (MD) simulation or Monte Carlo (MC) techniques, and this method allows explicit treatment of solvent molecules [36, 37, 38, 39, 40].

In the hybrid quantum mechanics-classical model, the solute is treated by using the quantum mechanical level, whereas the solvent is treated at the classical level [41, 42, 43, 44, 44, 46, 47, 48]. The interaction between the solute and solvent may include van der Waals terms, electrostatic interactions, or any term in the force field being used.

In the PCM-SCRF models, the solvent is characterized by its dielectric constant and the solute (including, when convenient, some solvent molecules, the whole being treated as supermolecule at quantum mechanics level in the case of the Discrete/Continuum model) is placed in a cavity representing the space occupied

by the solute in the solvent. Such models are also known as implicit solvation models. In the PCM-SCRF model, the solvent dielectric constant interacts with the solute charge distribution, generating a reaction field against it. The effect of this reaction field is introduced as a perturbation part into the Hamiltonian operater ($\hat{V_R}$).

$$(\hat{H^0} + \hat{V_R})\psi = E\psi \tag{1.17}$$

where H^0 is the Hamiltonian of the isolated molecule in gas phase. From the corresponding Schrödinger equation one obtains the energy of the molecule *in vacuo*.

$$E^0 = \langle \psi^0 | H^0 | \psi^0 \rangle \tag{1.18}$$

Various SCRF models were developed based on the cavity shape [49, 50, 35]. The simplest SCRF bearing the name of the Nobel prize laureate in chemistry in 1968 (Lars Onsager) [51]. In the Onsager model, the cavity that accommodates the solute is defined as a fixed spherical shape, whereas in the PCM model proposed by Miertus, Scrocco, and Tomasi [52, 53], the cavity is defined as interlocking atomic spheres.

In the continuum models, the solvation Gibbs energy G_{sol} is defined as a change in the Gibbs free energy when a molecule is transfered from gas phase to solution at constant temperature. The G_{sol} can thus be written as the sum of three terms.

$$G_{sol} = G_{ele} + G_{dr} + G_{cav} \tag{1.19}$$

The electrostatic interactions G_{ele} between a solute and solvent are always negative, i.e. attractive, and they are zero if the solute is characterized by no electrical moments. The presence of the electrostatic field leads to increasing the dipole of the solute. The solvent itself, seeing this increase, polarizes and moreover increases its own orientation to oppose solute's dipole and so on. Therefore the dipole moment of solute molecules in solution is larger than the corresponding dipole moments in the gas phase [54], and it has been confirmed that the dipole moment of small organic molecules increases by up to 30% in aqueous solutions compared to the gas phase values [55]. Indeed any property that depends on the electronic structure will tend to have different expectation values in solution than in the gas phase, and this depends on the strength of the solute-solvent interaction.

The non-electrostatic contributions that affect the solvation process are cavation

G_{cav} and dispersion-repulsion G_{dr} energies. The cavation energy is the energy required to create a cavity of vacuum within the solvent into which the solute will be accommodated in the second step. After the solute is inserted into a cavity, that has the shape of solute, it will experience favorable dispersion interactions with the surrounding solvent. Although the nature of the dispersion energy is electrostatic, it is always discussed separately from the solute-solvent electrostatic interaction. The dispersion and repulsion term G_{dr} is computed by classical approximation proposed by Floris and Tomasi [56].

The advantage of the PCM-SCRF method is that it provides a fast representation of solvent effects and allows one to consider polarization effects explicitly, which are neglected or partially considered in classical and QM classical calculations. The quality of the SCRF methods depends on the definition of the reaction field and the shape of the surface used to simulate the solute-solvent interface. The PCM can be implemented by using different levels of theory: Density Functional Theory (DFT) [57, 58], Hartree-Fock (HF) [59], Møller-Plesset perturbation theory (MP_n) [60], Multi-Configurational Self-Consistent Field (MCSCF) [61], and Quadratic Configuration Interaction Singles and Doubles (QCISD) [62].

The use of the DFT methods within the continuum model provides a good way to describe the solvent effects [63, 64], therefore in the current work, we performed DFT method to describe the solvent effect by using two different solvation models:

[1] Pure Continuum Model.

[2] Discrete/Continuum Model.

1.3.1 Pure Continuum Model

Among all SCRF methods, the original PCM proposed by Miertus, Scrocco, and Tomasi [52, 53] used the description of perterbation operator in terms of molecular electrostatic potential, and it has proved to be a reliable tool for describing the electrostatic interaction between the solute and solvent [65]. In the present work, the Integral Equation Formalism (IEF) [50, 49, 66, 67, 68] version of the polarized continuum model (PCM) [49, 52, 69] was used as a solvation model. The solute molecule is placed into a cavity, and the water molecules were considered at 298K with a dielectric constant of 78.39.

The most important fundamental quantity describing the interaction of a solute with surrounding solvent is solvation energy, which refers to the change in the

energy of a molecule leaving the gas phase and entering the aqueous phase (in the case of water). In the pure PCM model, the relative energy of solvation $E_{\mathrm{sol},1}$ can be written as the difference between the energy of the molecule in the continuum $E_{\mathrm{solute,PCM}}$ and the energy of the molecule in gas phase $E_{\mathrm{solute,g}}$.

$$\Delta E_{\mathrm{sol},1} = E_{\mathrm{solute,PCM}} - E_{\mathrm{solute,g}} \tag{1.20}$$

1.3.2 Discrete/Continuum Model

One of the deficiencies of the pure continuum model is that it includes only long-range interactions between the solvent and solute. In order to overcome such a deficiency, we also used the Discrete/Continuum model to allow for specific short-range interactions such as the hydrogen bonds. In this model, three water molecules were explicity considered and distributed near the hydrophilic regions of the solute inside the cavity and considered as the first solvation shell; those water molecules were also treated quantum mechanically as the solute molecule, while the remaining infinite number of solvent molecules are approximated by the continuum model. The combination Discrete/Continuum has been used for many years [70, 71, 72, 73, 74, 75, 76].

In the Discrete/Continuum model, we define an energy of solvation, $\Delta E_{\mathrm{sol},2}$, as

$$\Delta E_{\mathrm{sol},2} = E_{\mathrm{complex,PCM}} - E_{\mathrm{solute,gas}} - E_{(\mathrm{H_2O})_3,\mathrm{PCM}} \tag{1.21}$$

where $E_{(\mathrm{H_2O})_3,\mathrm{PCM}}$ represents the energy of three water molecules calculated in PCM and oriented as found for the complex of interest.

1.4 Definition of Cavity

In continuum models, the solute is placed in a cavity representing the space occupied by the solute in the solvent. The cavity is the basic concept in the PCM-SCRF method [77]. The shape and size of the cavity is differently defined in various versions of the continuum models. A very critical point in solvent calculations is the selection of the cavity size. A cavity that is too large will underestimate the solvent effect, whereas a cavity that is too small will overestimate it. The appropriate choice of the size of the cavity should be in a way that approximately mimics the first solvation shell [78] so that the cavity should be placed around 1.20-1.25 times

the van der Waals radii (e.g. 1.2 for water). Such a modification contributes to the electrostatic part of the free energy.

In the present work, the molecular cavity was build by using the United Atom Topological model (UAO), whereby the cavity is constructed through the interlocking sphere centered on heavy (non-hydrogen) atoms. The radii were obtained by scaling the corresponding van der Waals radius by factor of 1.2 [49, 78]. The surface is smoothed by adding some other spheres, not centered on atoms, to simulate the solvent-excluding surface by using the GEnerating POLyhedra (GEPOL) method [77]. Then the cavity surface is partitioned into small domains called tesserae. The number of tesserae influences the accuracy of the results and computational time. In our calculations we used the default number of initial tesserae, 60 per sphere.

1.5 Computational Details

All the calculations were performed using the Gaussian03 program package [79]. The calculations in both gas phase and aqueous phase were performed by using the hybrid functional DFT- the B3LYP [34], including a combination of Becke's 3-parameter and nonlocal exchange functional with the correlation functional of Lee-Yang-Parr [33]. The basis set 6-31+G(d,p) was used. The 6-31+G(d,p) indicates a single basis set consisting of 6 Gaussian functions for inner electrons and two separate basis functions, one consisting of 3 Gaussian functions, and the other Gaussian function for valence electrons. The diffuse functions help us deal with unshared pairs of electrons; the basis set also implies the addition of a set of p (added to the hydrogen atoms) and d orbitals to provide polarization.

The implementation of a PCM model in Gaussian03 can be invoked using the SCRF keyword. An additional option has been specified at the end of the input file and read in using a read modifier of the SCRF keyword. This option corresponds to scaling all radii by a factor of 1.20. In the case of Discrete/Continuum calculations the values of OFac and RMin parameters of the GEPOL algorithm [77] were changed to 0.8 and 0.5 from 0.89 and 0.2 respectively. In both gas phase and aqueous phase calculations, all stationary points were characterized as minima in the potential energy surface with no imaginary frequency.

2 Clusters

2.1 Introduction

Clusters are aggregates of atoms or molecules, which may contain any number of particles from three to thousands. The clusters can be considered nanoparticles when such aggregates reach sizes with diameters in nanometers. The clusters could be formed from one type of atom (in the case of atomic clusters), leading to homo-atomic clusters, or different types of atoms leading to hetero-atomic clusters. Clusters are a new type of material and have properties different from individual atoms and molecules or bulk matter.

Atomic clusters are formed by most of elements in the periodic table, even including the inert gases. Clusters may be held together by different kind of forces: ionic forces between the oppositely charged ions (as in NaCl clusters), van der Waals attraction as in the case of rare gases (He and Ar clusters), covalent chemical bonds (as in the Si clusters), or metallic bonds (as in Na and Cu clusters). The interest of studying clusters is due to their size-dependent properties such as geometric, electronic structure, and binding energy. In fact, both the geometric shape and the energetic stability may change with the size. Moreover, clusters can be studied isolated or in several media such as molecular beams, the vapor phase, colloidal suspensions, and deposited in inert matrices or on surfaces [80, 81].

From a practical standpoint, the interest in studying clusters is due to the variety of their applications. For instance, there has been traditional interest in the application to catalysis because of the properties of surface/volume ratio. Nanoclusters have been used to build devices for variety of applications, including electronic, optical, magnetic, and mechanical ones.

Due to their individual and unique properties, clusters have been the subject of intensive studies from both experimental and theoretical approaches. The history of scientific interest in studying clusters goes back to Faraday's experiments with colloidal golds in 1857. Interest in the theoretical study of clusters started in the

1970s. One of the important characteristics of clusters is the variety of structures they exhibit. The number of structures increases exponentially with the size of the clusters, and as a result of this both physical and chemical properties change significantly with the size [82].

The first point to understand the properties of clusters is to study their structures. One of the challenges in investigating clusters is to find the global minimum structures in the potential energy surface, which is not an easy task due to the complexity of their energy landscape. The determination of the global minimum structures has been a topic that has attracted considerable attention. In order to search for the lowest minima structures, we required intelligent methods that search the structure space. Numerous approaches have been developed for searching the global minima structures, for example but not limited to Aufbau/Abbau method [83, 84, 85], Basin-Hopping method [86], and Genetic algorithms [87, 88, 89, 90, 91, 92, 93, 94, 95, 96, 97, 98].

Metallic clusters from across the periodic table form a wide variety of clusters. From these clusters, alkali metal clusters consituting any of the six chemical elements that make up Group 1 (Ia) of the periodic table, namely lithium (Li), sodium (Na), potassium (K), rubidium (Rb), cesium (Cs), and francium (Fr), played an important role in the development of clusters physics as a branch of modern physics and chemistry. Alkali-metal clusters have been subject to different experimental and theoretical studies. Interested readers are referred to the review article by Balletto and Ferrando [80] and the papers cited therein.

Interest in studying of the alkali-metal clusters grew with the pioneering work of Knight and coworkers [99, 100, 101]. They have discovered that certain clusters, those with the magic numbers 8, 20, and 40 .. of atoms, are more stable and consequently were found more abundantly in the mass spectra of these clusters. The existence of the magic number cluster is attributed to the electronic shell structures of the clusters. Many properties of alkali metal clusters can be explained with help of the jellium model and its extensions [102, 103].

2.2 Clusters On Surfaces

There is much known about the properties of metal clusters in gas phase compared to their properties when the clusters are deposited on surfaces. Clusters deposited on surfaces play a significant role in chemical processes such as cataly-

sis. Metal clusters deposited on surfaces have different applications, for instance, in the growth of nanostructure materials [104] and in nano and biotechnologies [105, 106, 107]. When clusters are deposited on surfaces, their properties might change. Subsequently the deposited clusters may have properties different from those obtained in gas phase.

Clusters on surfaces have been of great interest in both experimental and theoretical studies. Experimental information about clusters deposited on surfaces has been acquired by several means, including scanning tunneling microscopy [108, 109, 110], scanning transmission electron microscopy [111], and field ion microscopy (FIM) [112]. Among these studies, Wang *et al.* [113] studied the properties of iridium clusters (up to 13 atoms) on Ir(111) surface by using FIM and investigated the arrangement of iridium atoms in the clusters in relation to the binding sites for single atom on an Ir(111) surface. Theoretically, there are many calculations devoted to the study of clusters on surfaces by using semi-empirical methods such as Embedded Atom Method (EAM). For example but not limited to, the study of Ni_n/Ni(111) and Pt_n/Pt(111) [114, 115, 116, 117]. Schwoebel *et al.* studied the properties of small Pt clusters on the Pt(001) surface [118]. Both the energetics and structural properties of Ni, Pd, and Pt on Pt(001) surface have been investigated [119]. The structural properties of Pd and Pt clusters on Ag(110) surface was studied by Roy *et al.* [120]. The primary interest of theoretical studies has focused on the geometric structures assumed by clusters on surfaces, which reflect fundamental aspects of adatom-adatom and adatom-substrate interaction and offer insights into the initial stage of cluster growth.

2.3 Potassium Clusters

There was interest early on in investigating the properties of isolated potassium clusters, and much is known about their properties in gas phase, e.g. the spherical jellium model showed discontinuities of total energies for the isolated potassium clusters as a function of cluster size due to the existence of the electronic shell structure [121] such as that reported for sodium clusters, with peaks or steps for those clusters that contain N = 2, 8, 20, and 40 atoms [99, 100]. This study has been confirmed experimentally by the mass spectra of potassium cluster beams [101]. Besides this study, potassium clusters have been subject to different experimental studies [122, 123, 124, 125, 126, 127, 128, 129].

Potassium clusters have been investigated by different theoretical methods. Most of these studies were limited to small sizes; potassium clusters up to 8 atoms have been studied by using pseudopotential calculations [130]. An *ab initio* study of both neutral and ionic structures of potassium clusters was carried out by using the configuration interaction (CI) method [131, 132]. The structures and binding energies for cluster sizes between four and six atoms were also investigated by using diatomics in molecules (DIM) approximation [133]. The valence-only self consistent field calculations were used to study the neutral and singly ionized K clusters with up to four atoms [134]. K_9, K_{15}, and K_{27} have been studied by using the SCF $X\alpha$ (LSD) SW (local spin density-scattered wave) method [135]. The potassium clusters K_N ($N \leq 7$) have been investigated by using Hartree-Fock many-body perturbation [136]. Florez and co-workers [137] investigated the properties of potassium clusters up to eight atoms by applying two types of exchange-correlation functionals. Recently Banerjee *et al.* [138] studied the properties of various isomers of potassium clusters containing even numbers of atoms up to 20 atoms by employing the all-electron density functional theory with a gradient-corrected, exchange-correlation functional to calculate the binding energies, ionization potential, and static polarizability with respect to the cluster size. Among the wide theoretical studies that the potassium clusters received, it is quite surprising that there were no attempts to find the global minima structures, considering the fact that the experimental results for the ionization potential, static polarizability, and photoabsorption spectra of potassium clusters as a function of cluster size was reported very early [101, 123]. On the other hand, potassium clusters of up to 60 atoms were investigated by using Gupta potential combined with both genetic and basin-hopping algorithms [139] to search for the global minima. Such a model was not suitable for describing the electronic effects but rather the packing effects; thus the particularly stable clusters were not in agreement with those obtained from the experiments and the spherical jellium model [121, 101]. Therefore, one needs to apply a model that takes into account the electronic degree of freedom. In this work, the global minima structures of potassium clusters up to 20 atoms were obtained by utilizing the Density Functional Tight Binding (DFTB) method combined with the genetic algorithm. We analyzed both energetic and structural properties as a function of the cluster size.

In order to study the effect of a surface on the properties of potassium clusters, we softly deposited the clusters on K(100) and K(110) surfaces. We shall focus on

changes in the structures due to adsorption as well as the energetics related to the adsorption.

2.4 Theoretical Method

2.4.1 Density Functional Tight Binding Method

The Density Functional Tight Binding (DFTB) method based on the density functional theory of Hohenberg and Kohn [24] in the framework of Kohn and Sham [25] has been used to optimize the structures of potassium clusters in this work. DFTB method has been developed by Seifert *et al.* [140, 141, 142, 143, 144]. In the DFTB, the linear combination of the atomic orbital (LCAO) for Kohn-Sham wave functions $\psi(r)$ is written as.

$$\psi(r) = \sum_{\mu} C_{\mu}\phi_{\mu}(r - R_j) \tag{2.1}$$

Atomic-like wave functions ϕ_μ used as basis functions are centered at the atomic sites R_j. The LCAO leads to secular equations in the form of:

$$\sum_{\mu} C_{\mu}(h_{\mu\nu} - \varepsilon_i S_{\mu\nu}) = 0 \tag{2.2}$$

These equations can be solved by diagonalization of the secular matrix. The matrix elements of the Hamiltonian $h_{\mu\nu}$ and the overlap matrix elements $S_{\mu\nu}$ are defined as:

$$h_{\mu\nu} = \langle \phi_\mu \mid \hat{h} \mid \phi_\nu \rangle \tag{2.3}$$

$$S_{\mu\nu} = \langle \phi_\mu \mid \phi_\nu \rangle \tag{2.4}$$

$$\hat{h} = \hat{t} + V_{eff}(r) \tag{2.5}$$

where $\hat{t}$ is the operator of kinetic energy ($\hat{t} = \frac{1}{2}\nabla^2$), and V_{eff} is the effective Kohn-Sham potential (one particle potential), consisting of an electron-nuclear part V_{ext}, the mean field electron interaction contribution (Hartree potential V_H), and the exchange-correlation part V_{xc} in the local density approximation (LDA).

$$V_{eff} = V_{ext} + V_H + V_{xc} \tag{2.6}$$

The effective Kohn-Sham potential $V_{eff}(r)$ is approximated as a sum of potentials V_j^0 of neutral atoms:

$$V_{eff}(r) = \sum_j V_j^0(\mid r - R_j \mid) \tag{2.7}$$

where R_j is the position of the jth atom. Furthermore, we make tight-binding approximation, so that:

$$h_{\mu\nu} = \langle \phi_\mu \mid \hat{t} + \sum_j V_j^0 \mid \phi_\nu \rangle = \langle \phi_\mu \mid \hat{t} + V_{j\mu}^0 + (1 - \delta_{j\nu,j\mu}) V_{j\nu}^0 | \phi_\nu \rangle \tag{2.8}$$

The Kronecker-δ is included in order to assure that the potential is not double counted for j_ν=j_μ. Through this approximation, the two center terms ($h_{\mu\nu} = \langle \phi_\mu \mid \hat{h} \mid \phi_\nu \rangle$, $S_{\mu\nu} = \langle \phi_\mu \mid \phi_\nu \rangle$) are calculated exactly within the Kohn-Sham basis.

Using the Kohn-Sham eigenvalues ε_i, the total energy ($E[\rho(r)]$) can be written as:

$$E[\rho(r)] = \sum_i^{occ} \varepsilon_i - \frac{1}{2}[\int d^3 r V_{eff} \rho - \int d^3 r V_{ext} \rho] + E_{xc} - \frac{1}{2} \int d^3 r V_{xc} \rho + E_N \tag{2.9}$$

The V_{ext} is the electron-nucleus external potential; E_{xc} is the exchange-correlation energy; V_{xc} is the corresponding potential, E_N is the nuclear-nuclear repulsion energy, and $\rho(r)$ is the electron density. The electron density and potential can be approximated in the following form.

$$\rho = \sum_j \rho_j \tag{2.10}$$

$$V = \sum_j V_j \tag{2.11}$$

so that the terms corresponding to equation (2.9) can be written as:

$$\frac{1}{2} \int d^3 r V_{eff} \rho = \frac{1}{2} \sum_j \sum_{\grave{j}} \int d^3 r V_j \rho_{\grave{j}} \tag{2.12}$$

$$\frac{1}{2} \int d^3 r V_{ext} \rho = \frac{1}{2} \sum_j \sum_{\grave{j}} \int d^3 r \frac{Z_j \rho_{\grave{j}}}{r_j} \tag{2.13}$$

$$E_{xc} - \frac{1}{2} \int d^3 r V_{xc} \rho = \frac{1}{2} \sum_j \sum_{\grave{j}} d^3 r \tilde{V_{xc_j}} \rho_{\grave{j}} \tag{2.14}$$

$$E_N = \frac{1}{2}\sum_j \sum_{\grave{j},j\neq\grave{j}} \int d^3r \frac{Z_j Z_{\grave{j}}}{R_{j\grave{j}}} \tag{2.15}$$

$R_{j\grave{j}}$ stand for the internuclear distance: $R_{j\grave{j}}$=$\mid R_j - R_{\grave{j}} \mid$. Special care is need in the treatment of the contribution for E_{xc}. For the representation of V_{xc_j} in terms of E_{xc} and V_{xc}. For the large internuclear distances, the electron-nucleus energy strongly compensates the nuclear repulsion energy, and the two center terms with the potential vanish also : $\int d^3r V_j \rho_{\grave{j}}$=0 for $j \neq \grave{j}$, due to screening of the potential (Wigner-Seitz limit). Assuming additionally that $\int d^3r V_{xc_j}\rho_{\grave{j}}$=0, and writting the total energy as single atom E_j in the corresponding form as above, one can evaluate the binding energy approximately by the Kohn-Sham eigenvalues and Kohn-Sham energies ε_{nj} of the atomic orbital n_j.

$$\varepsilon_B = E - \sum_j E_j \approx \sum_j^{occ} \varepsilon_i - \sum_j \sum_{nj} \varepsilon_{nj} \tag{2.16}$$

Such an expression holds only more or less strictly for large interatomic distances. The difference between ε_B and the binding energy from a full SCF-LDA calculation (E_B) for diatomic molecule increase with decreasing internuclear distance. Instead of calculating the binding energy from the total energy as written in equation (2.16), it reasonable to approximated as:

$$E_B = \sum_j^{occ} \varepsilon_i - \sum_j \sum_n \varepsilon_{jn} + \frac{1}{2}\sum_{j\neq\grave{j}} U_{j\neq\grave{j}}(R_j - R_{\grave{j}}) \tag{2.17}$$

$$E_B = \varepsilon_B + \frac{1}{2}\sum_{j\neq\grave{j}} U_{j\neq\grave{j}}(R_j - R_{\grave{j}}) \tag{2.18}$$

where $U(R_{j\grave{j}})$ is a set of short-ranged, repulsive pair potentials. These are obtained by requiring that the total energy of diatomic molecules (in our case, of K_2) as a function of interatomic distance is accurately reproduced.

In the DFTB method, we considered only the valence electrons (in our case only the $4s$ electron of the K atom), whereas the core electrons are treated as frozen.

The minimization of total energy is performed by using forces. The force F^j acting on atom j is divided into a nuclear part F_n^j and electronic part F_e^j.

$$F^j = -\delta E/\delta R^j = F_e^j + F_n^j \tag{2.19}$$

$$F_n^j = -\sum_{j\neq\grave{j}} \frac{\delta}{\delta R_{\grave{j}}}\left(\frac{Z_{\grave{j}} Z_j}{|R_{\grave{j}} - R_j|}\right) \tag{2.20}$$

The electronic part of force can be written as a sum of orbital contributions.

$$F_e^j = \sum_i n_i F_i^j = -\frac{\delta}{\delta R_j}\left(\sum_i (\psi_i|\hat{h}|\psi_i)\right) \tag{2.21}$$

where n_i is the occupation number of orbital i. Finally, F_i^j can be written as:

$$F_i^j = \sum_\mu \sum_\nu C_\mu^i C_\nu^i \left(-\frac{\delta H_{\mu\nu}}{\delta R_j} + \varepsilon_i \frac{S_{\mu\nu}}{\delta R_j} + \frac{\delta V_{\mu\nu}^{ee}}{\delta R_j}\right) \tag{2.22}$$

where $V_{\mu\nu}^{ee}$ are the matrix elements of the electron-electron interaction potential (V^{ee}=V_H+V_{xc}). The nuclear repulsion force F_n^j and the contribution arising from $\frac{\delta V_{\mu\nu}^{ee}}{\delta R_j}$ compensate strongly so that instead LCAO basis sets are needed to calculated the force accurately. This two terms are approximated by the repulsive term U(R).

$$U(R) = a(R - R_1)^2 \tag{2.23}$$

for $R < R_1$ and zero for $R \geq R_1$. The force acting on an atom at R_j can be calculated as:

$$F^j = -\bigtriangledown_i E_{tot} = \sum_i^{occ} \sum_\mu \sum_\nu C_\mu^i C_\nu^i \left(-\frac{\delta H_{\mu\nu}}{\delta R_j} + \varepsilon_i \frac{\delta S_{\mu\nu}}{\delta R_j}\right) + \frac{1}{2} \sum_{j\neq\grave{j}} \frac{\delta}{\delta R_j} U(|R_j - R_{\grave{j}}|) \tag{2.24}$$

2.4.2 2.4.2 Genetic Algorithm (GA)

The most important point in studying clusters is to find the global minima structures. The principal difficulty arises from the increase of the number of local minima structures with the number of atoms. An example is the cluster of 13 atoms: Lennard-Jones (LJ) has at least 1,506 numbers of local minima [145, 146].

The genetic algorithm is inspired by concepts from Darwinian natural evolution and is used as an effective tool for global geometry optimization. The main idea of GA is based on survival of the fittest. The fittest candidates pass their genetic characteristics on to the next generation through selective breeding and mutation.

The genetic algorithm has been used for optimizing the cluster geometries; for instance, Xiao and Williams [87] applied it to benzene, naphthalene, and anthracene clusters. Deaven *et al.* [88] used the genetic algorithm to locate the global minima of C_{60}. Hartke has used the method to Si_{10} [89]. Niesse and Mayne applied the technique to silicon clusters up to 10 atoms [90]. Morris also used the method to find the lowest energy configration of N-point changes on a unit sphere. The genetic algorithm has been used to optimize the morse clusters of 19-50 atoms [92].

The version of GA used in the present work has been applied to obtain the global minimum structures of monoatomic (Au, Al, Na, Ge, Si), diatomic (SiGe, AlO), and triatomic (HAlO) [93, 94, 95, 96, 97, 98]. Using GA, the global optimization of isolated potassium clusters up to 20 atoms was done in the following way: first we optimized the structures of K_N cluster; from these structures we randomly generated initial structures for K_{N+1} cluster by adding one atom; such structures were called parent structures. The parent structures were relaxed near the local minimum by using the geometry optimization method. By cutting the parents into two parts (mating) the next set of structures was obtained; those structures were called children structures and were also optimized. From the parent and children structures, the structures with the lowest energies are kept and used as parent structures for the next generation. This procedure is repeated until the lowest energy is unchanged for large number of generations.

Bibliography

[1] I. L. Finar, *Organic Chemistry: The Fundamental Principles*, Fourth Edition, vol.1 Longman and Green Co Ltd. 1963.

[2] R. W. Taft, E. D. Raczynska, P. C. Maria, I. Leito, W. Lewandowski, R. Kurg, J. F. Gal, M. Decouzon, and F. F. Anvia, *J. Anal. Chem.* **355**, 412 (1996).

[3] E. D. Raczynska and C. Laurence, *J. Chem. Res.* **5**, 338 (1990).

[4] A. H. de Vries and P. Th. van Duijnen, *Biophys. Chem.* **43**, 139 (1992).

[5] E. D. Raczynska and R. W. Taft, *Polish J. Chem.* **72**, 1054 (1998).

[6] R. Caminiti, A. Pieretti, L. Bencivenni, F. Ramondo, and N. Sanna, *J. Phys. Chem.* **100**, 10928 (1996).

[7] M. Remko, O. A. Walsh, and W. G. Richards, *Chem. Phys. Lett.* **336**, 156 (2001).

[8] M. Remko, O. A. Walsh, and W. G. Richards, *Phys. Chem. Chem. Phys.* **3**, 901 (2001).

[9] N. Marchand-Geneste and A. Carpy, *J. Mol. Struct. (THEOCHEM)* **465**, 209 (1999).

[10] M. Remko, O. A. Walsh, and W. G. Richards, *J. Phys. Chem. A* **105**, 6926 (2001).

[11] M. Remko, P. Th. van Duijnen, and M. Swart, *Struct. Chem.* **14**, 271 (2003).

[12] E. B. Fisher and J. R. Van Wazer, *Phosphorus and its componds. Vol.II Technology, Biological Functions, and Applications,* Interscience, INC., New York 1961.

[13] J. W. Bücher, R. Schiebs, G. Winter, and K. H. Büchel, *In Industrial Organic Chemistry*, VCH, New York, 1989.

[14] F. Cramer, *Angew. Chem.* **72**, 236 (1960).

[15] O. I. Kolodiazhnyi and N. Prynada, *Tetrahedron Lett.* **41**, 7997 (2000).

[16] A. R. Katritzky and J. M. Lagowski, *Advances in Heterocyclic Chemistry*, Academic Press, New York. 1963.

[17] M. M. Karelson, A. R. Katritzky, M. Szafran, and M. C. Zerner, *J. Chem. Soc. Perkin Trans. 2.* **1990**, 195 (1990).

[18] H. S. Rzepa, M. Y. Yi, M. M. Karelson, and M. C. Zerner, *J. Chem. Soc. Perkin Trans. 2.* **1991**, 635 (1991).

[19] H. B. Schlegel, P. Gund, and E. M. Fluder, *J. Am. Chem. Soc.* **104**, 5347 (1982).

[20] M. J. Scanlan,I. H. Hillier, and A. A. MacDowell, *J. Am. Chem. Soc.* **105** 3568 (1983).

[21] S. Woodcock, D. V. S. Green, M. A. Vincent, I. H. Hillier, M. F. Guest, and P. Sherwood, *J. Chem. Soc. Perkin Trans. 2.* **1992**, 2151 (1992).

[22] F. J. Luque, J. M. López-Bes, J. Cemeli, M. Aroztegui, and M. Orozco, Theor. Chem. Acc. **96**, 105 (1997).

[23] P. I. Nagy, F. R. Tejada, and W. S. Messer Jr., *J. Phys. Chem. B* **109**, 22588 (2005).

[24] P. Hohenberg and W. Kohn, *Phys. Rev.* **136**, B 864 (1964).

[25] W. Kohn and L. J. Sham, *Phys. Rev.* **140**, A1133 (1965).

[26] S. H. Vosko, L. Wilk, and M. Nusair, *Can. J. Phys.* **58**, 1200 (1980).

[27] A. D. Becke, *Phys. Rev. A* **38**, 3098 (1988).

[28] J. P. Perdew, *Phys. Rev. B***33**, 8822 (1986).

[29] J. P. Perdew and Y. Wang, *Phys. Rev. B***45**, 13244 (1992).

[30] J. P. Perdew, J. A. Chevary, S. H. Vosko, K. A. Jackson, M. R. Pederson, D. J. Singh, and C. Fiolhais, *Phys. Rev. B* **46**, 6671 (1992).

[31] A. D. Becke, *J. Chem. Phys.* **104**, 1040 (1996).

[32] J. P. Perdew, K. Burke, and M. Ernzerhof, *Phys. Rev. Lett.* **77**, 3865 (1996).

[33] C. Lee, W. Yang, and R. G. Parr, *Phys. Rev. B* **37**, 785 (1988).

[34] A. D. Becke, *J. Chem. Phys.* **98**, 5648 (1993).

[35] M. Springborg, in A. Hinchliffe (Ed.), Specialist Periodical Reports: Chemical Modelling, Applications and Theory, vol. 5, Royal Society of Chemistry, Cambridge, UK, 2008.

[36] W. L. Jorgensen, *Acc. Chem. Res.* **22**, 184 (1989).

[37] D. L. Beveridge and F. M. DiCapua, *Ann. Rev. Biophys. Chem.* **18**, 431 (1989).

[38] P. A. Bash, U. C. Singh, R. Langridge, and P. A. Kollman, *Science* **236**, 564 (1987).

[39] J. K. Buckner and W. L. Jorgensen, *J. Am. Chem. Soc.* **111**, 2507 (1989).

[40] J. A. McCammon and M. Karplus, *Acc. Chem. Res.* **16**, 187 (1983).

[41] A. Warshel and M. Levitt, *J. Mol. Biol.* **103**, 227 (1976).

[42] A. Warshel, *J. Phys. Chem.* **83**, 1640 (1979).

[43] A. Warshel and S. T. Russell, *Quart. Rev. Biophys.* **17**, 283 (1984).

[44] V. Luzhkov and A. Warshel, *J. Am. Chem. Soc.* **113**, 4491 (1991).

[45] V. Luzhkov and A. Warshel,*J. Comp. Chem.* **13**, 199 (1992).

[46] J. Gao, *J. Phys. Chem.* **96**, 537 (1992).

[47] J. Gao and J. J. Pavelites, *J. Am. Chem. Soc.* **114**, 1912 (1992).

[48] J. Gao and X. Xia, *Science* **258**, 631 (1992).

[49] J. Tomasi and M. Persico, *Chem. Rev.* **94**, 2027 (1994).

[50] J. Tomasi, B. Mennucci, and R. Cammi, *Chem. Rev.* **105**, 2999 (2005).

[51] L. Onsager, *J. Am. Chem.Soc.***58**, 1486 (1936).

[52] S. Miertuŝ, E. Scrocco, and J. Tomasi, Chem. Phys. **55**, 117 (1981).

[53] S. Miertuŝ and J. Tomasi, *Chem. Phys.* **65**, 239 (1982).

[54] C. J. Cramer, *Essential of computaional chemistry*, 2nd Edition, John Wiley and Sons, Ltd. 2004.

[55] G. Alagona, C. Ghio, and P. I. Nagy, *Int. J. Quantum. Chem.* **99**, 161 (2004).

[56] F. M. Floris, J. Tomasi, and J. L. Pascual-Ahuir, *J. Comput. Chem.* **12**, 784 (1991).

[57] C. Alemána and S. E. Galembeck. *Chem. Phys.* **232**, 151 (1998).

[58] A. Jezierska, J. Panek, and S. Ryng, *J. Mol. Struct. (Theochem)* **636**, 203 (2003).

[59] I. Tuñôn, M. F. Ruiz-Lôpez, D. Rinaldi, and J. Bertrân, *J. Comput. Chem.* **17**, 148 (1996).

[60] M. W. Wong, K. B. Wiberg, and M. J. Frisch, *J. Am. Chem. Soc.* **114**, 523 (1992).

[61] K. V. Mikkelsen, A. Cesar, H. Ågren, and H. J. A. Jensen, *J. Chem. Phys.* **103**, 9010 (1995).

[62] M. W. Wong, M. J. Frisch, and K. B. Wiberg, *J. Am. Chem. Soc.* **113**, 4776 (1991).

[63] R. J. Hall, M. M. Davidson, N. A. Burton, and I. H. Hillier, *J. Phys. Chem.* **99**, 921 (1995).

[64] M. Namazian, *J. Mol. Struct. (Theochem)* **664**, 273 (2003).

[65] M. Cossi, V. Barone, R. Cammi, and J. Tomasi, *Chem. Phys. Lett.* **255**, 327 (1996).

[66] E. Cancès, B. Mennucci, and J. Tomasi, *J. Chem. Phys.* **107**, 3032 (1997).

[67] B. Mennucci, E. Cancès, and J. Tomasi, *J. Phys. Chem. B.* **101** 10506 (1997).

[68] E. Cancès, and B. Mennucci, *J. Math. Chem.* **23**, 309 (1998).

[69] R. Cammi and J. Tomasi, *J. Comput. Chem.* **16**, 1449 (1995).

[70] M. J. Huron, and P. Claverie, *J. Phys. Chem.* **76** 2123 (1972).

[71] M. J. Huron, and P. Claverie, *J. Phys. Chem.* **78**, 1853 (1974).

[72] M. J. Huron, and P. Claverie, *J. Phys. Chem.* **78** 1862 (1974).

[73] G. W. Schnuelle and D. L. Beveridge, *J. Phys. Chem.* **79**, 2566 (1975).

[74] J. H. McCreey, R. E. Christoffersen, and G. G. Hall, *J. Am. Chem. Soc.* **98**, 7191 (1976).

[75] H. S. Rzepa and M. Y. Yi, *J. Chem. Soc. Perkin Trans. 2.* **1991**, 531 (1991).

[76] P. Claverie, J. P. Daudey, J. Langlet, B. Pullman, D. Piazzola, and M. J. Huron, *J. Phys. Chem.* **82** 405 (1978).

[77] J. L. Pascual-Ahuir, E. Silla, J. Tomasi, and R. Bonaccorsi, *J. Comp. Chem.* **8**, 778 (1987).

[78] F. J. Luque, M. J. Negre, and M. Orozco, *J. Phys. Chem.* **97**, 4386 (1993).

[79] M. J. Frisch, G. W. Trucks, H. B. Schlegel, G. E. Scuseria, M. A. Robb, J. R. Cheeseman, J. A. Montgomery, Jr., T. Vreven, K. N. Kudin, J. C. Burant, J. M. Millam, S. S. Iyengar, J. Tomasi, V. Barone, B. Mennucci, M. Cossi, G. Scalmani, N. Rega, G. A. Petersson, H. Nakatsuji, M. Hada, M. Ehara, K. Toyota, R. Fukuda, J. Hasegawa, M. Ishida, T. Nakajima, Y. Honda, O. Kitao, H. Nakai, M. Klene, X. Li, J. E. Knox, H. P. Hratchian, J. B. Cross, V. Bakken, C. Adamo, J. Jaramillo, R. Gomperts, R. E. Stratmann, O. Yazyev, A. J. Austin, R. Cammi, C. Pomelli, J. W. Ochterski, P. Y. Ayala, K. Morokuma, G. A. Voth, P. Salvador, J. J. Dannenberg, V. G. Zakrzewski, S. Dapprich, A. D. Daniels, M. C. Strain, O. Farkas, D. K. Malick, A. D. Rabuck, K. Raghavachari, J. B. Foresman, J. V. Ortiz, Q. Cui, A. G. Baboul, S. Clifford, J. Cioslowski, B. B. Stefanov, G. Liu, A. Liashenko, P. Piskorz, I. Komaromi, R. L. Martin, D. J. Fox, T. Keith, M. A. Al-Laham, C. Y. Peng, A. Nanayakkara, M. Challacombe, P. M. W. Gill, B. Johnson, W. Chen, M. W. Wong, C. Gonzalez, and J. A. Pople, *Gaussian 03; Revision D.01*; Gaussian, Inc., Wallingford, CT, 2004.

[80] F. Baletto and R. Ferrando, *Rev. Mod. Phys.* **77**, 371 (2005).

[81] R. Ferrando, J. Jellinek, and R. L. Johnston, *Chem. Rev.* **108**, 845 (2008).

[82] T. Kondow and F. Mafunè, *Progress in experimental and theoretical studies of clusters.*, World Scientific PublishIng Co. Pte. Ltd. 2003.

[83] V. G. Grigoryan and M. Springborg, *Phys. Chem. Chem. Phys.* **3**, 5135 (2001).

[84] V. G. Grigoryan and M. Springborg, *Chem. Phys. Lett.* **375**, 219 (2003).

[85] V. G. Grigoryan and M. Springborg, *Phys. Rev. B.* **70**, 205415 (2004).

[86] D. J. Wales and J. P. K. Doye, *J. Phys. Chem. A* **101**, 5111(1997).

[87] Y. Xiao and D. E. Williams, *Chem. Phys. Lett.* **215**, 17 (1993).

[88] D. M. Deaven and K. M. Ho, *Phys. Rev. Lett.* **75**, 288 (1995).

[89] B. Hartke, *Chem. Phys. Lett.* **240**, 560 (1995).

[90] J. A. Niesse and H. R. Mayne, *Chem. Phys. Lett.* **261**, 576 (1996).

[91] J. R. Morris, D. M. Deaven, and K. M. Ho, *Phys. Rev.B* **53**, R1740 (1996).

[92] C. Roberts, R. L. Johnston, and N. T. Wilson, *Theor. Chem. Acc.* **104**, 123 (2000).

[93] Y. Dong and M. Springborg, *J. Phys. Chem. C* **111**, 12528 (2007).

[94] Y. Dong and M. Springborg, *Eur. Phys. J. D* **43**, 15 (2007).

[95] V. Tevekeliyska, Y. Dong, M. Springborg, and V. G. Grigoryan, *Eur. Phys. J. D* **43**, 19 (2007).

[96] H. ur Rehman, M. Springborg, and Y. Dong, *Eur. Phys. J. D* **52**, 39 (2009).

[97] H. ur Rehman, M. Springborg, and Y. Dong, *J. Phys. Chem. A* **115**, 2005 (2011).

[98] Y. Dong and M. Springborg, *Am. Inst. Phys. Conf. Proc.* **1148**, 342 (2009).

[99] W. D. Knight, W. A. de Heer, K. Clemenger, and W. A. Saunders, M. Y. Chou, M. L. Cohen, *Phys. Rev. Lett* **52**, 2141 (1984).

[100] W. D. Knight, W. A. de Heer, K. Clemenger, and W. A. Saunders, *Phys. Rev. B***31**, 2539 (1985).

[101] W. D. Knight, W. A. de Heer, K. Clemenger, and W. A. Saunders, *Solid State Commun.* **53**, 445 (1985).

[102] W. D. de Heer, *Rev. Mod. Phys.* **65**, 611 (1993).

[103] M. Barck, *Rev. Mod. Phys.* **65**, 677 (1993).

[104] P. Jesen, *Rev. Mod. Phys.* **71**, 1695 (1999).

[105] C. Binns, *Surface Science Reports* **44**, 1 (2001)

[106] U. Heiz and W.-D Schneider, *J. Phys. D: Appl. Phys.* **33**, R85 (2000).

[107] R. E. Plamer, S. Pratontep, and H. -G. Boyen, *Nature Materials* **2**, 443 (2003).

[108] J. A. Golovchenko, *Science* **232**, 48 (1986).

[109] R. J. Hamers, *Annu. Rev. Phys. Chem.* **40**, 531 (1989).

[110] R. M. Tromp, *J. Phys. Condens. Matter* **1**, 10211 (1989).

[111] A. V. Crewe, *Science* **221**, 325 (1983).

[112] J. A. Panitz, *J. Phys. E Sci. Instrum.* **15**, 1281 (1982).

[113] S. C. Wang and G. Ehrlich, *Surf. Sci.* **239**, 301 (1990).

[114] M. C. Fallis, M. S. Daw, and C. Y. Fong, *Phys. Rev. B* **51**, 7817 (1995).

[115] R. C. Longo, C. Rey, L. J. Gallego, *Surf. Sci.* **424**, 311 (1999).

[116] M. Breeman, G. T. Barkema, and D. O. Boerma, *Surf. Sci.* **323**, 71 (1995).

[117] C. -L. Liu and J. B. Adams, *Surf. Sci.* **268**, 73 (1992).

[118] P. R. Schwoebel, S. M. Foiles, C. L. Bisson, and G. L. Kellogg, *Phys. Rev. B* **40**, 10639 (1989).

[119] A. F. Wright, M. S. Daw, and C. Y. Fong, *Phys. Rev. B* **42**, 9409 (1990).

[120] H. -V. Roy, P. Fayet, F. Patthey, W. -D. Schneider, B. Delley, and C. Massorbrio, *Phys. Rev. B* **49**, 5611 (1994).

[121] M. Y. Chou, A. Cleland, and M. L. Cohen, *Solid State Commun.* **52**, 645 (1984).

[122] G. A. Thompson, and D. M. Lindsay, *J. Chem. Phys.* **74**, 959 (1981).

[123] W. A. Saunders, K. Clemenger, W. A. de Heer, and W. D. Knight, *Phys. Rev. B* **32**, 1366 (1985).

[124] W. D. Knight, W. A. de Heer, and W. A. Saunders, *Z. Phys. D* **3**, 109 (1986).

[125] C. Brèchignac and Ph. Cahuzac, *Chem. Phys. Lett.* **117**, 365 (1985).

[126] C. Brèchignac and Ph. Cahuzac, *Z. Phys. D* **3**, 121 (1986).

[127] M. M. Kappes, M. Schär, P. Radi, and E. Schumacher, *J. Chem. Phys.* **84**, 1863 (1986).

[128] M. M. Kappes, P. Radi, M. Schär, and E. Schumacher, *Chem. Phys. Lett.* **113**, 243 (1985).

[129] A. Kornath, R. Ludwig, and A. Zoermer, *Angew. Chem. Int. Ed.* **37**, 1575 (1998).

[130] H. Soll, J. Flad, E. Golka, and Th. Krüger, *Surf. Sci.* **106**, 251 (1981).

[131] G. Pacchioni, H. O. Beckmann, and J. Koutecký, Chem. Phys. Lett. **87**, 151 (1982).

[132] F. Spiegelmann and D. J. Pavolini, *Chem. Phys.* **89**, 4954 (1988).

[133] S. C. Richtsmeier, D. A. Dixon, and J. L. Gole, *J. Phys. Chem.* **86**, 3942 (1982).

[134] J. Flad, G. Igel, M. Dolg, H. Stoll, and H. Preuss, *Chem. Phys.* **75**, 331 (1983).

[135] A. Pellegatti, B. N. McMaster, and D. R. Salahub, *Chem. Phys.* **75**, 83 (1983).

[136] A. K. Ray and S. D. Altekar, *Phys. Rev. B* **42**, 1444 (1990).

[137] E. Florez and P. Fuentealba, *Int. J. Quant. Chem.* **109**, 1080 (2009).

[138] A. Banerjee, T. K. Ghanty, and A. Chakrabarti, *J. Phys. Chem. A* **112**, 12303 (2008).

[139] S. K. Lai, P. J. Hsu, K. L. Wu, W. K. Liu, and M. Iwamatsu, *J. Chem. Phys.* **117**, 10715 (2002).

[140] P. Blaudeck, Th. Frauenheim, D. Porezag, G. Seifert and E. Fromm, *J. Phys: Condens Matter* **4**, 6389 (1992).

[141] D. Porezag, Th. Frauenheim, Th. Köhler, G. Seifert and R. Kaschner, *Phys. Rev. B* **51**, 12947 (1995).

[142] G. Seifert, D. Porezag, and Th. Frauenheim *Int. J. Quantum. Chem.***58**, 85 (1996).

[143] G. Seifert, *J. phys. Chem. A* **111**, 5609 (2007).

[144] G. Seifert and J.-O. Joswig, WIREs Comput Mol Sci. doi: 10.1002/WCMS.1094.

[145] C. Tasi and K. Jordan, *J. Phys. Chem.* **97**, 11227 (1993).

[146] S. F. Chekmarev, *Phys. Rev. E* **64**, 036703 (2001).

Theoretical Study of the Effects of Solvation, Substitution, and Structure on the Properties of Imidazolines, Oxazolines, and Thiazolines

Sahar Abdalla* and Michael Springborg*

Physical and Theoretical Chemistry, University of Saarland, 66123 Saarbrücken, Germany

Received: October 26, 2009; Revised Manuscript Received: April 1, 2010

Different isomers and tautomers of methylphosphino- and phenylphosphino-substituted cyclic imidazoline, oxazoline, and thiazoline have been investigated theoretically in gas and aqueous phases. Special emphasis is put on the relative total energies and on the changes in the structure due to substitution or solvation. The calculations were carried through using the B3LYP/6-31+G(d,p) method. To include the effects of the solvent, we used the polarizable-continuum approach both without and with the inclusion of explicit water molecules. Lacking experimental information on the systems, the results were compared with those for nitrogen-containing compounds. In gas phase the cyclic moiety of these molecules show clear deviations from planarity. Only moderate changes in the structure due to solvation were found. On the other hand, the solvent affects strongly the relative stability of different tautomers and isomers. The inclusion of explicit water molecules changes the order of stability due to the presence of intermolecular hydrogen bonds. On the basis of the Bader theory of atoms in molecules, we identify the critical points of the hydrogen bonds as well as properties of the electron density at those points. Thereby, we can quantify the strength of the hydrogen bonds. Finally, we report energies of solvation for the systems of our study.

I. Introduction

The theoretical determination of tautomerization in heterocyclic systems is far from trivial,[1] and a number of theoretical approaches have been applied for this purpose, ranging from semiemprical molecular orbital methods[2,3] to parameter-free methods that may even include electron correlation.[4,5] Also, the influence of a solvent on the tautomeric equilibrium of heterocyclic, five-membered ring systems has been the subject of many studies.[2,6−8] A comparison of the relative energies of different tautomers in two different solvents gives direct information on the influence of the solvent.

In several recent studies, systems containing the amidine group −NH−C(R)═N− were examined.[9−16] As a natural extension of those we shall here investigate the isoelectronic systems containing the −PH−C(R)═N− group. Phosphorus compounds have been investigated as relevant materials for a large number of different applications, including as lubricants, oil additives, water treatment cleaners, flame-retarding agents, fertilizers, plasticizers, and pesticides.[17,18] Phosphorus and organophosphorus compounds were also recognized to have important biological functions, including that they are essential constituents of the protoplasm.[19] Of direct relevance to the present work is that proton transfer processes between nitrogen and phosphorus were investigated by Kolodiazhnyi et al.,[20] who concluded that the tautomeric equilibrium depends both on the nature of the solvent and on the substituents at these atoms.

The present work reports a systematic theoretical examination of the methyl- and phenyl-substituted phosphino and phosphinidene tautomers of cyclic imidazoline, oxazoline, and thiazoline (which we shall label Me−NH, Me−O, Me−S, Ph−NH, Ph−O, and Ph−S) in gas phase and in aqueous phase. In particular, we shall focus on the relative energies and molecular geometries and how these properties change upon solvation. Due to the absence of theoretical and experimental data for these compounds, we shall compare them with their nitrogen analogues.

Theoretical studies of tautomerization in solution depend critically on being able to calculate the free energy of solvation, that is, the free-energy difference between tautomers in gas phase and in aqueous phase. Over the years, many different approaches have been suggested (see, e.g., refs 21 and 22). In one class of approaches, the free energy of solvation is calculated with the help of the self consistent reaction field (SCRF) continuum models, which replace the microscopic description of the solvent by a polarizable dielectric medium. Alternatively, in particular when hydrogen bonding between the solvent and the solute may exist, it is more realistic to use so-called explicit models whereby a part of the solvent is treated fully quantum mechanically, whereas the rest is treated within the polarizable continuum model. Such a so-called discrete/SCRF approach has been used over many years[23−29] and has been found to provide reliable estimates of the solvation energy even with a modest numbers of solvent molecules.[29] In the present work, we shall consider both approaches, that is, the SCRF approach and the discrete/SCRF approach.

II. Computational Details

We studied the systems shown in Figure 1. All calculations were performed with the Gaussian03 program suite[30] and with the B3LYP[31−33] density functional using a 6-31+G(d,p) basis set. From the vibrational frequencies it was confirmed that all obtained structures indeed correspond to stable ones.

Solvent effects were studied by using two different approaches. In one, only the solute was treated quantum-mechanically, whereas in the other up to three water molecules were also treated quantum-mechanically. The (rest of the) solvent was treated using the integral equation formalism (IEF)[22,34−37] of the polarized continuum model (PCM)[34,38,39] of the SCRF, and the relative dielectric constant of water was set

* To whom correspondence should be addressed. E-mail: s.abdalla@mx.uni-saarland.de (S. A.), m.springborg@mx.unisaarland.de (M. S.).

10.1021/jp9102096
Published on Web 04/20/2010

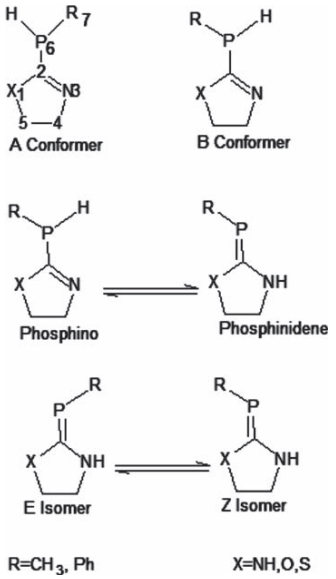

Figure 1. Structures and atom numbering of the tautomers and isomers of methylphosphino-substituted cyclic imidazoline, oxazoline, and thiazoline (Me−NH, Me−O, Me−S) and phenylphosphino-substituted cyclic imidazoline, oxazoline, and thiazoline (Ph−NH, Ph−O, Ph−S).

equal to 78.39. The molecular cavity was constructed by using the united atom topological model (UAO), whereby the cavity gets the shape of interlocking spheres centered on heavy (i.e., non-hydrogen) atoms with radii equal to van der Waals radii scaled by a factor of 1.20.[34] In the discrete/SCRF model, the values of the OFac and RMin parameters for the GEPOL algorithm[40] were changed to 0.8 and 0.5 from 0.89 and 0.2, respectively.

In both treatments of the solvent, the changes in the total energy contain more different contributions. One of those is the change in the total energy of the solute in gas phase when changing the structure from the optimized one to that in the solvent. This change is, per construction, always positive. Another is the electrostatic interaction energy between solvent and solute which, according to the present calculations, always is negative. The last contribution is the energy that is needed for creating the cavity in the solvent. Also, this contribution is always positive.

In the SCRF calculations, the energy of solvation, $\Delta E_{sol,1}$, was calculated as the difference between the energy of the molecule in the continuum and the energy of the molecule in gas phase,

$$\Delta E_{sol,1} = E_{solute,PCM} - E_{solute,gas} \quad (1)$$

In this expression, none of the total energies includes zero-point corrections. Thereby, we assume that the vibrational properties of the solute change only marginally, so that $\Delta E_{sol,1}$ represents the experimentally measurably solvation energy (within the PCM).

On the other hand, in the Discrete/SCRF model, we calculate the relative energies of solvation, $\Delta E_{sol,2}$, according to

$$\Delta E_{sol,2} = E_{complex,PCM} - E_{solute,gas} - E_{(H_2O)_3,PCM} \quad (2)$$

where $E_{(H_2O)_3, PCM}$ represents the energy of three water molecules in PCM oriented as found for each complex.

TABLE 1: Various Properties As Found in the Gas Phase (Marked Gas), in the PCM Calculations (Marked PCM), and in the PCM Calculations with the Inclusion of 3 Explicit Water Molecules (Marked PCM + $3H_2O$)[a]

system	isomer	ΔE (Gas)	ΔE (PCM)	ΔE (PCM + $3H_2O$)	$\Delta E_{sol,1}$	$\Delta E_{sol,2}$
Me−NH	B	0.00	0.00	0.00	−17.15	3.61
	A	−4.42	−2.52	−3.85	−15.38	3.44
	E	12.49	3.82	−1.25	−25.79	−10.82
Me−O	B	0.00	0.00	0.00	−12.34	10.82
	A	−3.14	−1.57	2.33	−10.58	15.62
	E	33.46	20.86	15.62	−24.84	−6.17
	Z	31.72	21.69	20.11	−21.95	−0.72
Me−S	B	0.00	0.00	0.00	−11.22	16.65
	A	−4.41	−2.59	6.24	−9.45	21.71
	E	23.89	14.77	1.59	−20.19	−7.70
	Z	21.24	13.42	3.99	−18.75	−4.77
Ph−NH	B	0.00	0.00	0.00	−19.07	−11.76
	A	5.78	3.21	2.40	−21.63	−15.00
	E	4.01	−4.56	−12.99	−27.72	−29.64
Ph−O	B	0.00	0.00	0.00	−15.70	−2.71
	A	1.83	1.29	19.52	−16.67	11.94
	E	20.47	10.81	12.89	−25.16	−11.94
	Z	27.74	15.21	25.26	−27.88	−7.29
Ph−S	B	0.00	0.00	0.00	−14.74	16.27
	A	−0.24	0.39	−10.49	−14.10	11.74
	E	13.50	7.44	−9.55	−21.15	−3.78
	Z	17.45	8.88	−12.65	−23.08	−9.74

[a] All quantities, except for the solvation energies, are given relative to the B isomer. The quantities are E, the total energy at $T = 0$ (with the inclusion of zero-point energy), and the two solvation energies. Energies are given in kJ/mol. Finally, the different isomers are shown in Figure 1.

The strength of the intermolecular hydrogen bonds of the complexes was studied by using the atoms in molecules (AIM) theory of Bader[41] as follows. From the electron density we identify the bond critical point (BCP) of a hydrogen bond, $\vec{r}_{cp}$. Subsequently, we calculate $\rho(\vec{r}_{cp})$ and $\nabla^2\rho(\vec{r}_{cp})$. These two parameters can be used in quantifying the strength of a hydrogen bond.[42] All AIM calculations were carried through using the AIMPAC series of programs.[43−45]

III. Results and Discussion

Our main findings about the energetics for all the systems of our study are collected in Table 1. These include relative energies (at $T = 0$ with the inclusion of zero point corrections), and solvation energies.

A. Gas Phase Calculations. Previous DFT calculations on similar systems[12,16] have shown that the most stable structures are stabilized via intramolecular hydrogen bonds (which are identified by their lengths that are smaller than the sum of the van der Waals radii of the atoms,[46] that is, 2.75, 2.72, 3.00, and 3.00 Å for H···N, H···O, H···P, and H···S interatomic distances, respectively; for the interatomic distances of the present systems, see the Supporting Information). This is also to some extent the case here.

Our DFT calculations show that the phosphino derivatives of methyl- and phenyl-substituted cyclic imidzoline, oxazoline, and thiazoline, respectively, may exist in two forms (conformers A and B, cf. Figure 1). The methyl substitution in all case stabilizes the A form over the B form by around 3.14−4.41 kJ mol^{-1}. Moreover, the stability of the sulfur derivative is characterized by the presence of intramolecular hydrogen bonding between the hydrogen atoms of the methyl group and N(3), and the rotation of the methyl group increases the possibility of forming hydrogen bonds via a "bifurcated" hydrogen bond, that is, X < $(C-H)_2$. The phenyl substitution (X = NH, O) stabilizes the B form by 1.83 and 5.78 kJ mol^{-1}, respectively, which also is due to hydrogen bonding between

TABLE 2: Selected Bond Lengths (in Å) of the Various Isomers in Gas Phase[a]

	X = NH				X = O				X = S			
	A	B	E	E	A	B	Z	E	A	A	Z	E
bond length	Me	Ph	Me	Ph	Me	Ph	Me	Ph	Me	Ph	Me	Ph
$d[X_1-C_2]$	1.399	1.397	1.389	1.385	1.371	1.369	1.363	1.363	1.809	1.809	1.782	1.785
$d[C_2-N_3]$	1.285	1.286	1.383	1.375	1.275	1.276	1.387	1.373	1.274	1.272	1.386	1.369
$d[N_1-H]$	1.013	1.013	1.011	1.010								
$d[X_1-C_5]$	1.475	1.475	1.465	1.465	1.457	1.456	1.449	1.446	1.841	1.842	1.846	1.844
$d[C_4-C_5]$	1.550	1.550	1.535	1.537	1.549	1.547	1.529	1.531	1.546	1.547	1.528	1.529
$d[N_3-C_4]$	1.479	1.479	1.466	1.464	1.477	1.478	1.462	1.461	1.466	1.465	1.461	1.459
$d[C_2-P_6]$	1.851	1.852	1.738	1.747	1.846	1.850	1.724	1.733	1.848	1.856	1.722	1.732
$d[N_3-H]$			1.009	1.010			1.011	1.011			1.013	1.013
$d[P_6-C_7]$	1.860	1.857	1.886	1.860	1.863	1.852	1.881	1.865	1.865	1.846	1.878	1.864
$d[P_6-H]$	1.424	1.416			1.422	1.416			1.423	1.419		

[a] For the atom numbering, see Figure 1.

P(6)−H and N(3). For the phenyl phosphino of the sulfur compound the A conformer is stabilized due to the presence of intramolecular hydrogen bonding between P(6)−H and S, whose length is 2.97 Å.

It is worthwhile to mention that when comparing our results with those for the nitrogen analogues[16] we find two factors that influence the hydrogen bonding, that is, the increase of the bond length C(2)−P(6) by about 0.5 Å as a result of replacing the nitrogen atom by the phosphorus in position 6 and the fact that the phosphorus atom is a weaker proton donor than nitrogen.[47,48]

The phosphinidene tautomers of the oxygen- and sulfur-based compounds exist in two geometrical isomers (Z and E). Methyl substitutions (X = O, S) stabilize the Z isomer by around 1.74 and 2.66 kJ mol^{-1}, respectively, whereas phenyl substitution stabilizes the E isomer over the Z one by about 7.27 and 3.95 kJ mol^{-1}, respectively. In the case of phenyl substitution this stability can be explained through three-center bonds, P(6)−C(2)−N(3). The considerable elongation (by about 0.4 Å) of the N(3)−H···S hydrogen bond in the Z isomer of Ph-S compared to the N(3)−H···O length in the X = O compound causes a weakening in the stability of the Z isomer for the sulfur species.

From the relative energies in Table 1 we see that, in all cases the phosphino form was found to be more stable than the phosphinidene form. The stability of the endocyclic double bond is in agreement with the results obtained by Remko et al. in their investigation of amino ↔ imino tautomers for the same cyclic species.[16]

Our optimized structures in gas phase show that the ring moieties adopt nonplanar configurations in agreement with results of previous calculations on the nitrogen-based compounds.[16] All molecules have C_1 symmetries. In Table 2 we give the most important geometric parameters of the most stable isomers. Small differences for the substituted phosphino and phosphinedene tautomers are found for the C(2)−P(6) bond length which is shorter by about 0.1 Å, confirming the tautomerization. The 2-phosphino substituents [P(6)−H group] are oriented so as to form intramolecular hydrogen bonds, leading to an increased stability of these isomers. Other geometric parameters are given in the Supporting Information.

B. Aqueous Solution Calculations. ***1. SCRF Calculations.*** In this subsection we shall report the results of the calculations for which the complete solvent was treated within the PCM approach, that is, no water molecule was treated explicitly. From the values of the total relative energy, ΔE (see Table 1), we find that the phosphino forms are the most stable species except for Ph−NH, for which the phosphinidene tautomer (in the E form) is the most stable tautomer.

When comparing with the gas phase results, we see that the relative order of stability of isomers and tautomers in several cases has changed. For instance, the A isomers of Ph−S are less preferred in the solution when compared to B. This may be explained as related to the larger dipole moment of the B structure, which leads to an attractive interaction with the polarized continuum. Table 3 lists the dipole moment of the studied species in gas phase and in aqueous phase. Without exception, the dipole moment increases when the molecule is being solvated. The reason is that an increased stabilizing electrostatic interaction between solvent and solute is thereby obtained.

TABLE 3: Dipole Moment (in Debye) for the Various Structures (cf. Fig. 1) in Gas Phase and As Found in Aqueous Solution Using the PCM

isomer	gas phase (μ)	PCM (μ)	isomer	gas phase (μ)	PCM (μ)
Me−NH			Ph−NH		
B	2.31	3.57	B	3.79	5.09
A	1.66	3.77	A	3.09	3.91
E	4.45	6.31	E	4.77	6.76
Me−O			Ph−O		
B	2.14	2.65	B	2.32	2.91
A	1.58	1.94	A	1.69	2.04
E	5.21	7.29	E	5.34	7.52
Z	4.49	6.27	Z	5.09	7.04
Me−S			Ph−S		
B	1.87	2.09	B	1.98	2.53
A	1.53	1.89	A	1.79	2.18
E	4.86	6.85	E	4.99	7.10
Z	3.74	5.35	Z	4.18	5.83

Unfortunately, there is no experimental information about the tautomeric equilibrium in these compounds. Since also no experimental information on the dipole moment for the molecules of our structures is available, it may be relevant to compare with results of theoretical studies on smaller, organic molecules. For those, the PCM predicts an increase of the dipole moment by up to 30% in aqueous solution compared to gas phase values.[49]

For our compounds, only moderate changes in the geometric parameters were found when comparing gas-phase and solution results. In Table 4 we give some of the most important geometric parameters. Other geometric parameters are available in the Supporting Information. To get further information about the effects of the solvent on the solute, the Mulliken net charges[50] are given in the Supporting Information. In general, the atomic charges are only weakly affected by the aqueous media.

2. Discrete/SCRF Calculations. When including three explicit water molecules in the calculations we obtain the relative energies listed in Table 1. The inclusion of explicit water molecules changes the relative order of stability compared to the results from the gas-phase and the PCM calculations. The stability of the B form for Me-O is due to the hydrogen bonding stabilization between the heteroatoms (oxygen and nitrogen) and the water molecules as well as a contribution from bifurcated

TABLE 4: Selected Bond Lengths (in Å) As Found in the PCM Calculations[a]

	X = NH				X = O				X = S			
	A	B	E	E	A	B	E	E	A	B	Z	E
bond length	Me	Ph	Me	Ph	Me	Ph	Me	Ph	Me	Ph	Me	Ph
$d[X_1-C_2]$	1.394	1.390	1.371	1.365	1.369	1.365	1.362	1.359	1.809	1.808	1.780	1.785
$d[C_2-N_3]$	1.289	1.290	1.379	1.374	1.276	1.278	1.364	1.358	1.273	1.275	1.372	1.357
$d[N_1-H]$	1.015	1.014	1.011	1.012								
$d[X_1-C_5]$	1.477	1.476	1.469	1.469	1.461	1.461	1.454	1.456	1.842	1.842	1.847	1.846
$d[C_4-C_5]$	1.548	1.548	1.535	1.536	1.548	1.547	1.529	1.531	1.545	1.544	1.527	1.528
$d[N_3-C_4]$	1.483	1.483	1.468	1.468	1.479	1.481	1.465	1.464	1.469	1.469	1.463	1.463
$d[C_2-P_6]$	1.849	1.853	1.754	1.764	1.847	1.851	1.738	1.745	1.856	1.856	1.733	1.740
$d[N_3-H]$			1.014	1.013			1.011	1.012			1.016	1.013
$d[P_6-C_7]$	1.863	1.852	1.885	1.858	1.861	1.849	1.884	1.861	1.846	1.848	1.879	1.861
$d[P_6-H]$	1.424	1.417			1.421	1.417			1.419	1.418		

[a] The numbering of the atoms is given in Figure 1.

hydrogen bonding between the hydrogen atoms of the methyl group and the oxygen of the water molecules. For Ph−O, there is hydrogen bonding involving the α hydrogen of the phenyl ring in addition to hydrogen bond between the explicit water molecules. The fact that phosphorus has a lower tendency to act as the proton donor in hydrogen bonding explains why the oxygen of the water molecule prefers to form hydrogen bonding with the hydrogen atoms of the methyl group or with α phenyl hydrogen. Figure 2 shows the structures including hydrogen bonding for the most stable species.

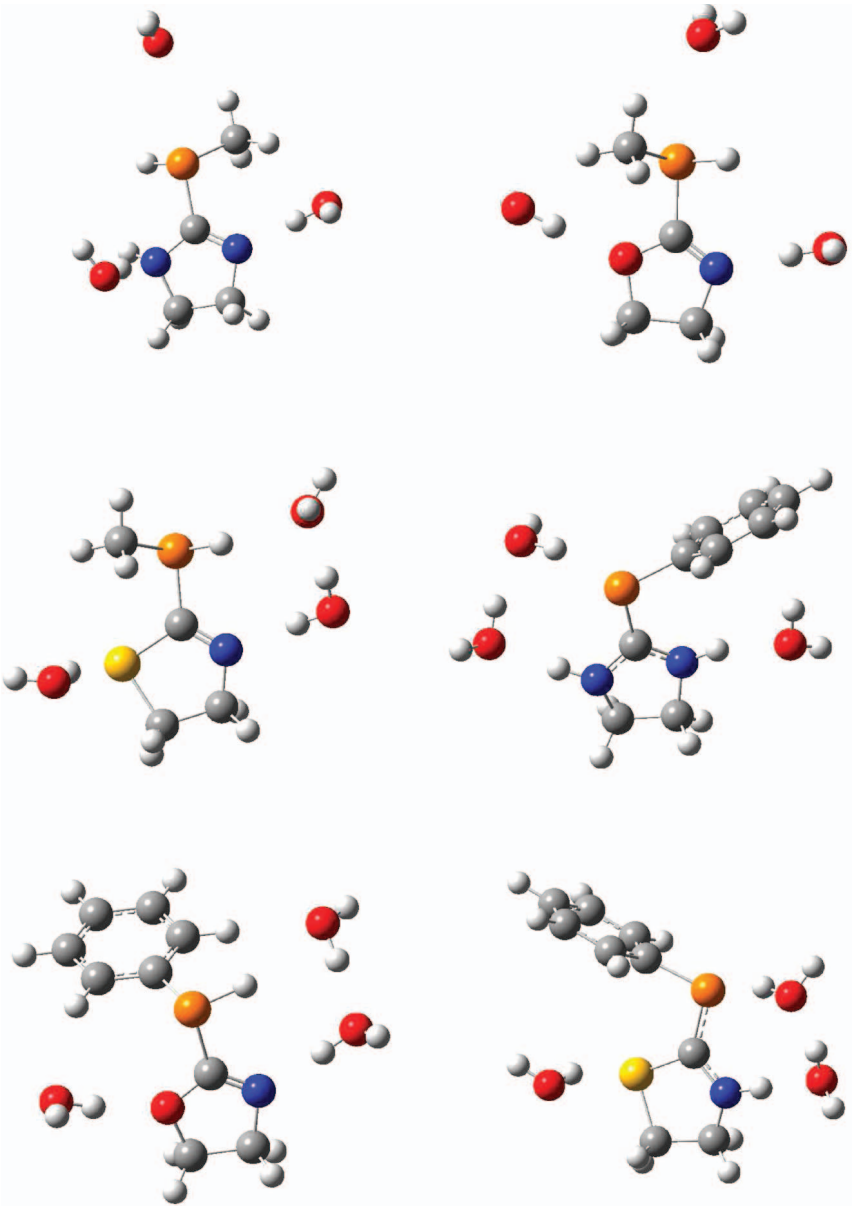

Figure 2. Molecular geometries of the most stable complexes as found in solution with the inclusion of three explicit water molecules.

TABLE 5: Hydrogen Bond (HB) Distances, $R_{H\cdots Y}$ (in Å), As Well As the Electron Density $\rho(\vec{r}_{cp})$ and Its Laplacian $\nabla^2\rho(\vec{r}_{cp})$ at the Hydrogen-Bond Critical Points in Atomic Unit[a]

system	isomer	HB	$R_{H\cdots Y}$	$\rho(\vec{r}_{cp})$	$\nabla^2\rho(\vec{r}_{cp})$	system	isomer	HB	$R_{H\cdots Y}$	$\rho(\vec{r}_{cp})$	$\nabla^2\rho(\vec{r}_{cp})$
Me−NH	A	$N_1\cdots H_w$	2.01	0.028	0.086	Ph−NH	B	$N_1\cdots H_w$	2.03	0.016	0.054
		C_7—H$\cdots O_w$	2.51	0.024	0.023			C_8—H$\cdots O_w$	2.42	0.015	0.031
	E	$N_1\cdots H_w$	2.00	0.019	0.067			$O_w\cdots H_w$	1.79	0.029	0.056
		$P_6\cdots H_w$	2.45	0.019	0.031		E	$P_6\cdots H_w$	2.36	0.056	−0.001
		N_3—H$\cdots O_w$	1.96	0.021	0.081			N_3—H$\cdots O_w$	1.98	0.029	0.066
								N_1—H$\cdots O_w$	1.91	0.026	0.077
								$O_w\cdots H_w$	1.79	0.035	0.101
								$N_3\cdots H_w$	1.79	0.026	0.089
Me−O	B	$O_1\cdots H_w$	1.97	0.021	0.066	Ph−O	B	$O_1\cdots H_w$	1.99	0.021	0.065
		$N_3\cdots H_w$	1.89	0.003	0.009			$N_3\cdots H_w$	1.82	0.024	0.090
		C_7—H$\cdots O_w$	2.52	0.006	0.023			C_8—H$\cdots O_w$	2.37	0.020	0.037
	E	$O_1\cdots H_w$	1.98	0.008	0.023			$O_w\cdots H_w$	1.79	0.032	0.099
		$P_6\cdots H_w$	2.49	0.005	0.012		E	$O_1\cdots H_w$	2.11	0.013	0.055
		N_3—H$\cdots O_w$	1.91	0.017	0.078			$P_6\cdots H_w$	2.44	0.027	0.043
								N_3—H$\cdots O_w$	1.91	0.029	0.083
								$O_w\cdots H_w$	1.89	0.024	0.069
Me−S	B	$S_1\cdots H_w$	2.54	0.006	0.021	Ph−S	A	P_6—H$\cdots O_w$	2.44	0.022	0.023
		P_6—H$\cdots O_w$	2.65	0.002	0.008			$N_3\cdots H_w$	1.92	0.029	0.019
		$N_3\cdots H_w$	1.98	0.039	0.093			C_8—H$\cdots O_w$	2.49	0.015	0.019
		$O_w\cdots H_w$	1.92	0.033	0.096			$O_w\cdots H_w$	1.87	0.004	0.014
	E	$S_1\cdots H_w$	2.69	0.007	0.029		Z	$S_1\cdots H_w$	2.56	0.019	0.028
		$P_6\cdots H_w$	2.42	0.003	0.023			N_3—H$\cdots O_w$	1.87	0.029	0.085
		N_3—H$\cdots O_w$	1.95	0.021	0.072			$O_w\cdots H_w$	1.79	0.029	0.096
		$O_w\cdots H_w$	1.85	0.003	0.006						

[a] The subscript "w" marks atoms from the water molecules, whereas the other atoms are numbered according to Figure 1.

The hydrogen acceptor and donor distances are listed for the most stable complexes in Table 5. Our calculations gave that not all hydrogen bonds contribute to the stability of the compounds, and that, instead, in some cases hydrogen bonding between the explicit water molecules was formed. It was, on the other hand, important that the number of explicit water molecules is sufficiently large so that they can surround the hydrophilic regions of the compound.

3. Analysis of Intermolecular Hydrogen Bond Using AIM Theory. One geometrical parameter that can be used in characterizing hydrogen bonds is the distance between the proton and the acceptor atom, which should be shorter than the sum of their van der Waals radii.[46] Alternatively, one may used parameters based on Bader's AIM theory, according to which properties of the electron density, that is, $\rho(\vec{r}_{cp})$ and $\nabla^2\rho(\vec{r}_{cp})$, at the bond critical point $\vec{r}_{cp}$ are relevant. It has been found that $\rho(\vec{r}_{cp})$ and $\nabla^2\rho(\vec{r}_{cp})$ should lie in the ranges 0.002−0.035 au and 0.024−0.139 au, respectively, for a hydrogen bond.[42]

In Table 5 we present our results for the analysis of the intermolecular hydrogen bonds for our most stable complexes. It is seen that the values of $\rho(\vec{r}_{cp})$ are within the above range, but for the case of the Laplacian $\nabla^2\rho(\vec{r}_{cp})$ some values are smaller than what is usually found, suggesting that these interactions at most can be characterized as weak hydrogen bonds.

4. Free Energies of Solvation. The free energies of solvation predicted from the PCM-SCRF calculations (i.e., $\Delta E_{sol,1}$ and $\Delta E_{sol,2}$, respectively) are listed in Table 1.

The solvation of the phosphino tautomer of the methyl substitution is generally less favored according to the discrete/SCRF model, whereas for the phenyl substitution the phosphino tautomers of the sulfur species show a lower solubility when explicit water molecules are included. The A conformer of Ph−O is unsolvable according to the calculations with three explicit water molecules. The results of such calculations are strongly affected by the number of the explicit water molecules around the solute[51,52] that can form strong hydrogen bonding. It is easy to recognize from our model that not all intermolecular hydrogen bonding in our discrete/SCRF calculations contribute to the stability of the complexes except for the phoshinidene tautomer of Ph−NH. This might be attributed to the problems related to the construction of the cavity that is not the most appropriate approach when studying aggregation in solution.[53] From extra calculations with just one explicit water molecule placed at various positions near to the solute, we found that not all the hydrogen bonds are stable.

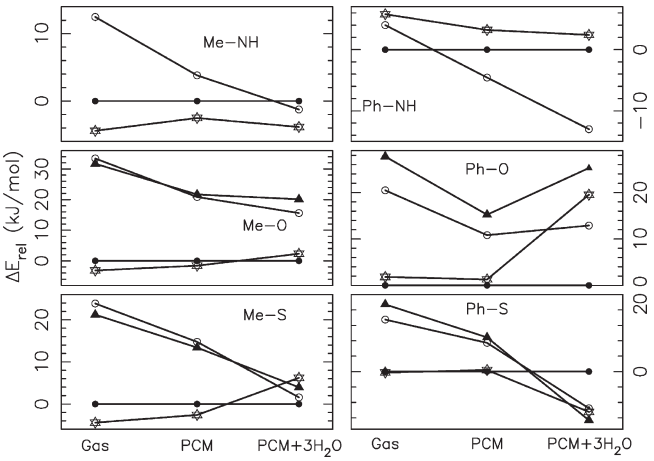

Figure 3. The relative energies for the various systems as found in gas phase, using the PCM model, and with the PCM model plus 3 explicit water molecules. The energies are given relative to the B isomer (dark circles). Stars, white circles, and dark triangles mark the A, E, and Z isomers, respectively.

IV. Conclusions

In this study we used the B3LYP/6-31+G(d,p) approach to calculate the properties of a set of related molecules both in gas phase and in aqueous solution. Special emphasis was put on relative energies and solvation energies. The calculated tautomers showed a large preference for the phosphino tautomer in gas phase relative to phosphinidene one. In studying the effects of the solvent we studied two different approaches, that is, the PCM-SCRF and the discrete/SCRF method.

Our main findings concerning the energetics are summarized in Figure 3. We see that the order of stability of the isomers changes when comparing the gas phase with the aqueous phase. Moreover, there are clear differences between the results of the

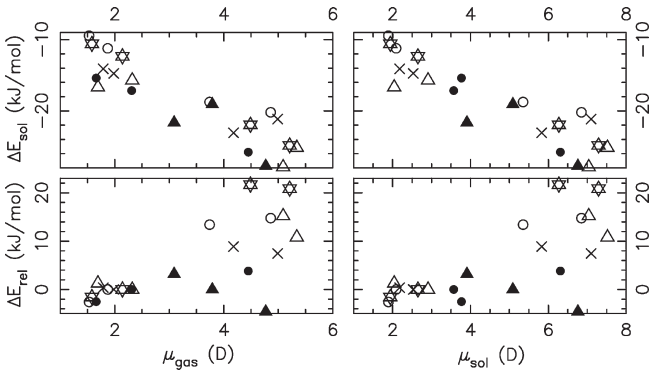

Figure 4. The relative energies (lower panels; given relative to those of the B isomers) and solvation energies from the PCM calculations (upper panels) as function of the dipole moment in the gas phase (left panels) and the dipole moment in the PCM calculations (right panels) for the various systems. White circles, stars, crosses, dark circles, white triangles, and dark triangles mark Me−S, Me−O, Ph−S, Me−NH, Ph−O, and Ph−NH, respectively.

pure PCM calculations and those of the calculations that include three explicit water molecules except for Ph−NH, where the order of stability in solution is unchanged independent of the model adopted. From additional calculations with three water molecules in the gas phase, we found that the problem related to the construction of the cavity is the reason behind the unstability of the hydrogen bonds, implying that the pure PCM approach is too inaccurate for the present type of systems. The figure also indicates that the phosphino isomers respond differently from the phosphinidene isomers.

Some of our results could be correlated to the dipole moment. We demonstrate this further in Figure 4, where we show the relative energies and the solvation energies from the PCM calculations as functions of the dipole moment in the gas phase and in the PCM approach. The relative free energies have no common energy scale when comparing the different systems, but even when just looking at one of the isomers there is hardly a correlation between this quantity and any of the dipole moments. This is different when looking at the energy of solvation. Here, we clearly see a correlation between dipole moment and stability of the system in solution, irrespectively of whether we use the gas phase or the PCM value for the dipole moment. When studying the molecular geometries we found only smaller differences between gas phase and aqueous phase. These could also be used in clearly identifying hydrogen bonding between the solute and explicit water molecules around the hydrophilic region of the solute. From the analysis of the properties of the electron density at hydrogen bond critical point we found that some intermolecular hydrogen bonds at most are weak hydrogen bonds.

Finally, the calculations of the free energies of solvation indicate that the selected hydrophilic regions are not the preferred solvation sides.

Acknowledgment. The authors thank Deutscher Akademischer Austauschdienst (DAAD) for the financial support of this work.

Supporting Information Available: The optimized geometric parameters (bond length, angle, and dihedral angle), atomic coordinate (*XYZ*), and Milliken net charges of the atoms for both gas phase and PCM calculations as obtained from B3LYP/6-31+G(d,p) method are available free of charge via the Internet at http://pubs.acs.org.

References and Notes

(1) Katritzky, A. R.; Lagowski, J. M. *Advances in Heterocyclic Chemistry*; Academic Press: New York, 1963; Vol II, pp 1−81.
(2) Karelson, M. M.; Katritzky, A. R.; Szafran, M.; Zerner, M. C. *J. Chem. Soc., Perkin Trans.* **1990**, *2 1990*, 195–201.
(3) Rzepa, H. S.; Yi, M. Y.; Karelson, M. M.; Zerner, M. C. *J. Chem. Soc., Perkin Trans.* **1991**, *2 1991*, 635–637.
(4) Schlegel, H. B.; Gund, P.; Fluder, E. M. *J. Am. Chem. Soc.* **1982**, *104*, 5347–5351.
(5) Scanlan, M. J.; Hillier, I. H.; MacDowell, A. A. *J. Am. Chem. Soc.* **1983**, *105*, 3568–3571.
(6) Woodcock, S.; Green, D. V. S.; Vincent, M. A.; Hillier, I. H.; Guest, M. F.; Sherwood, P. *J. Chem. Soc., Perkin Trans.* **1992**, *2 1992*, 2151–2154.
(7) Luque, F. J.; López-Bes, J. M.; Cemeli, J.; Aroztegui, M.; Orozco, M. *Theor. Chem. Acc.* **1997**, *96*, 105–113.
(8) Nagy, P. I.; Tejada, F. R.; Messer, W. S. *J. Phys. Chem. B* **2005**, *109*, 22588–22602.
(9) de Vries, A. H.; van Duijnen, P. *Biophys. Chem* **1992**, *43*, 139–147.
(10) Raczynska, E. D.; Taft, R. W.; Polish, J. *Chem.* **1998**, *72*, 1054–1067.
(11) Caminiti, R.; Pieretti, A.; Bencivenni, L.; Ramondo, F.; Sanna, N. *J. Phys. Chem.* **1996**, *100*, 10928–10935.
(12) Remko, M.; Walsh, O. A.; Richards, W. G. *Chem. Phys. Lett.* **2001**, *336*, 156–162.
(13) Remko, M.; Walsh, O. A.; Richards, W. G. *Phys. Chem. Chem. Phys.* **2001**, *3*, 901–907.
(14) Marchand-Geneste, N.; Carpy, A. *J. Mol. Struct. Theochem* **1999**, *465*, 209–217.
(15) Remko, M.; Walsh, O. A.; Richards, W. G. *J. Phys. Chem. A* **2001**, *105*, 6926–6931.
(16) Remko, M.; van Duijnen, Ph. T.; Swart, M. *Struct. Chem.* **2003**, *14*, 271–278.
(17) Fisher, E. B.; Van Wazer, J. R. *Phosphorus and Its Componds: Technology, Biological Functions, and Applications*; Interscience, Inc.: New York, 1961; Vol II, pp 1897−1929.
(18) Bücher, J. W.; Schiebs, R.; Winter, G.; Büchel, K. H. In *Industrial Organic Chemistry*; VCH: New York, 1989.
(19) Cramer, F. *Angew. Chem.* **1960**, *72*, 236–249.
(20) Kolodiazhnyi, O. I.; Prynada, N. *Tetrahedron Lett.* **2000**, *41*, 7997–8000.
(21) Springborg, M. In *Specialist Periodical Reports: Chemical Modelling, Applications and Theory*; Hinchliffe, A. Ed.; Royal Society of Chemistry: Cambridge, UK, 2008;Vol 5.
(22) Tomasi, J.; Mennucci, B.; Cammi, R. *Chem. Rev.* **2005**, *105*, 2999–3094.
(23) Huron, M. J.; Claverie, P. *J. Phys. Chem.* **1972**, *76*, 2123–2133.
(24) Huron, M. J.; Claverie, P. *J. Phys. Chem.* **1974**, *78*, 1853–1861.
(25) Huron, M. J.; Claverie, P. *J. Phys. Chem.* **1974**, *78*, 1862–1867.
(26) Schnuelle, G. W.; Beveridge, D. L. *J. Phys. Chem.* **1975**, *79*, 2566–2573.
(27) McCreey, J. H.; Christoffersen, R. E.; Hall, G. G. *J. Am. Chem. Soc.* **1976**, *98*, 7191–7197.
(28) Claverie, P.; Daudey, J. P.; Langlet, J.; Pullman, B.; Plazzola, D.; Huron, M. J. *J. Phys. Chem.* **1978**, *82*, 405–418.
(29) Rzepa, H. S.; Yi, M. Y. *J. Chem. Soc., Perkin Trans.* **2 1991**, *1991*, 531–537.
(30) Frisch, M. J.; Trucks, G. W.; Schlegel, H. B.; Scuseria, G. E.; Robb, M. A.; Cheeseman, J. R.; Montgomery, J. A., Jr.; Vreven, T.; Kudin, K. N.; Burant, J. C.; Millam, J. M.; Iyengar, S. S.; Tomasi, J.; Barone, V.; Mennucci, B.; Cossi, M.; Scalmani, G.; Rega, N.; Petersson, G. A.; Nakatsuji, H.; Hada, M.; Ehara, M.; Toyota, K.; Fukuda, R.; Hasegawa, J.; Ishida, M.; Nakajima, T.; Honda, Y.; Kitao, O.; Nakai, H.; Klene, M.; Li, X.; Knox, J. E.; Hratchian, H. P.; Cross, J. B.; Bakken, V.; Adamo, C.; Jaramillo, J.; Gomperts, R.; Stratmann, R. E.; Yazyev, O.; Austin, A. J.; Cammi, R.; Pomelli,C.; Ochterski, J. W.; Ayala, P. Y.; Morokuma, K.; Voth, G. A.; Salvador, P.; Dannenberg, J. J.; Zakrzewski, V. G.; Dapprich, S.; Daniels, A. D.; Strain, M. C.; Farkas, O.; Malick, D. K.; Rabuck, A. D.; Raghavachari, K.; Foresman, J. B.; Ortiz, J. V.; Cui, Q.; Baboul, A. G.; Clifford, S.; Cioslowski, J.; Stefanov, B. B.; Liu, G.; Liashenko, A.; Piskorz, P.; Komaromi, I.; Martin, R. L.; Fox, D. J.; Keith, T.; Al-Laham, M. A.; Peng, C. Y.; Nanayakkara, A.; Challacombe, M.; Gill, P. M. W.; Johnson, B.; Chen, W.; Wong, M. W.; Gonzalez, C.; Pople, J. A. *Gaussian 03; Revision D.01*; Gaussian, Inc.: Wallingford, CT, 2004.
(31) Becke, A. D. *J. Chem. Phys.* **1993**, *78*, 5648–5652.
(32) Lee, C.; Yang, W.; Parr, R. G. *Phys. Rev. B* **1988**, *37*, 785–789.
(33) Soua, S. F.; Fernandes, P. A.; Ramos, M. J. *J.Phys. Chem A* **2007**, *111*, 10439–10452.
(34) Tomasi, J.; Persico, M. *Chem. Rev.* **1994**, *94*, 2027–2094.
(35) Cances, E.; Mennucci, B.; Tomasi, J. *J. Chem. Phys.* **1997**, *107*, 3032–3041.

(36) Mennucci, B.; Cances, E.; Tomasi, J. *J. Phys. Chem. B* **1997**, *101*, 10506–10517.
(37) Canc, E.; Mennucci, B. *J. Math. Chem.* **1998**, *23*, 309–326.
(38) Miertus, S.; Scrocco, E.; Tomasi, J. *Chem. Phys.* **1981**, *55*, 117–129.
(39) Cammi, R.; Tomasi, J. *J. Comput. Chem.* **1995**, *16*, 1449–1458.
(40) Pascual-Ahuir, J. L.; Silla, E.; Tomasi, J.; Bonaccorsi, R. *J. Comput. Chem.* **1987**, *8*, 778–787.
(41) Bader, R. F. W. *J. Phys. Chem. A* **1998**, *102*, 7314–7323.
(42) Koch, U.; Popelier, P. L. A. *J. Phys. Chem.* **1995**, *99*, 9747–9754.
(43) Biegler-Koenig, F. W.; Bader, R. F. W.; Tang, T.-H. *J. Comput. Chem.* **1982**, *3*, 317–328.
(44) Bader, R. F. W.; Tang, T. H.; Tal, Y.; Biegler-Koenig, F. W. *J. Am. Chem. Soc.* **1982**, *104*, 946–952.
(45) Bader, R. F. W. *AIMPAC, a suite of program for the Theory of Atoms in Molecules*; McMaster University: Hamilton Ontario, Canada.
(46) Bondi, A. *J. Phys. Chem.* **1964**, *68*, 441–451.
(47) Topp, W. C.; Allen, L. C. *J. Am. Chem. Soc.* **1974**, *96*, 5291–5293.
(48) Pogorelyi, V. K. *Russ. Chem. Rev.* **1977**, *46*, 316–337.
(49) Alagona, G.; Ghio, C.; Nagy, P. I. *Int. J. Quantum Chem.* **2004**, *99*, 161–178.
(50) Mulliken, R. S. *J. Chem. Phys.* **1962**, *36*, 3428–3439.
(51) Aleman, C.; Galembeck, S. E. *Chem. Phys.* **1998**, *232*, 151–159.
(52) Aleman, C. *Chem. Phys.* **1999**, *244*, 151–162.
(53) Pitarch, J.; Moliner, V.; Pascual-Ahuir, J.; Silla, E.; Tunñón, I. *J. Phys. Chem.* **1996**, *100*, 9955–9959.

JP9102096

Supporting information for: Theoretical Study of the Effects of Solvation, Substitution, and Structure on the Properties of Imidazolines, Oxazolines, and Thiazolines

Sahar Abdalla* and Michael Springborg†

Physical and Theoretical Chemistry,

University of Saarland, 66123 Saarbrücken, Germany

(Dated: February 12, 2010)

* e-mail: s.abdalla@mx.uni-saarland.de

† e-mail: m.springborg@mx.uni-saarland.de

TABLE I: Selected optimized geometries of the isomer studied in gas phase. For the structures of isomers see Fig. 1; bond lengths are in Å; X=NH, O and S mark the various species; A and B refer to the Phosphino forms whereas E and Z refer the Phosphinidene forms.

			X=NH			X=O			X=S			
	A	B	E	E	A	B	Z	E	A	A	Z	E
Parameter	Me	Ph	Me	Ph	Me	Ph	Me	Ph	Me	Ph	Me	Ph
$\Theta[C_2 - X_1 - C_5]$	106.14	105.92	110.29	110.57	106.11	105.88	109.34	109.27	88.58	88.56	92.27	91.64
$\Theta[X_1 - C_5 - C_4]$	100.53	100.59	100.58	100.59	103.68	103.46	103.56	103.68	104.61	104.54	104.04	103.94
$\Theta[C_2 - N_1 - H]$	117.69	117.39	117.27	117.94								
$\Theta[X_1 - C_2 - C_3]$	116.20	116.49	106.43	106.53	118.53	118.51	108.19	108.49	117.32	117.41	108.79	109.14
$\Theta[C_5 - C_4 - N_3]$	105.65	105.56	100.57	100.56	104.93	104.73	99.09	99.21	110.11	110.05	104.43	104.62
$\Theta[C_2 - N_3 - C_4]$	106.42	106.21	110.75	111.13	106.75	106.44	109.19	110.33	112.79	112.73	114.84	116.74
$\Theta[X_1 - C_2 - P_6]$	119.59	120.15	124.21	123.21	114.87	114.69	125.44	119.55	119.48	119.88	127.44	120.89
$\Theta[C_2 - P_6 - C_7]$	100.43	100.65	99.21	99.47	99.77	100.84	99.68	97.83	100.39	101.69	101.16	99.08
$\Theta[C_2 - P_6 - H]$	95.59	94.37			93.18	93.83			95.49	95.74		
$\Theta[C_2 - N_3 - H]$			118.23	118.62			117.29	118.46			116.03	117.48
$\Phi[C_2 - X_1 - C_5 - C_4]$	20.94	21.23	−28.99	27.74	0.88	8.75	−20.78	21.75	20.44	−20.29	−23.41	27.32
$\Phi[C_5 - C_4 - N_3 - C_2]$	13.66	14.14	−27.21	26.64	0.61	7.16	−30.91	27.36	20.50	−21.38	−41.16	34.93
$\Phi[X_1 - C_2 - N_3 - C_4]$	0.26	−0.06	10.09	−10.28	−0.04	−1.69	19.93	−15.57	−3.62	4.65	23.14	−13.93
$\Phi[X_1 - C_5 - C_4 - N_3]$	−21.02	−21.51	32.06	−30.89	−0.91	−9.67	30.09	−28.41	−26.76	27.10	37.91	−37.45
$\Phi[X_1 - C_2 - P_6 - C_7]$	162.79	−53.93	−179.26	178.04	154.69	−67.78	3.35	177.23	141.35	−124.49	4.23	175.06
$\Phi[X_1 - C_2 - P_6 - H]$	62.66	−153.25			54.42	−166.96			41.13	−25.44		
$\Phi[C_2 - P_6 - C_7 - C_8]$		114.31		−116.56		110.99		109.13		−88.67		−106.06
$\Phi[C_5 - C_4 - N_3 - H]$			−170.33	173.76			−170.23	173.44			176.54	−172.16
$\Phi[N_3 - C_2 - N_1 - H]$	−149.52	−149.14	153.99	−155.59								
$d[P_6 - H...N_3]$	3.56	2.78			3.53	2.76			3.57	3.63		
$d[P_6 - H...X_1]$	3.05	3.69			2.83	3.65			3.06	2.97		
$d[C_{7,8} - H...X_1]$	4.22	4.05	4.32	5.13	4.12	3.86	2.91	4.96	4.40	5.41	3.09	5.28
$d[C_{7,8} - H...N_3]$	2.89	5.29	2.89	4.39	2.99	5.24	4.34	4.23	2.98	3.40	4.35	4.18

The optimized geometries of the most stable isomers in gas phase and in solution as well as the Mulliken gross populations are collected in this part.

TABLE II: Selected optimized geometries of the isomer studied in continuum model. The notation is as in Table I.

			X=NH				X=O				X=S	
	A	B	E	E	A	B	E	E	A	B	Z	E
Parameter	Me	Ph	Me	Ph	Me	Ph	Me	Ph	Me	Ph	Me	Ph
$\Theta[C_2 - X_1 - C_5]$	106.23	106.26	111.07	111.27	106.21	106.24	109.16	109.19	88.71	88.59	92.22	91.61
$\Theta[X_1 - C_5 - C_4]$	100.68	100.51	100.80	100.85	103.57	103.58	103.68	103.70	104.41	104.66	104.09	103.99
$\Theta[C_2 - N_1 - H]$	117.93	118.54	119.98	119.86								
$\Theta[X_1 - C_2 - C_3]$	116.29	116.32	107.05	107.25	118.44	118.54	108.84	109.06	117.19	117.33	109.12	109.35
$\Theta[C_5 - C_4 - N_3]$	105.62	105.49	100.81	100.86	104.97	104.94	99.51	99.53	110.07	110.02	104.75	104.94
$\Theta[C_2 - N_3 - C_4]$	106.29	106.13	110.52	110.84	106.77	106.67	110.93	111.14	112.73	112.77	115.89	117.43
$\Theta[X_1 - C_2 - P_6]$	119.99	120.39	128.97	129.93	114.51	114.96	119.48	118.67	119.12	120.02	126.56	120.45
$\Theta[C_2 - P_6 - C_7]$	100.71	101.63	99.91	100.79	100.56	101.64	99.21	99.25	102.49	102.27	101.43	99.96
$\Theta[C_2 - P_6 - H]$	96.09	94.59			95.32	94.14			95.44	95.14		
$\Theta[C_2 - N_3 - H]$			118.53	119.23			120.86	120.53			117.79	119.02
$\Phi[C_2 - X_1 - C_5 - C_4]$	20.70	21.38	−25.15	24.51	−1.96	1.39	−21.85	−20.83	−20.69	20.54	−23.92	27.3
$\Phi[C_5 - C_4 - N_3 - C_2]$	13.16	14.19	−27.08	25.53	−1.67	1.24	−24.67	−24.15	−21.49	20.56	−37.93	32.06
$\Phi[X_1 - C_2 - N_3 - C_4]$	0.59	−0.06	12.36	−11.19	0.45	−0.38	12.55	12.62	4.39	−3.62	19.49	−11.01
$\Phi[X_1 - C_5 - C_4 - N_3]$	−20.54	−21.53	29.64	−28.30	2.19	−1.59	27.43	25.82	26.22	−26.83	36.44	−35.87
$\Phi[X_1 - C_2 - P_6 - C_7]$	−145.67	−52.90	1.37	0.46	−152.69	−63.15	−178.39	−178.04	−127.30	42.25	4.39	175.29
$\Phi[X_1 - C_2 - P_6 - H]$	−45.41	−152.77			−52.19	−162.83			−27.63	142.21		
$\Phi[C_2 - P_6 - C_7 - C_8]$		114.27		−122.774		109.66		−72.83		73.44		−105.96
$\Phi[C_5 - C_4 - N_3 - H]$			−169.99	171.18			−175.48	−176.78			173.59	−168.62
$\Phi[N_3 - C_2 - N_1 - H]$	−149.68	−151.03	156.62	−159.38								
$d[P_6 - H...N_3]$	3.59	2.79			3.54	2.78			3.63	2.84		
$d[P_6 - H...X_1]$	2.89	3.68			2.81	3.64			2.96	4.03		
$d[C_{7,8} - H...X_1]$	4.46	4.07	2.94	4.45	4.45	3.83	4.32	4.46	4.22	4.18	3.08	5.29
$d[C_{7,8} - H...N_3]$	2.99	5.31	4.35	2.94	3.06	5.24	2.99	3.27	3.88	4.13	3.34	4.20

TABLE III: The Optimzed Atomic Coordinates in Gas Phase

Me-NH(A)	X	Y	Z	Me-O(A)	X	Y	Z	Me-S(A)	X	Y	Z
N1	1.123628	-1.087656	0.235347	O1	1.024909	-1.113742	0.146693	S1	1.196383	-1.201328	0.253610
C2	0.114883	-0.145179	0.007399	C2	0.116317	-0.108611	-0.059564	C2	-0.101209	0.006900	-0.108427
N3	0.495525	1.077047	-0.107319	N3	0.547091	1.084605	-0.189147	N3	0.251900	1.224633	-0.232392
C4	1.967181	1.072655	0.044391	C4	2.017279	1.021885	-0.067260	C4	1.679166	1.432075	0.031818
C5	2.396025	-0.411524	-0.081811	C5	2.336437	-0.479551	0.146027	C5	2.446771	0.098504	-0.117371
P6	-1.639475	-0.708671	-0.171397	P6	-1.629730	-0.670874	-0.265459	P6	-1.827228	-0.577025	-0.416912
C7	-2.538269	0.897309	0.098195	C7	-2.524150	0.867867	0.284588	C7	-2.794740	0.759601	0.451847
Me-NH(E)	X	Y	Z	Me-O(Z)	X	Y	Z	Me-S(Z)	X	Y	Z
N1	0.507448	1.017448	0.089658	O1	0.436702	1.017068	0.001367	S1	-0.513161	-1.247320	0.034347
C2	-0.001176	-0.262422	-0.036902	C2	0.006951	-0.274847	-0.069469	C2	0.149803	0.403267	-0.067197
N3	1.093304	-1.111606	-0.142575	N3	1.117885	-1.093792	-0.203114	N3	-0.899387	1.297903	-0.207893
C4	2.322066	-0.404260	0.224415	C4	2.305193	-0.370706	0.248632	C4	-2.188310	0.813303	0.279027
C5	1.949983	1.031387	-0.172286	C5	1.879448	1.050416	-0.124760	C5	-2.244777	-0.643792	-0.178424
P6	-1.655708	-0.793754	-0.056874	P6	-1.637781	-0.786067	-0.003348	P6	1.805927	0.871675	-0.008590
C7	-2.512206	0.879600	0.101628	C7	-2.487324	0.890175	0.069542	C7	2.655133	-0.802152	0.048273

TABLE IV: The Optimzed Atomic Coordinates in Gas Phase

Ph-NH(B)	X	Y	Z	Ph-O(B)	X	Y	Z	Ph-S(A)	X	Y	Z
N1	-1.642777	-0.611233	-0.959029	O1	-1.742194	-0.408772	-1.055716	S1	2.707740	-0.944482	-0.473629
C2	-1.657638	0.401961	0.002739	C2	-1.656899	0.395804	0.049352	C2	1.351202	-0.077697	0.352327
N3	-2.712994	0.484323	0.732722	N3	-2.540815	0.273389	0.961652	N3	1.403575	1.192828	0.387949
C4	-3.616553	-0.593878	0.275323	C4	-3.487669	-0.758972	0.490936	C4	2.538773	1.733882	-0.364164
C5	-2.740127	-1.528475	-0.597359	C5	-2.845143	-1.323312	-0.798475	C5	3.628526	0.649447	-0.532651
P6	-0.319562	1.681852	0.026269	P6	-0.310631	1.663253	-0.019567	P6	0.023999	-1.046712	1.214645
C7	1.188467	0.600519	0.089708	C7	1.190354	0.581492	0.057838	C7	-1.500472	-0.406962	0.392903
Ph-NH(E)	X	Y	Z	Ph-O(E)	X	Y	Z	Ph-S(E)	X	Y	Z
N1	-1.431897	-0.930159	0.234973	O1	-2.866937	0.694487	-0.081443	S1	3.018408	-0.729037	0.009344
C2	-1.555881	0.407448	-0.057120	C2	-1.540407	0.381616	-0.088037	C2	1.274450	-0.355082	-0.068944
N3	-2.911850	0.688313	-0.049598	N3	-1.411594	-0.972596	0.095938	N3	1.098326	0.995617	0.069970
C4	-3.693732	-0.550032	-0.029220	C4	-2.662925	-1.538410	0.593594	C4	2.244562	1.762069	0.548967
C5	-2.708553	-1.494530	0.677009	C5	-3.643787	-0.522240	0.001693	C5	3.459129	1.060239	-0.058363
P6	-0.330922	1.611697	-0.375766	P6	-0.367130	1.637156	-0.313373	P6	0.104298	-1.611718	-0.295326
C7	1.191411	0.563662	-0.163087	C7	1.164685	0.588954	-0.132408	C7	-1.451113	-0.597768	-0.125821

TABLE V: Optimized Atomic Coordinates in the Polarized Continuum Model

Me-NH(A)	X	Y	Z	Me-O(A)	X	Y	Z	Me-S(A)	X	Y	Z
N1	-1.075241	-1.118611	0.043100	O1	-1.015375	-1.108296	0.159905	S1	-1.176058	-1.201887	0.263806
C2	-0.114362	-0.123422	-0.126910	C2	-0.118063	-0.098588	-0.065379	C2	0.099808	0.020956	-0.125432
N3	-0.556473	1.079748	-0.265642	N3	-0.562597	1.089214	-0.206363	N3	-0.276121	1.231784	-0.256629
C4	-2.033804	0.992570	-0.177980	C4	-2.033633	1.014451	-0.062288	C4	-1.704605	1.418753	0.031766
C5	-2.336081	-0.423366	0.370629	C5	-2.338583	-0.487928	0.150043	C5	-2.453264	0.074532	-0.101368
P6	1.659327	-0.584025	-0.378653	P6	1.628668	-0.659196	-0.277158	P6	1.830170	-0.545034	-0.444600
C7	2.509864	0.820502	0.500678	C7	2.545034	0.853834	0.301406	C7	2.802323	0.735800	0.497575
Me-NH(E)	X	Y	Z	Me-O(E)	X	Y	Z	Me-S(Z)	X	Y	Z
N1	0.510277	1.013025	0.081819	O1	1.024969	-1.139344	-0.077436	S1	-0.506633	-1.240601	0.057489
C2	0.011066	-0.259022	-0.035576	C2	0.008745	-0.236003	0.001011	C2	0.141479	0.414133	-0.049303
N3	1.091749	-1.109723	-0.136475	N3	0.539342	1.014397	0.124140	N3	-0.901109	1.298304	-0.171239
C4	2.334014	-0.407064	0.208774	C4	1.975933	1.004116	-0.164828	C4	-2.211650	0.802859	0.249771
C5	1.960030	1.035747	-0.157907	C5	2.288033	-0.458349	0.157258	C5	-2.239556	-0.655803	-0.202661
P6	-1.660682	-0.791166	-0.051195	P6	-1.636850	-0.794027	-0.041559	P6	1.812536	0.873140	-0.009978
C7	-2.532501	0.873636	0.092700	C7	-2.520951	0.867041	0.047685	C7	2.658409	-0.803871	0.025936

TABLE VI: Optimized Atomic Coordinates in the Polarized Continuum Model

Ph-NH(B)	X	Y	Z	Ph-O(B)	X	Y	Z	Ph-S(B)	X	Y	Z
N1	-1.657312	-0.627658	-0.935809	O1	-1.696941	-0.604385	-0.928142	S1	1.422215	-1.228702	-0.374834
C2	-1.664920	0.395377	0.005478	C2	-1.662086	0.388324	0.008702	C2	1.479506	0.552270	-0.068557
N3	-2.732575	0.506175	0.721467	N3	-2.599363	0.443134	0.875080	N3	2.555929	1.027459	0.421422
C4	-3.648738	-0.566897	0.263929	C4	-3.522976	-0.673855	0.572760	C4	3.547961	-0.011803	0.729654
C5	-2.773901	-1.525303	-0.579849	C5	-2.889605	-1.398440	-0.638234	C5	3.238973	-1.292969	-0.075008
P6	-0.311212	1.660844	0.025544	P6	-0.307784	1.630054	-0.218862	P6	0.075019	1.634359	-0.617897
C7	1.199406	0.590847	0.085533	C7	1.200390	0.579068	-0.013298	C7	-1.402106	0.627266	-0.151611
Ph-NH(E)	X	Y	Z	Ph-O(E)	X	Y	Z	Ph-S(E)	X	Y	Z
N1	-1.476587	-0.917112	0.279869	O1	2.864879	0.724327	-0.110386	S1	3.017510	-0.750576	0.002836
C2	-1.576185	0.401758	-0.058306	C2	1.553763	0.368397	-0.082904	C2	1.282119	-0.340628	-0.066850
N3	-2.913549	0.713556	-0.092510	N3	1.460528	-0.960099	0.181765	N3	1.127391	0.996939	0.110676
C4	-3.735262	-0.501535	-0.024429	C4	2.743252	-1.498999	0.638336	C4	2.296059	1.760020	0.552455
C5	-2.775795	-1.459567	0.698162	C5	3.687813	-0.470614	0.011448	C5	3.496144	1.032430	-0.054661
P6	-0.310042	1.584872	-0.387134	P6	0.346989	1.594710	-0.375884	P6	0.092270	-1.587120	-0.314547
C7	1.209271	0.540022	-0.161572	C7	-1.186688	0.564079	-0.153883	C7	-1.465593	-0.584359	-0.130362

TABLE VII: Mulliken net charges of the atoms in gas phase and in aqueous phase.

System	Medium	Isomer	X	C_2	C_4	C_5	P_6	N_3	C_7
Me-NH	Gas Phase	E	-0.307	-0.279	-0.176	-0.147	0.082	-0.330	-0.653
		A	-0.346	-0.089	-0.172	-0.241	0.367	-0.250	-0.663
	PCM-SCRF	E	-0.292	-0.273	-0.179	-0.143	0.206	-0.327	-0.681
		A	-0.379	-0.003	-0.162	-0.264	0.325	-0.327	-0.646
Me-O	Gas Phase	Z	-0.294	-0.197	-0.163	-0.048	0.222	-0.299	-0.652
		A	-0.319	0.017	-0.212	-0.084	0.368	-0.244	-0.655
	PCM-SCRF	Z	-0.299	-0.184	-0.179	-0.044	0.118	-0.307	-0.629
		A	-0.339	0.026	-0.207	-0.085	0.349	-0.285	-0.653
Me-S	Gas Phase	Z	0.283	-0.619	-0.122	-0.477	0.272	-0.165	-0.688
		A	0.151	-0.332	-0.226	-0.453	0.400	-0.102	-0.645
	PCM-SCRF	Z	0.266	-0.622	-0.132	-0.468	0.187	-0.175	-0.664
		A	0.122	-0.329	-0.214	-0.444	0.377	-0.138	-0.645
Ph-NH	Gas Phase	E	-0.255	-0.430	-0.173	-0.166	0.314	-0.255	-0.580
		B	-0.231	-0.352	-0.228	-0.177	0.485	-0.192	-0.415
	PCM-SCRF	E	-0.271	-0.371	-0.172	-0.179	0.186	-0.265	-0.749
		B	-0.252	-0.302	-0.229	-0.168	0.446	-0.285	-0.390
Ph-O	Gas Phase	E	-0.271	-0.296	-0.197	-0.033	0.369	-0.250	-0.472
		B	-0.249	-0.287	-0.289	-0.006	0.502	-0.151	-0.305
	PCM-SCRF	E	-0.292	-0.262	-0.206	-0.035	0.246	-0.255	-0.593
		B	-0.269	-0.227	-0.274	-0.026	0.475	-0.226	-0.291
Ph-S	Gas Phase	E	0.211	-0.609	-0.196	-0.440	0.288	-0.079	-0.267
		A	0.172	-0.527	-0.239	-0.469	0.552	-0.045	-0.158
	PCM-SCRF	E	0.156	-0.579	-0.195	-0.428	0.185	-0.081	-0.345
		A	0.115	-0.529	-0.211	-0.452	0.502	-0.057	-0.143

Journal of Molecular Structure: THEOCHEM 962 (2010) 101–107

Contents lists available at ScienceDirect

Journal of Molecular Structure: THEOCHEM

journal homepage: www.elsevier.com/locate/theochem

Theoretical study of tautomerization and isomerization of methylamino- and phenylamino-substituted cyclic azaphospholines, oxaphospholines and thiaphospholines in gas and aqueous phases

Sahar Abdalla *, Michael Springborg

Physical and Theoretical Chemistry, University of Saarland, 66123 Saarbrücken, Germany

ARTICLE INFO

Article history:
Received 28 June 2010
Received in revised form 21 September 2010
Accepted 22 September 2010
Available online 29 September 2010

Keywords:
Solvation
Stability
Tautomerization
Isomerization

ABSTRACT

Results of B3LYP/6-31+G(d,p) calculations are reported. Special emphasis is put on the effect of the environment on relative stability and structures of different isomers and tautomers of methylamino- and phenylamino-substituted cyclic azaphospholine, oxaphospholine and thiaphospholine in gas and aqueous phases. In the gas phase, the imino forms are found to be the most stable species for the cyclic azaphospholines and thiaphospholines, whereas for oxaphospholines, the amino species are predicted to be more stable. The calculations in the aqueous media were done by considering two different models, i.e., the PCM–SCRF and the Microsolvated/SCRF model. It is found that solvation shifts the stability towards the amino forms, except for the phenyl-substituted cyclic azaphospholine and thiaphospholine, for which the imino forms are more stable in solution. The molecular geometries change only little when going from the gas phase to the aqueous phase. The stability in gas phase and in PCM–SCRF is attributed to the presence of intramolecular hydrogen bonding. In the Microsolvated/SCRF model, the presence of intermolecular hydrogen bonds affects the relative stability of tautomers and isomers.

1. Introduction

Tautomeric equilibrium in heterocyclic systems has for a long time been of significant interest and importance [1], and it has accordingly been studied also theoretically using very many different theoretical methods ranging from semiempirical molecular orbital methods [2,3] to more sophisticated calculations that may include electron correlation [4,5]. As one important class of compounds, the effect of solvation on the tautomeric equilibrium of five-membered ring heterocyclic systems has been subject of many studies [2,6–8]. Through studies of the tautomerism in different environment it has been found that the environment is important for the relative stability of various tautomers.

During the last two decades, results of several studies on compounds containing the amidine group, –NH–C(R)=N–, have been reported [9–16]. As a natural extension of those we have recently started a theoretical study of the isoelectronic systems containing the –PH–C(R)=N– group obtained by replacing a single nitrogen atom by a phosphorous atom [17]. The present study is a continuation of this work.

Organophosphorus compounds have been found to be important in many different fields. This includes, for examples, as lubricants, oil additives, water treatment cleaners, flame retarding agents, fertilizers, plasticizers and pesticides [18,19]. Phosphorus and organophosphorus compounds have also been recognized to have important biological functions. For instance, they are essential constituents of the protoplasm [20].

The possibility of placing a proton either at the nitrogen or at the phosphorus atom, an issue that has direct relevance to this work, has earlier been investigated by Kolodiazhnyi et al. [21] for some other, related compounds. They concluded that the tautomeric equilibrium depends on the nature of the solvent and on the substituents at the nitrogen and phosphorous atoms. The tautomerization process in gas phase depends on the proton affinities of the proton donor and acceptor as well as the distances between those. In aqueous solution the process may be influenced by the presence of water molecules, which may provide additional proton acceptors and donors. In the present study we shall, however, not study proton transfer mechanisms, but instead the relative stability between tautomers in gas phase and in solution.

We shall report results of a theoretical investigation of the methylamino- and phenylamino-substituted cyclic azaphospholine, oxaphospholine, and thiaphospholine and their imino tautomers, both in gas phase and in aqueous solution. In particular we shall focus on how the relative stability and the molecular geometries change upon solvation. Earlier, the cyclic moieties, azaphospholine, oxaphospholine, and thiaphospholine, have been the studied by Cyrañski et al. [22] who focused on their aromatic properties.

* Corresponding author. Tel.: +49 6813022913; fax: +49 6813023857.
E-mail addresses: s.abdalla@mx.uni-saarland.de (S. Abdalla), m.springborg@mx.uni-saarland.de (M. Springborg).

0166-1280/$ - see front matter © 2010 Elsevier B.V. All rights reserved.
doi:10.1016/j.theochem.2010.09.024

Over the years many different approaches have been suggested for the study of solvation effects [23,24]. These methods include the self consistent reaction field (SCRF) continuum models. These so called implicit methods treat the effects of the solvent as those of a polarizable continuum with a given dielectric constant and with a cavity that is occupied by the solute. Alternatively, the inclusion of explicit solvent molecules can be important and necessary, in particular when hydrogen bonding between solvent and solute takes place. In that case a quantum-mechanical treatment of some few solvent molecules is useful and, in fact, such combined Microsolvated/SCRF approaches have been used over many years [25–31] . It has been found that they provide accurate estimates of solvation energy even with a modest number of solvent molecules [31].

In the present work we will consider both approaches, i.e., the SCRF approach and the Microsolvated/SCRF approach. Our aim is to explore the changes in the relative total energies and in the structures when the compounds are solvated.

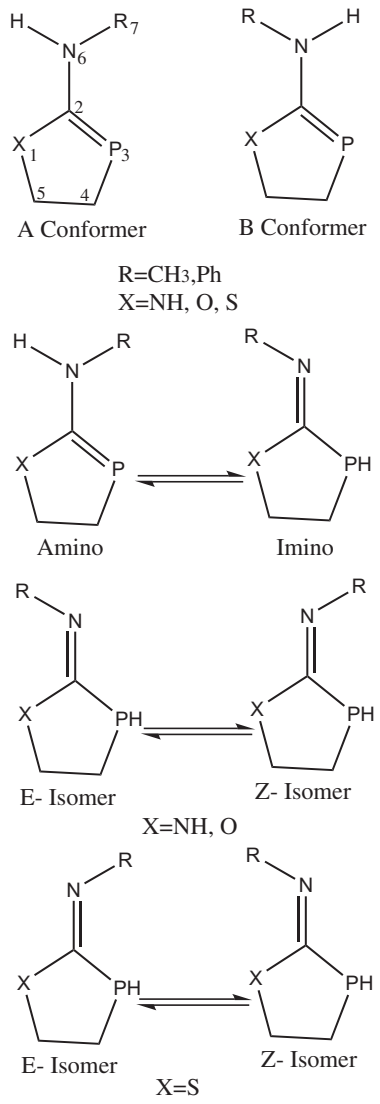

Fig. 1. Structure and atom numbering of the tautomers and isomers of methyl-amino-substituted cyclic azaphospholine, oxaphospholine, and thiaphospholine (Me–NH, Me–O, and Me–S) and phenylamino-substituted cyclic azaphospholine, oxaphospholine, and thiaphospholine (Ph–NH, Ph–O, and Ph–S).

The paper is organized as follows. Section 2 outlines the computational details. In Section 3, we present our results. Finally, the conclusions of the work are presented in Section 4.

2. Computational details

We carried gas phase, SCRF–PCM, and Microsolvated/SCRF calculations for different isomers and tautomers shown in Fig. 1. For the sake of simplicity we shall label the systems as Me–NH, Me–O, Me–S, Ph–NH, Ph–O, and Ph–S, respectively, where Me and Ph gives whether R in the figure is a methyl or a phenyl group, and where NH, O, and S represent X in the figure. In the calculations we used the Becke three parameter Lee–Yang–Parr (B3LYP) functional [32–34] together with the 6-31+G(d,p) basis set. All calculations were performed with the Gaussian 03 program package [35].

For the study of the influence of the solvent we considered two different models, i.e., the PCM–SCRF model whereby the solute is embedded inside a cavity surrounded by a continuum representing the water solvent, and the Microsolvated/SCRF method with which some (i.e., 3) explicit solvent molecules are treated quantum-mechanically. In the latter case, the three water molecules were placed around the hydrophilic regions of the solute as a first solvation shell, whereas the other solvent molecules were treated through the continuum model. The Integral Equation Formalism (IEF) [24,36–39] of the polarized continuum model (PCM) [36,40,41] of the self consistent reaction field (SCRF) was used to treat the continuum in both solvation models. For water we used a dielectric constant of 78.39.

For the construction of the cavity we used the United Atom Topological model (UAO) whereby the cavity is constructed through interlocking spheres centered on the heavy (that is, non-hydrogen) atoms. The radii were obtained by scaling the corre-

Table 1
Energy differences (ΔE, in kJ/mol) as found in the gas phase (marked gas), in the PCM calculations (marked PCM), and in the PCM calculations with the inclusion of three explicit water molecules (marked PCM + $3H_2O$) as well as the two solvation energies (at $T = 0$ K). All quantities, except for the solvation energies, are given relative to those of the B isomer and include zero-point energies. Finally, the different isomers are shown in Fig. 1.

System	Isomer	ΔE			$\Delta E_{sol,1}$	$\Delta E_{sol,2}$
		Gas	PCM	PCM + $3H_2O$		
Me–NH	B	0.00	0.00	0.00	−26.12	−9.69
	A	−6.60	−8.07	−16.86	−26.44	−18.51
	E	−9.82	−1.59	−0.18	−18.43	2.96
	Z	−17.10	−5.19	−19.72	−14.10	−9.98
Me–O	B	0.00	0.00	0.00	−16.99	−8.59
	A	−8.47	−7.09	2.09	−15.86	4.12
	E	−3.96	0.48	23.14	−13.62	15.14
	Z	2.63	2.35	20.13	−18.11	6.89
Me–S	B	0.00	0.00	0.00	−15.54	−4.89
	A	−9.31	−8.81	−0.03	−20.09	6.91
	E	−3.77	−1.00	24.05	−13.46	20.27
	Z	−11.42	−7.12	12.87	−12.18	23.29
Ph–NH	B	0.00	0.00	0.00	−24.04	−23.43
	A	0.33	−5.57	−0.29	−30.29	−22.54
	E	−17.55	−8.15	14.47	−15.06	7.13
	Z	−22.27	−19.12	−14.50	−21.15	−16.60
Ph–O	B	0.00	0.00	0.00	−18.59	−12.38
	A	−8.55	−7.44	0.34	−17.63	−5.14
	E	−7.89	0.39	22.52	−10.89	−16.72
	Z	−5.42	−3.12	3.86	−16.83	−3.74
Ph–S	B	0.00	0.00	0.00	−16.67	−1.29
	A	−6.60	−6.99	−7.98	−17.31	−3.14
	E	−9.91	−5.16	15.13	−12.49	22.03
	Z	−13.95	−7.16	−5.53	−10.58	9.53

Table 2
The dipole moment (in Debye) for various structures (cf. Fig. 1) in gas phase and as found in aqueous solution using PCM.

Isomer	Gas phase	PCM	Isomer	Gas phase	PCM
Me–NH			Ph–NH		
B	4.34	6.40	B	3.37	5.41
A	3.65	6.08	A	3.64	5.88
E	4.18	5.56	E	4.23	5.53
Z	2.66	3.59	Z	3.81	5.11
Me–O			Ph–O		
B	2.45	3.69	B	1.43	2.09
A	2.24	3.25	A	2.04	3.06
E	3.38	4.54	E	3.63	4.67
Z	3.29	4.38	Z	3.77	4.94
Me–S			P-h-S		
B	1.80	2.80	B	0.85	1.40
A	1.59	2.46	A	1.42	2.28
E	2.97	4.04	E	3.27	4.47
Z	2.72	3.70	Z	2.97	3.86

sponding van der Waals radius by a factor of 1.20 [36]. In the Microsolvated/SCRF, the calculations have problems and end with error messages due to overlapping spheres that construct the cavity around the solute. To avoid such errors the values of the OFac and RMin parameters for the GEPOL algorithm [42] were changed to 0.8 and 0.5 from 0.89 and 0.2, respectively. Exploratory calculations for a single solvated water molecule gave an unchanged solvation energy within 1 μhartree.

In the PCM–SCRF calculations, the energy of solvation $\Delta E_{sol,1}$ was calculated as the difference between the energy of the molecule in the continuum and the energy of the molecule in gas phase,

$$\Delta E_{sol,1} = E_{solute,PCM} - E_{solute,g}. \quad (1)$$

On the other hand, in the Microsolvated/SCRF calculations, the energy of solvation $\Delta E_{sol,2}$ was defined as

$$\Delta E_{sol,2} = E_{complex,PCM} - E_{solute,g} - E_{(H_2O)_3,PCM} \quad (2)$$

where $E_{(H_2O)_3,PCM}$ represents the energy of three water molecules calculated in PCM and oriented as found for the complex of interest.

3. Results and discussion

The aim of the present work is to address the influence of a solvent on the structural and energetic properties of the systems of interest. Thus, in presenting the results we will first discuss those for the gas phase and subsequently those for the aqueous phase.

3.1. Gas phase calculations

Relative energies, ΔE at $T = 0$ K with the inclusion of zero-point energies are listed in Table 1. We have here arbitrarily chosen to set the relative energy of the B isomers equal to 0.

We find that the most stable structures are stabilized by the presence of intramolecular hydrogen bonds, as also is the case for their nitrogen analogous [12,16]. The amino derivatives of the methyl and phenyl substituted cyclic azaphopholine, oxaphospholine, and thiaphospholine, respectively, may exists in two different forms (conformers A and B, cf. Fig. 1). The A forms are more stable over the B forms by around 6.60–9.31 kJ/mol with the exception of Ph–NH for which the B form is more stable than the A form by about 0.33 kJ/mol.

For the methyl substitution, the amino group (N_6–H) is so oriented that hydrogen bonds to the heteroatom (N, O, or S) can be formed. These hydrogen bonds have lengths of 2.48, 2.36, and 2.72 Å, respectively, i.e., significantly smaller than the sum of the van der Waals radii of the atoms [43] (2.75, 2.72, 3.00, and 3.00 Å for H···N, H···O, H···P, and H···S, respectively).

An interesting case is that of Ph–O and Ph–S. Here, two types of hydrogen bonds can be recognized with one type being the N_6–H···X (X = O or S) bond with a length of around 2.24 and 2.59 Å for oxaphospholine and thiaphospholine, respectively. The second type is found between the α hydrogen of the phenyl group and the phosphorus atom in position 3 with the C_8–H···P_3 bond length

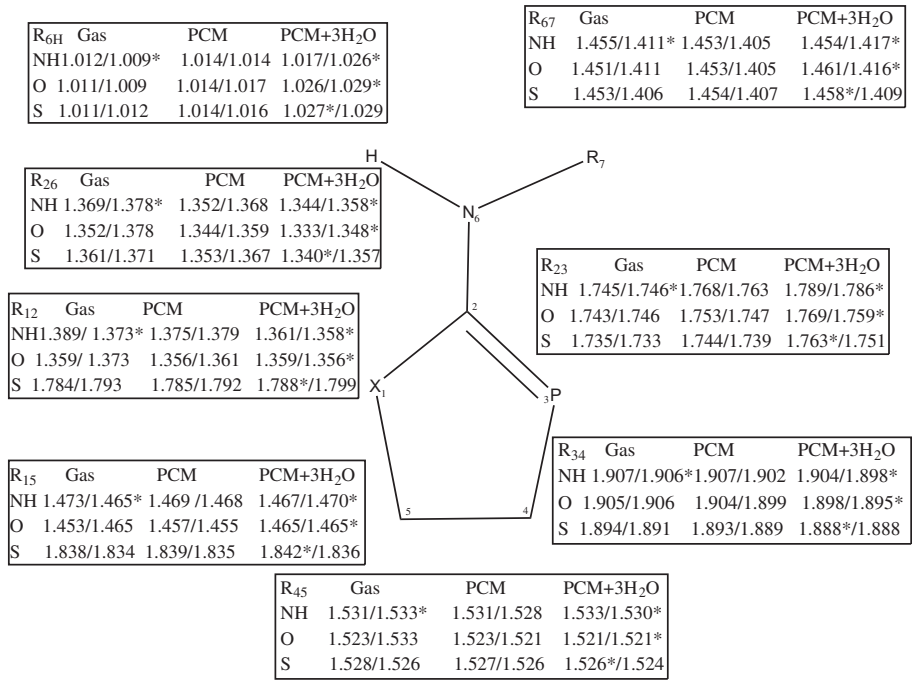

Fig. 2. Optimized amino species as found in the gas phase, the PCM and the PCM + $3H_2O$, R = CH_3 calculations, for R = CH_3, Ph and X = NH, O, and S. The bond lengths are given in Å. The two values for each entry correspond to the A and B isomers. In all cases, except those marked with an asterisk, the B isomer is the more stable one.

being 2.51 and 2.49 Å (X = O or S) for oxaphospholine and thiaphospholine, respectively.

Also the imino forms may exist in two different isomers (E and Z). Here, the Z isomers are the most stable structures for the cyclic azaphopholine and thiaphospholine. For the oxaphospholine compound, the E isomers are the more stable species.

Our finding of a stabilizing effect of the exo-cyclic double bond in the phenylamino-substituted cyclic azaphospholine is in an agreement with the results obtained by Remko et al. in their investigation of amino ↔ imino tautomers for similar species [16].

For the optimized structures in gas phase the ring moieties adopt a nonplanar configuration, which is in an agreement with results of previous calculations on similar systems [16,17]. The molecules have a low C_1 symmetry. Not surprising, upon tautomerization we find the largest changes in the C_2—N_6 and C_2—P_3 bond lengths that vary by about 0.1 Å for different tautomers. The amino substituents (N_6—H) group is so oriented that intramolecular hydrogen bonds are formed, which leads to an additional stabilization.

3.2. Aqueous solution calculations

3.2.1. SCRF calculations

From the relative energies (ΔE at $T = 0$ K with the inclusion of zero-point energies), as obtained with the PCM–SCRF calculations and given in Table 1, we see that the amino tautomers (in the A form) are the most stable species for Me–NH, Me–O, Me–S, and Ph–O, which can be ascribed to the presence of hydrogen bonds N_6—H···X (X = N, O, and S). The lengths of these hydrogen bonds are 2.51, 2.37, and 2.72 Å for the methyl substitution. For the phenyl substitution we identify two types of hydrogen bonds, i.e., N_6—H···X (X = O) with lengths of 2.25 Å, and C_8—H···P_3 with lengths of 2.50 Å. The imino forms (of the Z form) are the most stable isomers for Ph–NH and Ph–S. Here, the stability of the exo-cyclic double bond for the Ph–NH is in an agreement with our earlier results for similar systems [17].

Since the solute–solvent interactions have a strong dependence on the dipole moment of the solute, it is worth to mention that, although the E forms for Me–NH and Ph–NH have the larger dipole

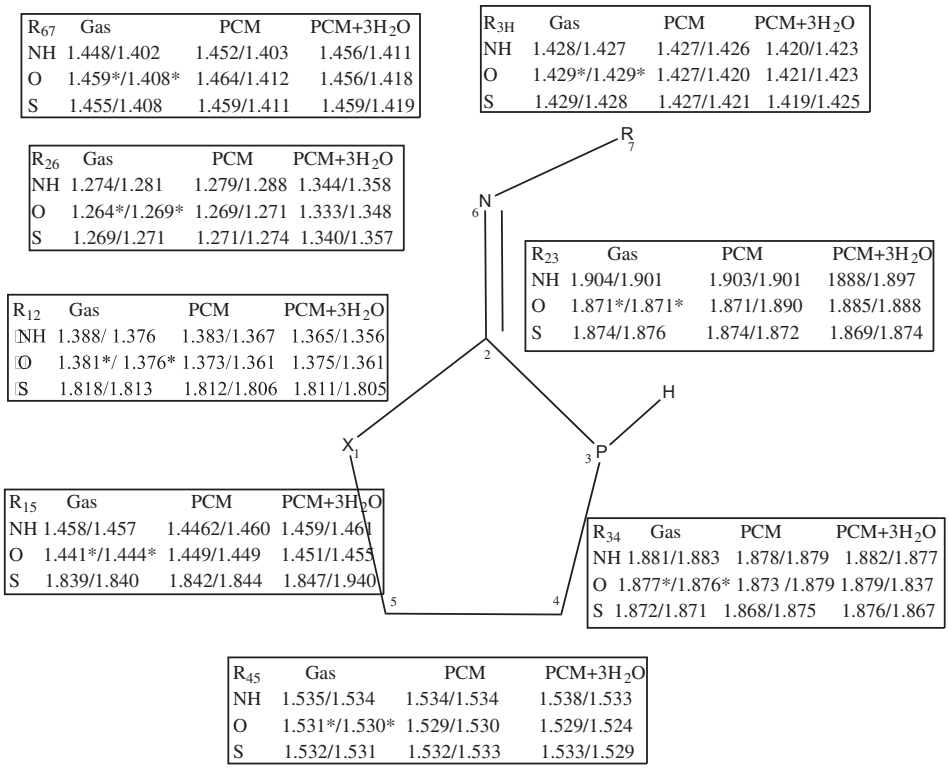

Fig. 3. Optimized imino species as found in the gas phase, the PCM and the PCM + $3H_2O$, R = CH_3 calculations, for R = CH_3, Ph and X = NH, O, and S. The bond lengths are given in Å. The two values for each entry correspond to the E and Z isomers. In all cases, except those marked with an asterisk, the E isomer is the more stable one.

Table 3
Hydrogen bond distances (Å) for the optimized complexes. The subscript *w* marks atoms from the water molecules, whereas the other atoms are numbered according to Fig. 1.

Bond	X = NH				X = O				X = S			
	A Me	B Ph	Z Me	Z Ph	B Me	B Ph	Z Me	Z Ph	B Me	A Ph	Z Me	Z Ph
$X_1 \cdots H_wO_w$					2.00	2.01	1.95	2.18	2.53	2.65	2.55	2.58
N_6—H···O_wH_w	2.04	1.91			1.86	1.85				1.88		
$N_6 \cdots H_wO_w$			1.72	1.77			1.97	1.88	1.86		1.96	1.95
$P_3 \cdots H_wO_w$	2.45	2.36			2.42	2.46			2.44	2.56		
$P_3 \cdots H_wO_w$	2.47											
P_3—H···O_wH_w			2.46	2.57			2.34	2.48			2.71	2.61
N_1—H···O_wH_w	2.14	2.01	1.96	1.93								
C_8—H···O_wH_w				2.45				2.41				
$O_w \cdots H_wO_w$		1.81	1.75	1.77	1.79	1.79	1.98	1.87	1.79	1.80	1.94	1.86

moment in gas phase, the Z forms are the more stable one in the PCM–SCRF calculations. This is due to the stabilizing effects of the intramolecular hydrogen bond $N_1—H\cdots N_6$ (length 2.52 and 2.53 Å, respectively) for the Z form.

Also for the A conformer for Ph–NH we find a stabilizing effect due to two intramolecular hydrogen bonds, $N_6—H\cdots N_1$ and $C_8—H\cdots P_3$, whose lengths are 2.40 and 2.47 Å, respectively. Similarly, for the A form of Me–O the intramolecular hydrogen bond $N_6—H\cdots O$ with a length of 2.37 Å makes that form stabler than the B form, although the latter has a higher dipole moment in the gas phase.

Since we have based parts of this discussion on the dipole moment, it would be useful to have experimental information on those, which, unfortunately, is not available. However, for some smaller organic molecules PCM calculations predict an increase of the dipole moments by up to 30% in aqueous solution compared to gas phase values [44]. This is also found in the present study, as can be seen in Table 2.

When comparing the geometries from the gas-phase calculations with those from the PCM–SCRF calculations we find only small changes, i.e., changes in the bond lengths by some thousandths of an angstrom and in the bond angles by around 1–2°. An exception is the A and B forms for Ph–NH where the relative stability is interchanged when going from gas phase to PCM, and where the structure of the exo-cyclic part changes significantly as is the case for the dihedral angle $\Phi[X_1—C_2—N_6—C_7]$ which ultimately leads to the formation of two hydrogen bonds, $C_8—H\cdots P_3$ and $N_6—H\cdots N_1$, with lengths of 2.47 and 2.40 Å, respectively.

Important geometric parameters are given in Figs. 2 and 3 for the amino and imino species, respectively. Other geometric parameters for both gas phase and PCM calculations are available in the Supplementary data.

From the Mulliken net atomic charges [45], which is also available, we can obtain a qualitative picture of charge transfer and polarization between different hydrogen bonded fragments. We find that these indeed are affected by the interaction of atoms with the aqueous medium, although no general trend can be identified.

3.2.2. Microsolvated/SCRF calculations

Since hydrogen bonds between solute and solvent may exist and since these are only poorly described by the PCM, we performed additional calculations with explicit consideration of three water

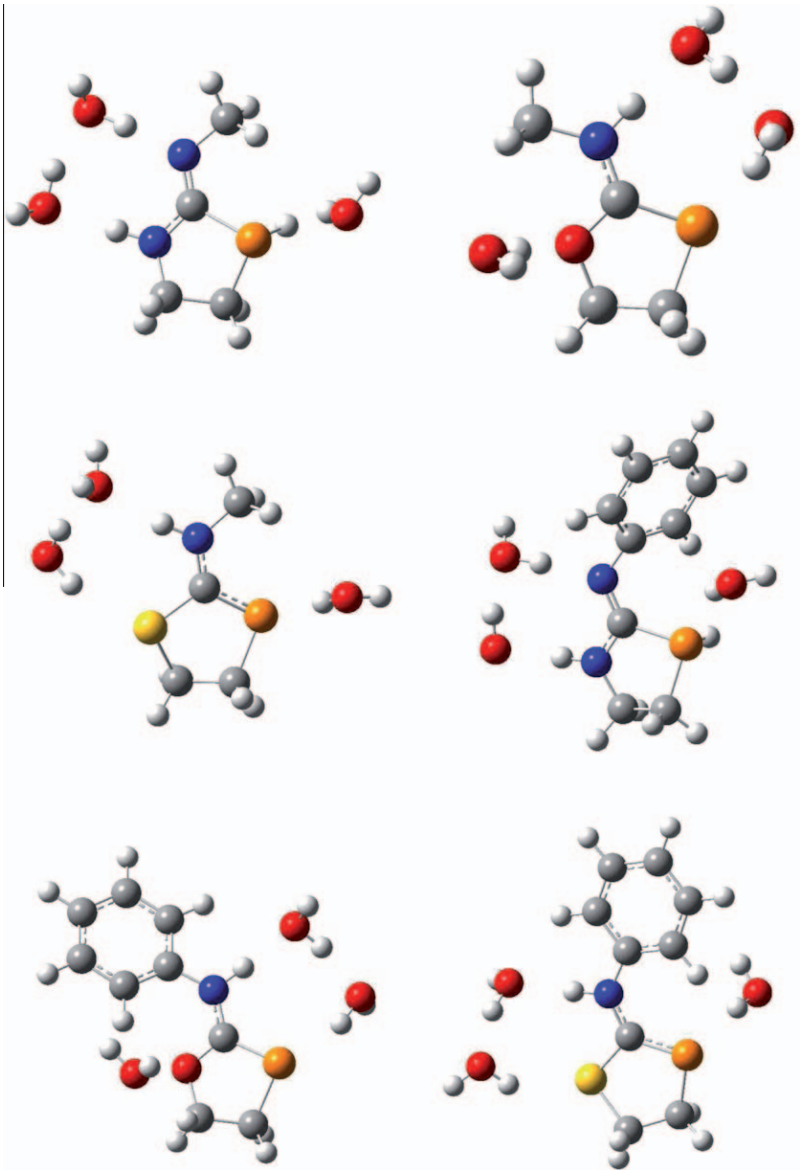

Fig. 4. Molecular geometries of the most stable complexes as found in solution in the calculations that include three explicit water molecules.

molecules. From the relative energies (ΔE at $T = 0$ K with the inclusion of zero-point energies), given in Table 1, we see that the amino tautomers in most cases are the most stable species with the exception of Me–NH and Ph–NH, where the imino forms are more stable than the amino one (of the Z form). For the Ph–NH we could identify an extra stabilizing hydrogen bond between the α hydrogen of the phenyl group and one of the extra water molecules, i.e., the C_8—H$\cdots$O$_w$ bond with a length of 2.45 Å. As also seen in Table 3, the inclusion of explicit water molecules changes the order of stability from that obtained in the gas-phase and in the PCM–SCRF calculations, which indeed is due to hydrogen bonding. This can be seen in Fig. 4 that shows the molecular geometries for the water-containing complexes for the most stable species.

The optimized hydrogen bond distances between water molecules and isomers are presented in Table 3 for the most stable species. In most cases we found hydrogen bonds between two water molecules although all water molecules participate in the first solvation shell. Thus, not all hydrogen bonds contribute to the stability of the compounds.

3.2.3. Free energies of solvation

The free energies of solvation as found in the PCM–SCRF and Microsolvated/SCRF calculations, i.e., $\Delta E_{sol,1}$ and $\Delta E_{sol,2}$, respectively, are listed in Table 1. From $\Delta E_{sol,1} - \Delta E_{sol,2}$ one obtains information on the hydrogen bonds between the explicit water molecules and the solute. Here, however, one has to be cautious since the Discrete/SCRF calculations often predict positive solvation energies, $\Delta E_{sol,2}$. The reason is partly a high energy for the construction of the cavity and partly an unrealistic solvation energy for a single water molecule (our calculations gave a value of 17.83 kJ/mol).

The results show also that the solvation of the imino tautomers of the methyl substituted compounds in general is less favored within the Microsolvated/SCRF model than the case for the amino tautomers. The only exception case is the Z isomer for Me–NH. For the phenyl substitution, the amino tautomers are well solvable. For the Ph–NH, the Z isomer is more solvable in contrast to the E isomer. This is due to bifurcated hydrogen bonds for the Z isomer between the water molecule and the P_3(P_3—H$\cdots$O$_w$H$_w$) from the one side and with the α hydrogen of the phenyl group (C_8—H$\cdots$O$_w$H$_w$) from the other side, as we also found in our earlier study on related systems [17].

Finally, from additional calculations where single water molecules were added one by one to the hydrophilic region we found that not all hydrogen bonds are stable.

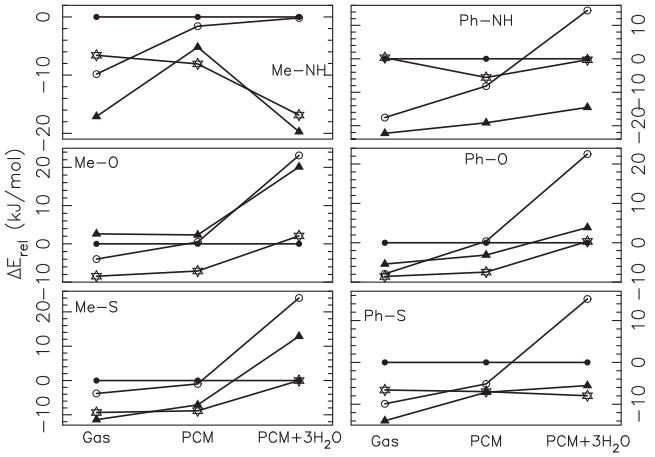

Fig. 5. The relative energies for the various systems as found in gas phase, using the PCM model, and with the PCM model plus three explicit water molecules. The energies are given relative to the B isomers (dark circles). Stars, white circles, and dark triangles mark the A, E, and Z isomers, respectively.

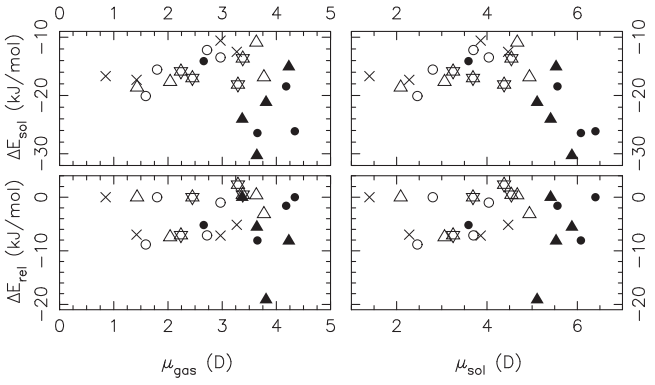

Fig. 6. The relative energies (lower panels; given relative to those of the B isomers) and solvation energies from the PCM calculations (upper panels) as function of the dipole moment in the gas phase (left panels) and the dipole moment in the PCM calculations (right panels) for the various systems. White circles, stars, crosses, dark circles, white triangles, and dark triangles mark Me–S, Me–O, Ph–S, Me–NH, Ph–O, and Ph–NH, respectively.

4. Conclusion

In this work we have studied theoretically the energetic and structural properties of some phosphorous analogues of some nitrogen-containing organic molecules and how these properties change when the molecules are solvated in water. In particular we focused on the relative stability of different isomers and tautomers.

In the first part we presented results for the molecules in gas phase. We found a strong preference for the imino tautomers in gas phase relative to amino ones with the exception of Me–O and Ph–O for which the amino forms were more stable. In the aqueous phase, the amino forms are more soluble species, this time with the exception of Me–S and Ph–NH for which the imine forms are more stable according to the PCM–SCRF calculations. In the Microsolvated/SCRF calculations, the only exception is found for Me–NH and Ph–NH.

The presence of water affects the relative stability and the order of stability of tautomers and isomers. Often intramolecular hydrogen bonds are responsible for the higher stability of isomers in gas phase and with the PCM–SCRF model. All our findings regarding the relative stability are summarized in Fig. 5. Here, we see that the order of stability change when comparing the gas phase with the pure PCM. Furthermore, the order of stability changes when the solvent effects are considered, independent of the model adopted.

From additional calculations with three water molecules in gas phase, we found that the construction of the cavity indeed the reason of the fact that some hydrogen bonds are not stable and have less contributions to the stability of the some complexes. It is worth to mention that the B3LYP approach understimates weak interactions, such as hydrogen bonds, which could, e.g., be improved by using Grimme's dispersion approach, B3LYP-D [46,47] in future studies.

In Fig. 6 we show the solvation energies and the relative energies as function of dipole moment in gas phase and in the PCM–SCRF calculations. In contrast to our earlier results on related systems [17], this figure does not show any correlation between the dipole moment and the stability of the system in solution, irrespectively of whether we use the dipole moment in gas phase or in aqueous phase. Similarly, for the relative energies it was not possible to identify a correlation to the dipole moment.

When looking at the structural properties, only small changes resulted from the solvation. Finally, the calculations of the energies of solvation indicate that not all the selected hydrophilic regions are preferred solvation sites.

Acknowledgement

The authors gratefully acknowledge Deutscher Akademischer Austauschdienst (DAAD) for sponsoring the fellowship for S.A.

Appendix A. Supplementary data

Supplementary data associated with this article can be found, in the online version, at doi:10.1016/j.theochem.2010.09.024.

References

[1] A.R. Katritzky, J.M. Lagowski, Advances in Heterocyclic Chemistry, vol. II, Academic Press, New York, 1963.
[2] M.M. Karelson, A.R. Katritzky, M. Szafran, M.C. Zerner, J. Chem. Soc., Perkin Trans. 2 (1990) (1990) 195.
[3] H.S. Rzepa, M.Y. Yi, M.M. Karelson, M.C. Zerner, J. Chem. Soc., Perkin Trans. 2 (1991) (1991) 635.
[4] H.B. Schlegel, P. Gund, E.M. Fluder, J. Am. Chem. Soc. 104 (1982) 5347.
[5] M.J. Scanlan, I.H. Hillier, A.A. MacDowell, J. Am. Chem. Soc. 105 (1983) 3568.
[6] S. Woodcock, D.V.S. Green, M.A. Vincent, I.H. Hillier, M.F. Guest, P. Sherwood, J. Chem. Soc., Perkin Trans. 2 (1992) (1992) 2151.
[7] F.J. Luque, J.M. López-Bes, J. Cemeli, M. Aroztegui, M. Orozco, Theor. Chem. Acc. 96 (1997) 105.
[8] P.I. Nagy, F.R. Tejada, W.S. Messer Jr., J. Phys. Chem. B 109 (2005) 22588.
[9] A.H. de Vries, van P.Th. Duijnen, Biophys. Chem. 43 (1992) 139.
[10] E.D. Raczynska, R.W. Taft, Polish J. Chem. 72 (1998) 1054.
[11] R. Caminiti, A. Pieretti, L. Bencivenni, F. Ramondo, N. Sanna, J. Phys. Chem. 100 (1996) 10928.
[12] M. Remko, O.A. Walsh, W.G. Richards, Chem. Phys. Lett. 336 (2001) 156.
[13] M. Remko, O.A. Walsh, W.G. Richards, Phys. Chem. Chem. Phys. 3 (2001) 901.
[14] N. Marchand-Geneste, A. Carpy, J. Mol. Struct. (THEOCHEM) 465 (1999) 209.
[15] M. Remko, O.A. Walsh, W.G. Richards, J. Phys. Chem. A 105 (2001) 6926.
[16] M. Remko, P.Th. van Duijnen, M. Swart, Struct. Chem. 14 (2003) 271.
[17] S. Abdalla, M. Springborg, J. Phys. Chem. A 114 (2010) 5823.
[18] E.B. Fisher, J.R. Van Wazer, Phosphorus and its componds, Technology, Biological Functions, and Applications, vol. II, Interscience, New York, 1961. p. 1897.
[19] J.W. Bücher, R. Schiebs, G. Winter, K.H. Büchel, Industrial Organic Chemistry, VCH, New York, 1989.
[20] F. Cramer, Angew. Chem. 72 (1960) 236.
[21] O.I. Kolodiazhnyi, N. Prynada, Tetrahedron Lett. 41 (2000) 7997.
[22] M.K. Cyrañski, T.M. Krygowski, A.R. Katritzky, P. von Ragué Schleyer, J. Org. Chem. 67 (2002) 1333.
[23] M. Springborg, in: A. Hinchliffe (Ed.), Specialist Periodical Reports: Chemical Modelling, Applications and Theory, vol. 5, Royal Society of Chemistry, Cambridge, UK, 2008.
[24] J. Tomasi, B. Mennucci, R. Cammi, Chem. Rev. 105 (2005) 2999.
[25] M.J. Huron, P. Claverie, J. Phys. Chem. 76 (1972) 2123.
[26] M.J. Huron, P. Claverie, J. Phys. Chem. 78 (1974) 1853.
[27] M.J. Huron, P. Claverie, J. Phys. Chem. 78 (1974) 1862.
[28] G.W. Schnuelle, D.L. Beveridge, J. Phys. Chem. 79 (1975) 2566.
[29] J.H. McCreey, R.E. Christoffersen, G.G. Hall, J. Am. Chem. Soc. 98 (1976) 7191.
[30] P. Claverie, J.P. Daudey, J. Langlet, B. Pullman, D. Plazzola, M.J. Huron, J. Phys. Chem. 82 (1978) 405.
[31] H.S. Rzepa, M.Y. Yi, J. Chem. Soc., Perkin Trans. 2 (1991) (1991) 531.
[32] A.D. Becke, J. Chem. Phys. 78 (1993) 5648.
[33] C. Lee, W. Yang, R.G. Parr, Phys. Rev. B 37 (1988) 785.
[34] S.F. Sousa, P.A. Fernandes, M.J. Ramos, J .Phys. Chem. A 111 (2007) 10439.
[35] M.J. Frisch, G.W. Trucks, H.B. Schlegel, G.E. Scuseria, M.A. Robb, J.R. Cheeseman, J.A. Montgomery Jr., T. Vreven, K.N. Kudin, J.C. Burant, J.M. Millam, S.S. Iyengar, J. Tomasi, V. Barone, B. Mennucci, M. Cossi, G. Scalmani, N. Rega, G.A. Petersson, H. Nakatsuji, M. Hada, M. Ehara, K. Toyota, R. Fukuda, J. Hasegawa, M. Ishida, T. Nakajima, Y. Honda, O. Kitao, H. Nakai, M. Klene, X. Li, J.E. Knox, H.P. Hratchian, J.B. Cross, V. Bakken, C. Adamo, J. Jaramillo, R. Gomperts, R.E. Stratmann, O. Yazyev, A.J. Austin, R. Cammi, C. Pomelli, J.W. Ochterski, P.Y. Ayala, K. Morokuma, G.A. Voth, P. Salvador, J.J. Dannenberg, V.G. Zakrzewski, S. Dapprich, A.D. Daniels, M.C. Strain, O. Farkas, D.K. Malick, A.D. Rabuck, K. Raghavachari, J.B. Foresman, J.V. Ortiz, Q. Cui, A.G. Baboul, S. Clifford, J. Cioslowski, B.B. Stefanov, G. Liu, A. Liashenko, P. Piskorz, I. Komaromi, R.L. Martin, D.J. Fox, T. Keith, M.A. Al-Laham, C.Y. Peng, A. Nanayakkara, M. Challacombe, P.M.W. Gill, B. Johnson, W. Chen, M.W. Wong, C. Gonzalez, J.A. Pople, Gaussian 03, Revision D.01, Gaussian Inc., Wallingford, CT, 2004.
[36] J. Tomasi, M. Persico, Chem. Rev. 94 (1994) 2027.
[37] E. Cancès, B. Mennucci, J. Tomasi, J. Chem. Phys. 107 (1997) 3032.
[38] B. Mennucci, E. Cancès, J. Tomasi, J. Phys. Chem. B 101 (1997) 10506.
[39] E. Cancès, B. Mennucci, J. Math. Chem. 23 (1998) 309.
[40] S. Miertus, E. Scrocco, J. Tomasi, Chem. Phys. 55 (1981) 117.
[41] R. Cammi, J. Tomasi, J. Comput. Chem. 16 (1995) 1449.
[42] J.L. Pascual-Ahuir, E. Silla, J. Tomasi, R. Bonaccorsi, J. Comput. Chem. 8 (1987) 778.
[43] A. Bondi, J. Phys. Chem. 68 (1964) 441.
[44] G. Alagona, C. Ghio, P.I. Nagy, Int. J. Quant. Chem. 99 (2004) 161.
[45] R.S. Mulliken, J. Chem. Phys. 36 (1962) 3428.
[46] S. Grimme, J. Comput. Chem. 25 (2004) 1463.
[47] S. Grimme, J. Comput. Chem. 27 (2006) 1787.

Supporting information for: Theoretical Study of Tautomerization and Isomerization of Methylamino and Phenylamino Substituted Cyclic azaphospholines, Oxaphospholines and Thiaphospholines in gas and aqueous phases

Sahar Abdalla* and Michael Springborg†

Physical and Theoretical Chemistry,

University of Saarland, 66123 Saarbrücken, Germany

(Dated: February 12, 2010)

* e-mail: s.abdalla@mx.uni-saarland.de

† e-mail: m.springborg@mx.uni-saarland.de

TABLE I: Selected optimized geometries of the various isomers in gas phase. For the structures see Fig. 1; bond lengths are in Å as well as bond and dihedral angles in degrees; X=NH, O and S mark the various species; A and B refer to the amino forms whereas E and Z refer the imino forms.

			X=NH			X=O			X=S			
	A	B	Z	Z	A	A	E	E	A	A	Z	Z
Parameter	Me	Ph	Me	Ph	Me	Ph	Me	Ph	Me	Ph	Me	Ph
$\Theta[C_2-X_1-C_5]$	111.19	112.53	116.36	117.91	110.05	110.09	113.63	113.81	93.43	93.89	96.25	95.71
$\Theta[X_1-C_5-C_4]$	105.93	105.28	105.63	105.74	108.54	108.54	108.98	109.06	107.98	107.55	109.56	109.49
$\Theta[C_2-N_1-H]$	115.46	120.33	114.84	116.67								
$\Theta[X_1-C_2-P_3]$	116.68	116.16	108.35	108.85	118.85	118.81	112.25	112.19	119.26	118.20	114.17	114.08
$\Theta[C_5-C_4-P_3]$	105.99	105.32	106.84	106.94	104.69	104.35	105.36	105.34	109.33	109.44	110.53	110.37
$\Theta[C_2-P_3-C_4]$	88.02	87.89	89.28	88.87	87.12	87.25	88.23	88.38	92.92	93.51	93.51	93.95
$\Theta[X_1-C_2-N_6]$	116.30	119.03	121.75	121.18	112.19	115.58	124.06	125.91	114.77	111.62	125.43	127.04
$\Theta[C_2-N_6-C_7]$	120.60	128.11	120.59	122.48	122.22	132.86	119.53	127.81	121.72	131.58	120.24	124.93
$\Theta[C_2-N_6-H]$	115.94	115.04			116.49	112.79			117.65	115.09		
$\Theta[C_2-P_3-H]$			93.97	94.71			94.59	94.66			94.75	94.41
$\Phi[C_2-X_1-C_5-C_4]$	34.89	−34.44	−39.19	−34.09	31.08	−30.74	32.09	−31.42	−35.95	−36.76	−32.23	−35.39
$\Phi[C_5-C_4-P_3-C_2]$	21.48	−24.22	−20.82	−23.07	22.37	−23.25	23.93	−23.82	−30.24	−29.89	−32.92	−30.27
$\Phi[X_1-C_2-P_3-C_4]$	−2.22	5.72	0.37	5.35	−6.27	7.53	−7.83	8.08	5.14	4.10	10.75	6.09
$\Phi[X_1-C_5-C_4-P_3]$	−34.72	36.13	35.64	34.66	−33.92	34.33	−35.69	35.18	44.74	44.89	44.48	44.73
$\Phi[X_1-C_2-N_6-C_7]$	169.91	30.37	−175.79	179.68	−178.77	15.42	−3.34	3.39	−179.41	−170.18	2.63	−0.548
$\Phi[X_1-C_2-N_6-H]$	21.83	−157.54			−15.29	170.96			22.49	11.76		
$\Phi[C_2-N_6-C_7-C_8]$		31.08		−55.17		−4.84		−8.09		−1.25		−53.09
$\Phi[C_5-C_4-P_3-H]$			73.09	71.55			−70.49	70.69			62.23	64.62
$\Phi[P_3-C_2-N_1-H]$	−152.53	166.27	168.49	171.67								
$d[P_6-H...P_3]$	3.65	2.87			3.67	2.82			3.64	3.67		
$d[P_6-H...X_1]$	2.48	3.23			2.36	3.17			2.72	2.56		
$d[C_{7,8}-H...X_1]$	4.03	2.76	3.93	4.11	3.98	2.22	2.48	2.24	4.47	4.65	2.81	2.89
$d[C_{7,8}-H...P_3]$	3.01	4.21	2.69	3.08	3.03	2.51	4.61	4.65	3.01	2.49	4.46	4.59

The optimized geometries of the most stable isomers in gas phase and in solution are collected in this part.

TABLE II: Selected optimized geometries (in Å) of the isomer studied in continuum model. The notation is as in Table I.

			X=NH			X=O			X=S			
	A	A	Z	Z	A	A	E	Z	A	A	Z	Z
Parameter	Me	Ph	Me	Ph	Me	Ph	Me	Ph	Me	Ph	Me	Ph
$\Theta[C_2{-}X_1{-}C_5]$	112.55	112.94	116.58	118.33	110.44	110.89	113.82	113.99	93.83	94.22	96.50	95.77
$\Theta[X_1{-}C_5{-}C_4]$	105.61	105.50	105.86	105.99	108.49	108.32	108.96	109.08	108.13	107.71	109.58	109.57
$\Theta[C_2{-}N_1{-}H]$	118.17	118.02	115.83	117.93								
$\Theta[X_1{-}C_2{-}P_3]$	115.46	114.76	108.43	108.89	118.20	117.47	112.37	111.21	118.71	117.76	114.04	113.27
$\Theta[C_5{-}C_4{-}P_3]$	105.59	105.59	106.76	106.86	104.62	104.69	105.36	102.72	109.39	109.46	110.37	106.67
$\Theta[C_2{-}P_3{-}C_4]$	87.99	88.57	89.44	89.02	87.39	88.01	88.25	87.56	93.23	93.83	93.61	93.84
$\Theta[X_1{-}C_2{-}N_6]$	118.01	114.67	122.08	121.52	112.88	109.70	123.45	118.26	115.33	112.02	125.19	126.59
$\Theta[C_2{-}N_6{-}C_7]$	122.66	131.18	120.06	122.15	122.63	130.93	118.16	120.84	122.33	131.39	119.59	124.10
$\Theta[C_2{-}N_6{-}H]$	118.74	115.23			117.30	113.58			118.82	115.43		
$\Theta[C_2{-}P_3{-}H]$			94.11	94.89			94.67	95.66			94.95	94.80
$\Phi[C_2{-}X_1{-}C_5{-}C_4]$	−35.26	35.35	−37.98	−32.01	−31.47	−31.67	−30.54	−30.38	−35.59	−36.39	−31.26	−34.53
$\Phi[C_5{-}C_4{-}P_3{-}C_2]$	−23.16	22.75	−21.06	−23.37	−22.33	−21.55	−24.61	−31.75	−30.05	−29.72	−33.66	−38.99
$\Phi[X_1{-}C_2{-}P_3{-}C_4]$	4.11	−3.62	1.25	6.78	6.02	4.97	9.34	17.70	5.26	4.25	12.17	16.43
$\Phi[X_1{-}C_5{-}C_4{-}P_3]$	35.84	−35.42	35.17	33.79	33.98	33.33	35.34	40.92	44.28	44.42	44.24	49.69
$\Phi[X_1{-}C_2{-}N_6{-}C_7]$	−179.37	174.89	−176.40	178.75	−178.82	−174.41	3.26	178.19	−177.80	−171.52	2.70	−4.09
$\Phi[X_1{-}C_2{-}N_6{-}H]$	10.48	−2.34			10.76	4.22			15.43	9.42		
$\Phi[C_2{-}N_6{-}C_7{-}C_8]$		4.86		−54.19		−4.96		−68.40		−2.40		126.74
$\Phi[C_5{-}C_4{-}P_3{-}H]$			73.01	71.44			69.89	−126.18			61.74	−135.47
$\Phi[P_3{-}C_2{-}N_1{-}H]$	159.78	−159.64	167.94	172.81								
$d[N_6{-}H...P_3]$	3.69	3.71			3.68	3.69			3.66	3.68		
$d[N_6{-}H...X_1]$	2.51	2.40			2.37	2.25			2.72	2.59		
$d[C_{7,8}{-}H...X_1]$	4.04	4.23	3.92	4.09	3.98	4.20	2.62	4.12	4.48	4.66	2.89	3.04
$d[C_{7,8}{-}H...P_3]$	3.03	2.47	2.67	3.06	3.07	2.50	4.45	3.34	3.15	2.48	4.47	4.59

TABLE III: The optimized atomic coordinates (in Å) in gas phase. For the structures of the isomers see Fig. 1

Me-NH(A)	X	Y	Z	Me-O(A)	X	Y	Z	Me-S(A)	X	Y	Z
N1	-0.595120	1.329940	0.180589	O1	-0.517526	-1.348271	-0.115150	S1	0.792323	-1.444103	-0.129051
C2	0.358566	0.333451	0.019757	C2	0.353894	-0.308581	-0.031745	C2	-0.498293	-0.216724	-0.019672
P3	-0.230138	-1.306900	-0.073204	P3	-0.278382	1.312548	0.075427	P3	-0.068499	1.463856	0.031277
C4	-1.988516	-0.621249	0.199592	C4	-2.003784	0.555145	-0.206312	C4	1.770927	1.101135	-0.236435
C5	-1.933661	0.853470	-0.206627	C5	-1.859974	-0.901189	0.216570	C5	2.110477	-0.261860	0.364814
N6	1.661882	0.746295	-0.046496	N6	1.641746	-0.716889	-0.077282	N6	-1.764052	-0.718077	-0.022867
C7	2.748861	-0.220222	0.005859	C7	2.752043	0.212345	0.021183	C7	-2.929159	0.147806	0.047445
Me-NH(Z)	X	Y	Z	Me-O(E)	X	Y	Z	Me-S(Z)	X	Y	Z
N1	-0.552900	1.359332	-0.178101	O1	-0.244650	1.127952	-0.049556	S1	0.195509	1.391811	-0.041123
C2	0.487958	0.448962	-0.055614	C2	-0.519827	-0.224533	-0.010687	C2	0.589243	-0.382925	-0.000315
P3	-0.250676	-1.305846	-0.027781	P3	1.035765	-1.263557	0.008980	P3	-0.913513	-1.501578	0.025158
C4	-1.968066	-0.560225	-0.205848	C4	2.018535	0.306591	-0.295528	C4	-2.101495	-0.106377	-0.355557
C5	-1.868123	0.900984	0.253312	C5	1.134997	1.444860	0.222151	C5	-1.608593	1.203874	0.266982
N6	1.704626	0.823363	-0.016721	N6	-1.686840	-0.710678	-0.032216	N6	1.756100	-0.877154	-0.019888
C7	2.775130	-0.151611	0.020232	C7	-2.839714	0.185031	-0.028174	C7	2.921413	-0.005174	-0.021944
Ph-NH(B)	X	Y	Z	Ph-O(A)	X	Y	Z	Ph-S(A)	X	Y	Z
N1	1.304337	0.813381	0.693155	O1	-2.200748	-1.326058	0.100445	S1	2.356513	-1.404869	-0.196804
C2	1.221237	-0.390631	0.039145	C2	-1.235786	-0.365790	-0.003865	C2	1.010778	-0.237821	0.007302
P3	2.719527	-1.030175	-0.589450	P3	-1.742888	1.297304	-0.057949	P3	1.397241	1.449080	0.105351
C4	3.615511	0.415643	0.270575	C4	-3.518910	0.687616	0.243171	C4	3.240376	1.163991	-0.208388
C5	2.559557	1.516659	0.416971	C5	-3.507493	-0.768934	-0.196882	C5	3.641081	-0.206951	0.329779
N6	0.005569	-1.036831	-0.020474	N6	-0.011504	-0.963065	-0.034436	N6	-0.204155	-0.871442	0.058286
C7	-1.284465	-0.465541	-0.037613	C7	1.281644	-0.418411	-0.015128	C7	-1.518008	-0.373262	0.026408
Ph-NH(Z)	X	Y	Z	Ph-O(E)	X	Y	Z	Ph-S(Z)	X	Y	Z
N1	-2.336796	1.214131	0.375574	O1	-1.258989	1.065537	0.017892	S1	-1.104335	1.306423	0.325031
C2	-1.129587	0.582253	0.184559	C2	-1.098737	-0.300789	-0.018773	C2	-0.918084	-0.434292	-0.145552
P3	-1.449436	-1.150326	-0.530114	P3	-2.736759	-1.203794	-0.047042	P3	-2.543427	-1.337045	-0.398288
C4	-3.280493	-0.724538	-0.644309	C4	-3.586265	0.453697	-0.267666	C4	-3.581011	0.205502	-0.191102
C5	-3.542854	0.396907	0.369445	C5	-2.611670	1.486820	0.301303	C5	-2.889535	1.189590	0.756523
N6	-0.021920	1.189580	0.397801	N6	0.008547	-0.919425	-0.072389	N6	0.169840	-1.069571	-0.314497
C7	1.223286	0.570187	0.218333	C7	1.305782	-0.372011	-0.040467	C7	1.456950	-0.516341	-0.172681

TABLE IV: The optimized atomic coordinates (in Å) in PCM-SCRF. For the structures of the isomers see Fig. 1

Me-NH(A)	X	Y	Z	Me-O(A)	X	Y	Z	Me-S(A)	X	Y	Z
N1	-0.592930	1.322244	-0.170139	O1	0.514774	-1.346839	-0.116409	S1	0.787872	-1.445538	-0.124925
C2	0.366856	0.344547	-0.051752	C2	-0.360674	-0.315040	-0.024049	C2	-0.505447	-0.220772	-0.012449
P3	-0.244410	-1.310516	0.065924	P3	0.284091	1.311664	0.079168	P3	-0.061033	1.465004	0.036069
C4	-1.998782	-0.610042	-0.195399	C4	2.006501	0.554154	-0.211193	C4	1.775716	1.099201	-0.240270
C5	-1.925091	0.856192	0.237555	C5	1.862494	-0.901454	0.211895	C5	2.115863	-0.266059	0.353887
N6	1.664529	0.723618	-0.065615	N6	-1.643608	-0.714291	-0.052041	N6	-1.766450	-0.709947	-0.003153
C7	2.759679	-0.225425	0.038997	C7	-2.755814	0.218377	0.007659	C7	-2.935047	0.153799	0.036784
Me-NH(Z)	X	Y	Z	Me-O(E)	X	Y	Z	Me-S(Z)	X	Y	Z
N1	-0.556992	1.361498	-0.164215	O1	0.267797	1.110359	-0.025465	S1	0.208553	1.382024	-0.025025
C2	0.485190	0.458902	-0.051956	C2	0.518625	-0.239016	-0.005918	C2	0.587415	-0.389805	0.003100
P3	-0.242328	-1.299566	-0.022155	P3	-1.051911	-1.254688	0.014409	P3	-0.926076	-1.493507	0.035764
C4	-1.962215	-0.571547	-0.214023	C4	-2.008172	0.323122	-0.310356	C4	-2.098458	-0.097267	-0.371812
C5	-1.878024	0.889288	0.245668	C5	-1.119568	1.451306	0.216948	C5	-1.605022	1.212029	0.250861
N6	1.707640	0.833120	-0.024176	N6	1.686794	-0.734023	-0.042819	N6	1.755421	-0.889724	-0.028929
C7	2.770022	-0.155616	0.016131	C7	2.826949	0.184605	-0.036340	C7	2.916710	-0.007045	-0.033916
Ph-NH(A)	X	Y	Z	Ph-O(A)	X	Y	Z	Ph-S(A)	X	Y	Z
N1	2.286065	1.296789	-0.120223	O1	-2.203044	-1.325519	0.086926	S1	2.362455	-1.406831	-0.169644
C2	1.235164	0.408736	-0.023574	C2	-1.232082	-0.375830	-0.002562	C2	1.006586	-0.247310	0.003815
P3	1.705215	-1.290180	0.015747	P3	-1.740223	1.295083	-0.039714	P3	1.393687	1.446919	0.076329
C4	3.511067	-0.747018	-0.232059	C4	-3.518588	0.691516	0.244996	C4	3.238434	1.167629	-0.221870
C5	3.574918	0.700956	0.252763	C5	-3.510881	-0.760269	-0.209419	C5	3.643028	-0.193649	0.335667
N6	-0.002635	0.990200	0.007563	N6	-0.010897	-0.970738	-0.032704	N6	-0.205209	-0.879050	0.053003
C7	-1.290011	0.426581	0.004907	C7	1.281694	-0.420592	-0.015252	C7	-1.518602	-0.375689	0.025264
Ph-NH(Z)	X	Y	Z	Ph-O(Z)	X	Y	Z	Ph-S(Z)	X	Y	Z
N1	2.337930	1.204218	-0.396995	O1	-2.326640	-1.182055	-0.520382	S1	1.075856	1.270582	-0.414777
C2	1.134833	0.587451	-0.194216	C2	-1.147065	-0.555702	-0.259290	C2	0.920820	-0.461855	0.072638
P3	1.444917	-1.146882	0.518807	P3	-1.431900	1.202536	0.373299	P3	2.568479	-1.334436	0.235257
C4	3.271189	-0.727512	0.659267	C4	-3.202143	0.693454	0.746262	C4	3.550373	0.261788	0.295470
C5	3.549750	0.390934	-0.352395	C5	-3.492166	-0.340272	-0.343909	C5	2.895912	1.218767	-0.707531
N6	0.020617	1.203138	-0.391930	N6	-0.068455	-1.197397	-0.457053	N6	-0.163037	-1.109674	0.239269
C7	-1.220913	0.575474	-0.212702	C7	1.186506	-0.587902	-0.240302	C7	-1.449504	-0.537249	0.144576

TABLE V: Mulliken net charges of the atoms in gas phase (to the left of the vertical line) and in aqueous phase (to the right of the vertical line).

System	Isomer	X_1	C_2	C_4	C_5	N_6	P_3	C_7	X_1	C_2	C_4	C_5	N_6	P_3	C_7
Me-NH	E	-0.333	-0.202	-0.517	-0.236	-0.17	0.486	-0.369	-0.344	-0.155	-0.512	-0.233	-0.248	0.425	-0.359
	Z	-0.193	-0.250	-0.467	-0.139	-0.294	0.373	-0.367	-0.224	-0.228	-0.467	-0.141	-0.351	0.349	-0.354
	B	-0.285	-0.249	-0.460	-0.282	-0.247	0.173	-0.307	-0.304	-0.215	-0.426	-0.274	-0.273	0.024	-0.315
	A	-0.233	-0.384	-0.386	-0.251	-0.295	0.207	-0.311	-0.241	-0.408	-0.360	-0.210	-0.309	0.049	-0.281
Me-O	E	-0.299	-0.091	-0.537	-0.084	-0.168	0.441	-0.349	-0.311	-0.054	-0.529	-0.083	-0.241	0.395	-0.341
	Z	-0.209	-0.129	-0.489	-0.032	-0.236	0.356	-0.342	-0.249	-0.105	-0.486	-0.033	-0.303	0.347	-0.338
	B	-0.299	-0.113	-0.505	-0.081	-0.282	0.153	-0.284	-0.306	-0.089	-0.478	-0.078	-0.302	0.043	-0.289
	A	-0.274	-0.233	-0.426	-0.077	-0.301	0.169	-0.287	-0.283	-0.229	-0.419	-0.059	-0.306	0.073	-0.286
Me-S	E	0.319	-0.555	-0.550	-0.413	-0.044	0.404	-0.329	0.234	-0.497	-0.540	-0.406	-0.103	0.388	-0.325
	Z	0.203	-0.545	-0.539	-0.412	-0.030	0.514	-0.374	0.181	-0.499	-0.521	-0.415	-0.093	0.458	-0.374
	B	0.235	-0.505	-0.503	-0.429	-1.999	0.213	-0.306	0.229	-0.512	-0.479	-0.412	-0.208	0.118	-0.322
	A	0.182	-0.562	-0.509	-0.404	-0.159	0.254	-0.300	0.172	-0.568	-0.498	-0.394	-0.165	0.169	-0.294
Ph-NH	E	-0.262	-0.103	-0.499	-0.259	-0.138	0.469	-0.604	-0.261	-0.060	-0.454	-0.305	-0.264	0.423	-0.497
	Z	-0.153	-0.239	-0.457	-0.116	-0.328	0.477	-0.360	-0.178	-0.205	-0.456	-0.122	-0.389	0.439	-0.334
	B	-0.267	-0.282	-0.475	-0.242	-0.287	0.321	-0.286	-0.288	-0.272	-0.464	-0.214	-0.295	0.115	-0.243
	A	-0.183	-0.192	-0.435	-0.223	-0.319	0.233	-0.554	-0.203	-0.198	-0.434	-0.196	-0.316	0.129	-0.471
Ph-O	E	-0.262	0.037	-0.563	-0.048	-0.135	0.451	-0.369	-0.269	0.109	-0.526	-0.077	-0.229	0.399	-0.322
	Z	-0.159	-0.104	-0.497	0.043	-0.280	0.443	-0.382	-0.214	0.017	-0.484	0.000	-0.331	0.409	-0.686
	B	-0.259	0.009	-0.564	-0.004	-0.299	0.197	-0.177	-0.281	-0.042	-0.564	0.025	-0.295	0.137	-0.192
	A	-0.233	-0.022	-0.484	-0.024	-0.348	0.208	-0.532	-0.239	-0.043	-0.482	-0.007	-0.349	0.149	-0.469
Ph-S	E	0.386	-0.651	-0.538	-0.442	-0.000	0.478	-0.322	0.257	-0.364	-0.468	-0.489	-0.064	0.383	-0.615
	Z	0.236	-0.491	-0.579	-0.387	0.016	0.505	-0.458	0.212	-0.374	-0.524	-0.437	-0.102	0.429	-0.455
	B	0.293	-0.559	-0.535	-0.395	-0.166	0.255	-0.464	0.263	-0.592	-0.515	-0.380	-0.164	0.208	-0.472
	A	0.177	-0.342	-0.550	-0.422	-0.129	0.242	-0.489	0.169	-0.389	-0.549	-0.404	-0.127	0.209	-0.439

Computational and Theoretical Chemistry 978 (2011) 143–151

Contents lists available at SciVerse ScienceDirect

Computational and Theoretical Chemistry

journal homepage: www.elsevier.com/locate/comptc

A DFT study of the properties of substituted pyrrolidines and phospholanes in gas and in aqueous phase

Sahar Abdalla *, Michael Springborg

Physical and Theoretical Chemistry, University of Saarland, 66123 Saarbrücken, Germany

ARTICLE INFO

Article history:
Received 19 July 2011
Received in revised form 2 October 2011
Accepted 3 October 2011
Available online 18 October 2011

Keywords:
Substitution
DFT
Relative energies
Solvation
Isomerization
Tautomerization

ABSTRACT

Properties of nitrogen-containing organic molecules and their phosphorous analogs are studied theoretically both in gas phase and in aqueous phase with the use of density functional calculations. In the aqueous phase calculations, both a pure continuum (PCM) and a supermolecular/continuum model was used. Particular emphasis is put on the changes of the properties due to the systematic replacement of nitrogen atoms by phosphorous atoms. The properties include the relative energies of different tautomers and isomers, their dipole moment, and their free energy of solvation. Both from gas phase and from pure PCM calculations, for the nitrogen-containing compounds the most stable structures are characterized by strong intramolecular hydrogen bonds formed with the nitrogen atoms and the hydrogen atoms located outside the ring. When replacing the nitrogen atoms by phosphorous atoms this formation of hydrogen bonds is strongly affected which, in turn, leads to changes in the relative energies of different iso- and tautomers. Intermolecular hydrogen bonds between the solute and (explicit) water molecules of the solvent are responsible for the stability in the supermolecular/continuum calculations, whereby stronger hydrogen bonds with the water molecules are formed for the nitrogen-containing molecules.

1. Introduction

The large attention [1–8] to compounds containing the amidine group, —NH—C(R)=N—, has recently encouraged us to study theoretically compounds obtained by substituting parts of the nitrogen atoms by phosphorus atoms, i.e., compounds containing —NH—C(R)=P— or —PH—C(R)=N—) groups [9,10]. A particularly interesting issue for those compounds is that of tautomerism and isomerism and how the stability of the different tautomers and isomers is affected by solvation effects. Actually, the proton transition involved in the tautomerization process in heterocyclic five-membered ring systems is of more general interest, [11–15] and has also been studied theoretically using different methods ranging from semiempirical molecular orbital methods [12,16] to more sophisticated calculations that include electron correlation effects [17,18].

Phosphorus-containing compounds are of wide interest due to various applications of organophosphorus as, e.g., lubricants, oil additives, water treatment cleaners, flame retarding agents, fertilizers, plasticizers, and pesticides [19,20]. Moreover, phosphorus and organophosphorus compounds have been recognized to have important biological functions, so that they, e.g., are essential constituents of the protoplasm [21].

The goal of the present work is to obtain a systematic understanding of the effects of substituting nitrogen atoms in compounds containing the amidine group —NH—C(R)=N— (which has been studied earlier by van Duijnen and coworkers [8]) by phosphorus atoms. To this end we have extended the earlier studies by calculations on the two sets of compounds containing either only N atoms or only P atoms so that we have considered all the compounds containing the amidine group —NH—C(R)=N— as well as the —PH—C(R)=N—, —NH—C(R)=P—, and —PH—C(R)=P— groups both in gas phase and in an aqueous phase. We shall focus on bond lengths, relative energies, dipole moment, and solvation energies.

The compounds of our study are presented in Fig. 1. In order to distinguish between the different classes of compounds (i.e., whether, which, and how many N atoms have been substituted by P atoms) we shall label those compounds that contain the amidene group as group [1] compounds. These have been studied in the gas phase by Remko et al. [8] Replacing the nitrogen atoms by phosphorus atoms at position 6 or 3 leads to group [2] and group [3] compounds, respectively, whereas double replacement gives group [4] compounds. Moreover, for the sake of simplicity we shall label our systems according to both the type of substitution, i.e., methyl or phenyl and to the type of the heteroatom in position 1. Thus, the compounds of our study are labeled Me—NH, Me—O, Me—S, Ph—NH, Ph—O, and Ph—S, respectively.

Since compounds like those of the present study very often are found in solution and not in a gas phase, it is highly relevant to

* Corresponding author. Tel.: +49 6813022913; fax: +49 6813023857.
E-mail addresses: s.abdalla@mx.uni-saarland.de (S. Abdalla), m.springborg@mx.uni-saarland.de (M. Springborg).

2210-271X/$ - see front matter © 2011 Elsevier B.V. All rights reserved.
doi:10.1016/j.comptc.2011.10.007

understand the effects of the solvent. To this end, a common approach for treating molecules in an aqueous solution treats the solvent by using the self-consistent reaction-field method, which allows for a quantum–mechanical description of the solute in the solvent continuum at a computational cost only slightly higher than that required for gas phase calculations. Although over the years much effort has been devoted to the development of accurate approaches for the inclusion of solvent effects into quantum calculations (see, e.g., [22,23]), some important electronic effects associated with specific solute–solvent interactions are not described accurately by the continuum model. One possible solution to this problem is to use a combined supermolecular/continuum model [24–30] which has been found to offer accurate descriptions of solvation processes even when including only a smaller number of solvent molecules [30]. Within this model, some few solvent molecules placed at realistic positions are treated explicitly using quantum-theoretical methods and are allowed to interact with specific part(s) of the solute, whereas the remaining parts of the solvent are treated as a polarizable continuum. Such a model provides accordingly a description of both short- and long-ranged solute–solvent interactions. In the present work we shall, accordingly, study the effects of the aqueous solution both by using only implicit model (i.e., the polarizable continuum model) and the combined explicit/implicit model in order to identify the effects of both the long- and the short-ranged solvent–solute interactions, separately.

2. Computational details

All compounds were optimized in gas phase and in aqueous phase using the Gaussian 03 program package [34]. We used the B3LYP functional [31–33] and the 6-31+G (d,p) basis set. For all structures it was checked that they correspond to local total-energy minima and have, accordingly, no imaginary vibrational frequencies.

As mentioned above, the solute–solvent interactions were described using two different approaches. In the polarized continuum model (PCM), the presence of the solute creates a cavity in the solvent, which has the shape related to that of the molecule, whereas the solvent is treated as a continuous dielectrics that can become polarized due to the presence of the solute. Water as the solvent is thus characterized by its relative dielectric constant of 78.39.

Alternatively, within the supermolecule/continuum (explicit/implicit) model we include three water molecules. The chosen number (3) of water molecules corresponds to the number of the hydrophilic regions of the solute. The remaining parts of the solvent were represented through the continuum model. Thus, the three water molecules are positioned near the hydrophilic regions of the solute without any distance restriction but so that the formation of intermolecular hydrogen bonds between the water molecules and the hydrophilic parts of the solute becomes possible.

In both solvation models the Integral Equation Formalism (IEF) [23,35–38] version of the polarized continuum model (PCM) [35,39,40] of the Self Consistent Reaction Field (SCRF) were used.

The molecular cavity was created using the United Atom topological model (UAO). In this model, the molecular cavity is constructed by using interlocking spheres centered on heavy (that is, non-hydrogen) atoms. The radius of each sphere was obtained by scaling the corresponding van der Waals radius by a factor of 1.20 [35]. A smooth surface is obtained with the help of extra spheres not centered on any atom using the GEnerating POLyhedra (GEPOL) method [41] and leading to the solvent-excluding surface. In the supermolecule/continuum model, the values of the OFac and RMin for the GEPOL algorithm were changed to 0.8 and 0.5 from 0.89 and 0.2, respectively.

In the first model we can calculate a relative energy of solvation $E_{sol,1}$ as the difference between the energy of the molecule in the continuum and the energy of the molecule in gas phase

$$\Delta E_{sol,1} = E_{solute,PCM} - E_{solute,g} \quad (1)$$

In the supermolecular/continuum model, we define an energy of solvation, $\Delta E_{sol,2}$, as

$$\Delta E_{sol,2} = E_{complex,PCM} - E_{solute,gas} - E_{(H_2O)_3,PCM} \quad (2)$$

where $E_{(H_2O)_3,PCM}$ represents the energy of three water molecule calculated in PCM and oriented as found for the complex of interest.

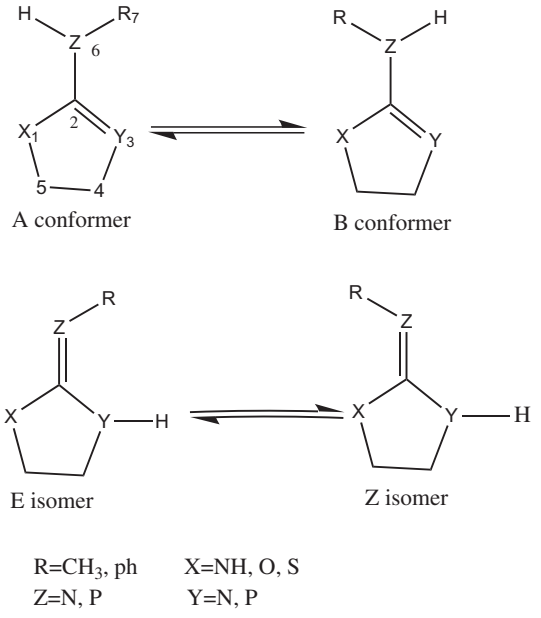

Fig. 1. Structures and atom numbering of the tautomers and isomers of substituted pyrrolidines and phospholanes. Notice that for Z = N, Y = P, and X = NH or O, the Z isomer is not stable but converts into the E isomer.

3. Results and discussion

3.1. Relative energies

3.1.1. Gas phase calculations

Relative energies ΔE (relative to those of the B isomers) in gas phase at $T = 0$ K with the inclusion of zero point energies are presented in Fig. 2 as function of substitution at positions 3 and 6. In all cases, the symmetry is low, i.e., C_1. For all the optimized structures the ring moieties adopt a non-planar configuration. Of the four iso- and tautomers we considered, two structures possess indocyclic double bonds (i.e., the A and B conformers). In general, the replacement of the nitrogen atoms by phosphorus atoms affects the order and the relative stability of isomers and tautomers for all systems.

The stability of group [1] can be explained as being due to intramolecular hydrogen bonds [8]. Actually, there are three different types of hydrogen bonds that can be recognized, of which one is the hydrogen bond between the hydrogen atom of the amino group and the nitrogen atom in position 3 (N_6—H···N_3), that have slightly different lengths for the B structures of Me—NH, Me—O, Ph—NH, Ph—O, and Ph—S, i.e., 2.47, 2.51, 2.45, 2.44, and 2.44 Å, respectively. The second type of hydrogen bond is found between the hydrogen atom of the amino group and the heteroatom in

position 1 (N_6—H···X), (with X = NH, O, or S). These are found in the A forms of Me—O, Ph—NH, Ph—O, and Ph—S and have lengths of 2.40, 2.45, 2.31, and 2.69 Å, respectively. Finally, the last type of hydrogen bond occurs between the hydrogen atoms of the methyl or phenyl group and the nitrogen atom in position 3 or the heteroatom in position 1, as in the A forms of Ph—NH and Ph—O (C_8—H···N_3), as well as the B form of Ph—S (C_8—H···X) whose lengths are 2.27, 2.29, and 2.75 Å, respectively. For the B form of Me—O and Me—S the hydrogen bond C_7—H···X (X = O or S) has a length of 2.51 and 2.82 Å, respectively. In the Z isomers of Me—O and Me—S systems the hydrogen bond C_7—H···X (again, X = O or S) has a length of 2.42 and 2.63 Å, respectively. We emphasize that in order to classify these bonds as being hydrogen bonds we have used that they all have lengths that are smaller than the sum of the van der Waal radii of the involved atoms [42].

When going from group [1] to group [2], i.e., replacing the nitrogen atom at position 6 by a phosphorus atom, the bond length C_2—Z increases by about 0.49 Å for the phosphino form and about 0.47 Å for the phosphinidene form. Due to this increase the formation of intramolecular hydrogen bonds becomes much more difficult. In addition, the phosphorus atom is a much weaker proton acceptor and donor compared to nitrogen [43,44]. Despite this, the stability of some isomers can still be interpreted as being due to hydrogen-bond formation.

The stability of the B form of Me—S for group [1] is due to intramolecular hydrogen bonding (C_7—H···S), and through a rotation of the methyl group, "bifurcated" hydrogen bonds (S < (C_7—H)$_2$) are formed. The stability of the A form of Ph—NH for group [2] is due to the C_8—H···N_3 hydrogen bonding being 2.63 Å. The Ph—S for group [2], stabilized the A conformer due to P_6—H···S hydrogen bond with a length of 2.97 Å. The phosphinidene form for methyl substitution (X = O or S) leads to a preference for the Z form, whereas the E form is the most stable one for their phenyl analogs due to the presence of three-center bonds, P_6—C_2—N_3. The considerable increase in the interatomic distances by about 0.4 Å of the N_3—H···S bond in the Z isomer for Ph—S compared to the N_3—H···O bond for Ph—O destabilizes the Z isomer for the sulfur species.

For group [3] the C_2—Y bond length increases by about 0.45 Å for the amino tautomers and 0.51 Å for the imino tautomers. In general, the relative total energy varies less than for group [2].

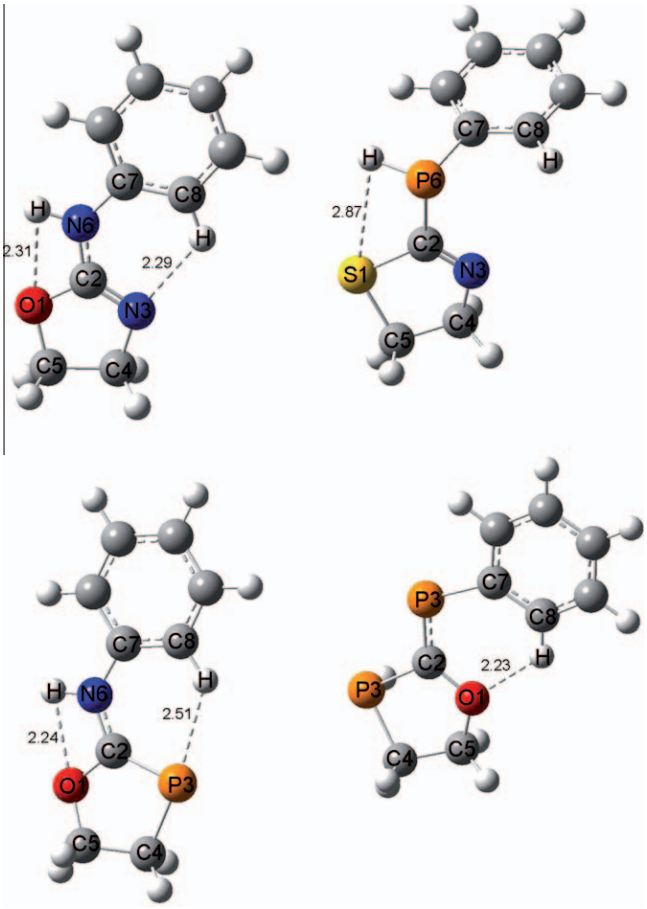

Fig. 3. Examples of intramolecular hydrogen bonds in the gas phase for four different molecules.

The most stable structures in this group are stabilized by the presence of intramolecular hydrogen bonds, similar to what we found for group [1]. The stability of the A form in the indocyclic double

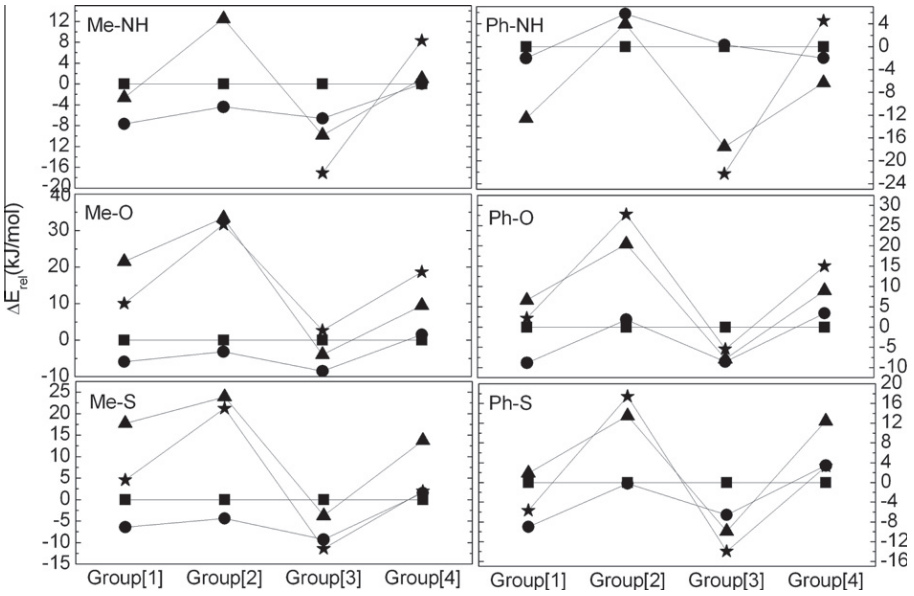

Fig. 2. The relative energies in gas phase as function of the substitution at position 3 and 6. The energies are given relative to B (squares). Circles, triangles, and stars mark the A, E, and Z isomers, respectively.

bond tautomers are still dominating with Ph—NH being an exception, where the B isomer is more stable. For the methyl substituted compounds, the amino group (N_6—H) is oriented so that hydrogen bonds with the heteroatom (X = N, O, or S) can be formed, having lengths of 2.48, 2.36, and 2.72 Å, respectively. For the phenyl substitution (X = O or S) two types of hydrogen bonds can be identified of which one is N_6—H···X with lengths of 2.24 and 2.59 Å, respectively, and the second is found between the α hydrogen of the phenyl group and the phosphorus atom in position 3 (C_8—H···P_3) with lengths of 2.51 and 2.49 Å for X = O and S, respectively. The Z isomers are more stable for the sulfur derivative of group [1], whereas the E isomers are more stable for the equivalent oxygen derivatives.

For group [4] the length of the C_2—Y bond increases by about 0.44 Å for the phosphino tautomers and 0.48 Å for phosphinidene tautomers. Simultaneously, the length of the C_2—Z bond increases by about 0.55 Å for the phosphino and 0.33 Å for the phosphinidene tautomers. As for group [3], also in this case the relative total energies show a fairly small spread. The A form for Me—NH is still the most stable tautomer. For the phosphino forms of Me—O, Me—S, Ph—O, and Ph—S, the B structures are the most stable species. For the phosphinidene forms, the E isomers are more preferred for the cyclic azaphospholine and oxaphospholine, whereas for the cyclic thiaphospholine the Z isomers are more stable. The stability of the E isomer for Ph—O can be explained as being due to the intramolecular hydrogen bond between the α hydrogen of the phenyl group and the oxygen atom (C_8—H···O) with a length of 2.23 Å.

In order to verify that our results on the the intramolecular hydrogen bonds are not due to our computational approach we performed additional gas-phase calculations for the most stable tautomers of Me—NH using the B3LYP/6-311++G (d,p) and the MP2/6-311++G (d,p) methods. We found that the lengths of the hydrogen bonds vary by only about 0.01 Å, with the only exceptional case being the E isomer of the group [1] where the C_7—H···N_3 hydrogen bond was reduced to 2.66 Å (which is now less than the sum of the van der Waal radii of nitrogen and hydrogen, i.e., 2.75 Å [42]), when the MP2/6-311++G (d,p) approach was used, compared to 2.77 Å for the B3LYP/6-31+G (d,p) and B3LYP/6-311++G (d,p) calculations.

Finally, in Fig. 3 we show some typical examples of intramolecular hydrogen bonds as found in the gas phase.

3.1.2. SCRF calculations

In the first set of calculations for the molecules in an aqueous solution the complete solvent was treated within the polarizable continuum model (PCM). The resulting relative total energies ΔE are shown in Fig. 4. When comparing with the results for the compounds in the gas phase (cf. Fig. 2) some differences are observed, mainly with respect to the absolute values of the relative energies, and partly to the relative ordering of the different structures, but only to a very small extend to the prediction of which structure is the most stable one. Thus, only for the Me—NH system of group [3], the Ph—NH system of group [1] and group [2], the Me—S system of group [3], and the Ph—S system of group [1] the structure that is the most stable one has changed. This means that the finding that the Z structure, the E structure, the B structure, the Z structure, and the A structure, respectively, is most stable in the gas phase is changed into that the A structure, the A structure, the E structure, the A structure, and the Z structure, respectively, is the most stable one in the aqueous solution. In all other cases, the two sets of calculations find the same structure to be the most stable one.

With the PCM, the only interactions between solvent and solute are of pure electrostatic nature: the solute has a certain charge distribution that leads to a polarization of the solvent which in turn polarizes the solute. Thus, structures that have a particularly polarized charge distribution (i.e., parts with large, positive or negative, charges) should be energetically favored within the PCM, neglecting all other effects. This effect can be partly quantified through the dipole moment, but it turns out (see below) that it is not possible to identify the most stable structures within the PCM as those that have the largest dipole moment. Thus, also the polarizability as well as the relative stability of the different structures in the gas phase have to be taken into account.

Despite this, the fact that the gas-phase and the PCM calculations lead to similar results suggests that the discussion of the relative stabilities in the gas phase also applies to the PCM results. In particular, many aspects can be explained through the existence (or absence) of intramolecular hydrogen bonding.

The changes of the lengths of the intramolecular hydrogen bonds when passing from the gas phase to PCM are only small. Thus, the stability of the A forms of Ph—NH and Ph—O systems of group [1] is due to the intramolecular hydrogen bond [C_8—H···N_3] with lengths of 2.31 and 2.33 Å in the PCM compared to 2.27 and

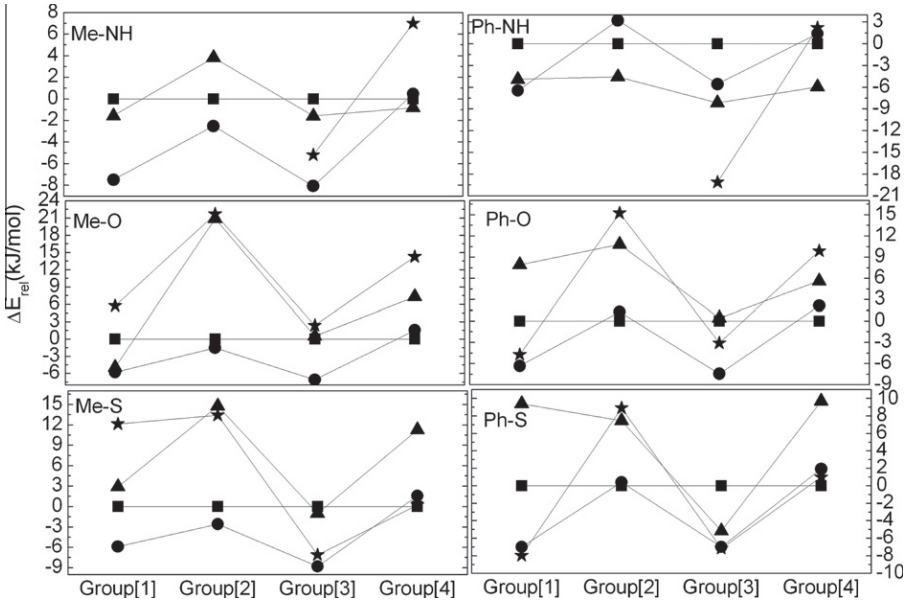

Fig. 4. Similar to Fig. 2, but for the PCM calculations in which the complete aqueous solvent is treated as a polarizable continuum.

2.29 Å in the gas phase. For the B form of Ph—O of group [1], the C_8—H···O hydrogen bond has a length of 2.25 Å in PCM compared to 2.21 Å in the gas phase.

3.1.3. Supermolecular/continuum calculations

Since we have found that intramolecular hydrogen bonding is important for our compounds, intramolecular solute–solvent hydrogen bonding may be so, too. To study this we included an explicit (quantum–mechanical) description of three water molecules together with that of the solute, whereas the remaining parts of the solvent were treated within the continuum approach. The positions of the three water molecules were chosen according to where we expected that hydrogen bonding might occur. The resulting hydrogen bonds are summarized in Table 1.

The fact that phosphorus has a lower tendency to act as the proton donor in hydrogen bonding explains why the oxygen of the water molecule prefers to form hydrogen bonding with the hydrogen atoms of the methyl group or with α phenyl hydrogen. A further result of our calculations is that not all hydrogen bonds contribute to the stability of the compounds, and that, instead, in some cases hydrogen bonding between the explicit water molecules was formed. It was, on the other hand, important that the number of explicit water molecules is sufficiently large so that they can surround the hydrophilic regions of the compound.

Next we turn our attention to the total energies. The results of the present calculations are shown in Fig. 5 in a presentation similar to that of Figs. 2 and 4. A comparison between Figs. 2 and 5 gives that the combined effects of the solvation and of the solvent–solute hydrogen bonding changes the relative stability significantly with the Me—NH system the only one for which the same structure is found to be the most stable one in both sets of calculations. This is in marked contrast to the results of Fig. 4, supporting that hydrogen bonding indeed is important for the present systems and implying that, for the present systems, treating the solvent with a solely implicit approach is not sufficiently accurate. In fact, the most stable isomers are stabilized via the intermolecular hydrogen bonds between water molecules and the heteroatoms.

3.2. Dipole moment

3.2.1. Gas phase

A single number that quantifies the charge distribution and that simultaneously is experimentally accessible is the dipole moment.

Table 1
Hydrogen bond (HB) distances (in Å) as obtained in the calculations with the explicit treatment of three water molecules. The subscript *w* marks atoms from the water molecules, whereas the other atoms are numbered according to Fig. 1.

System	HB	Group [1]		Group [2]		Group [3]		Group [4]	
		Isomer	Distance	Isomer	Distance	Isomer	Distance	Isomer	Distance
Me—NH	N_1···H_w	A		A	2.01	Z		A	
	N_1H···O_w		2.10				1.96		1.89
	HZ_6···H_w		2.11				1.72		2.53
	Y_3···H_w		1.84						2.50
	Y_3—H···O_w						2.46		
	C_7—H···O_w				2.51				2.88
	H_w···O_w		1.97				1.75		1.81
Me—O	O_1···H_w	Z	2.00	B	1.97	B	2.00	B	1.97
	HZ_6···H_w		1.73						
	Z_6H···O_w						1.86		
	Y_3···H_w				1.89		2.42		2.59
	Y_3—H···O_w		1.89						
	C_7—H···O_w				2.52				2.51
	H_w···O_w		1.75				1.79		
Me—S	S_1···H_w	Z	2.54	B	2.54	B	2.53	A	2.54
	HZ_6···H_w		1.76				1.86		
	Z_6H···O_w				2.65				
	Y_3···H_w				1.98		2.44		2.62
	Y_3—H···O_w		1.90						
	C_7—H···O_w								2.46
	H_w···O_w		1.75		1.92		1.79		
Ph—NH	N_1···H_w	B		E		Z		Z	
	N_1H···O_w		2.02		1.91		1.93		1.88
	HZ_6···H_w				2.36		1.77		2.44
	Z_6H···O_w		1.92						
	Y_3···H_w		1.69		1.79				2.57
	Y_3—H···O_w				1.98		2.57		
	C_8—H···O_w						2.45		
	H_w···O_w		1.75		1.79		1.77		1.79
Ph—O	O_1···H_w	Z	2.03	B	1.99	B	2.01	B	1.98
	HZ_6···H_w		1.79						
	Z_6H···O_w						1.85		2.67
	Y_3···H_w				1.82		2.46		2.59
	Y_3—H···O_w		1.87						
	C_8—H···O_w				2.37				2.39
	H_w···O_w		1.76		1.79		1.79		1.86
Ph—S	S_1···H_w	Z	2.53	Z	2.56	A	2.65	A	2.49
	HZ_6···H_w		1.82						
	Z_6H···O_w						1.88		3.01
	Y_3···H_w						2.56		2.62
	Y_3—H···O_w		1.88		1.87				
	C_8—H···O_w								2.39
	H_w···O_w		1.77		1.79		1.90		1.84

Therefore, we shall use this in studying the variation in the charge distribution for our systems.

Fig. 6 shows the dipole moment of our compounds in the gas phase. For group [1], the E isomers of the methyl substitutions (Me—NH, Me—O, and Me—S) have the largest dipole moment in gas phase and the amino tautomers of the A form have the lowest values. For the phenyl substitutions (Ph—NH, Ph—O, and Ph—S), the amino tautomers of the B form have the smallest dipole moment. For group [2], the phosphino tautomer of the forms A have the smallest values of dipole moment, whereas the E isomers have the largest values.

When comparing the results for the same system but differing in the number of nitrogen atoms that have been replaced by phosphorous atoms (i.e., when comparing the results for the different groups) it is at first clearly seen that the dipole moment depends strongly on the substitutions. Thus, replacing nitrogen by phosphorous leads to noticeable changes in the charge distribution. Moreover, one may compare the changes when going from group [1] to group [4] with the sum of the changes when going from group [1] to group [2] and going from group [1] to group [3]. As can be seen in the figure, these two sets of changes are not identical, implying that the double N → P substitution is not simply the sum of two single N → P substitutions, but cooperative effects show up. In fact, from the comparison just mentioned no trend can be identified, but each system seems to follow its own rules. Thus, the properties of the phosphorous-containing compounds are not trivially related to those of the nitrogen-containing compounds.

3.2.2. Aqueous phase

Here, we shall only discuss the results of the pure PCM calculations, since for those where also three water molecules are treated

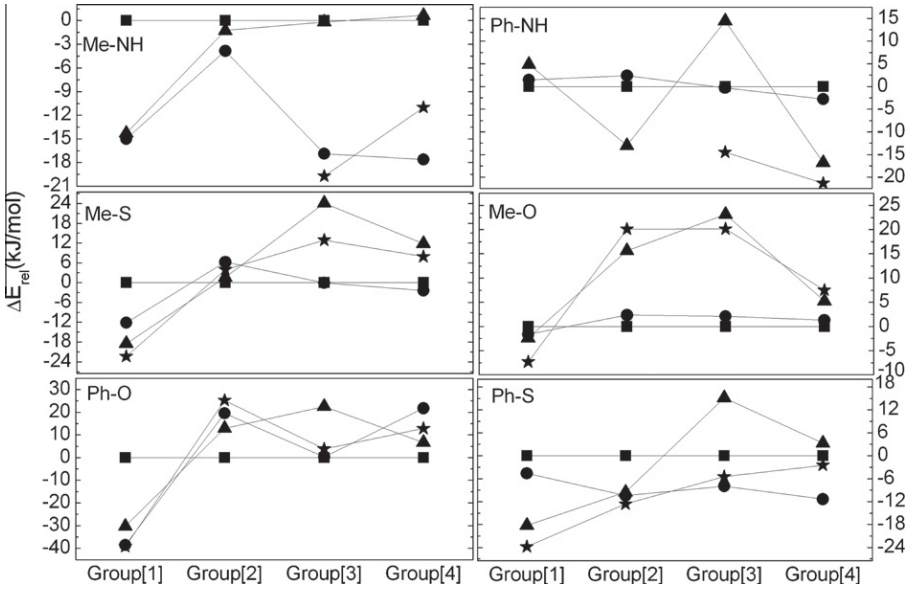

Fig. 5. Similar to Fig. 2, but for the PCM calculations in which three water molecules are treated explicitly, whereas the remaining parts of the aqueous solvent are treated as a polarizable continuum.

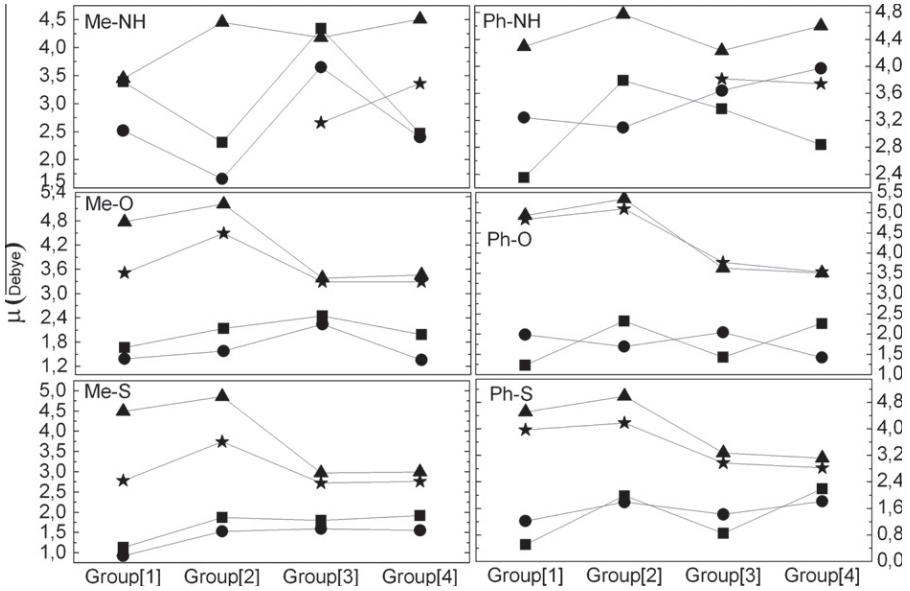

Fig. 6. Similar to Fig. 2, but for the dipole moment in the gas phase.

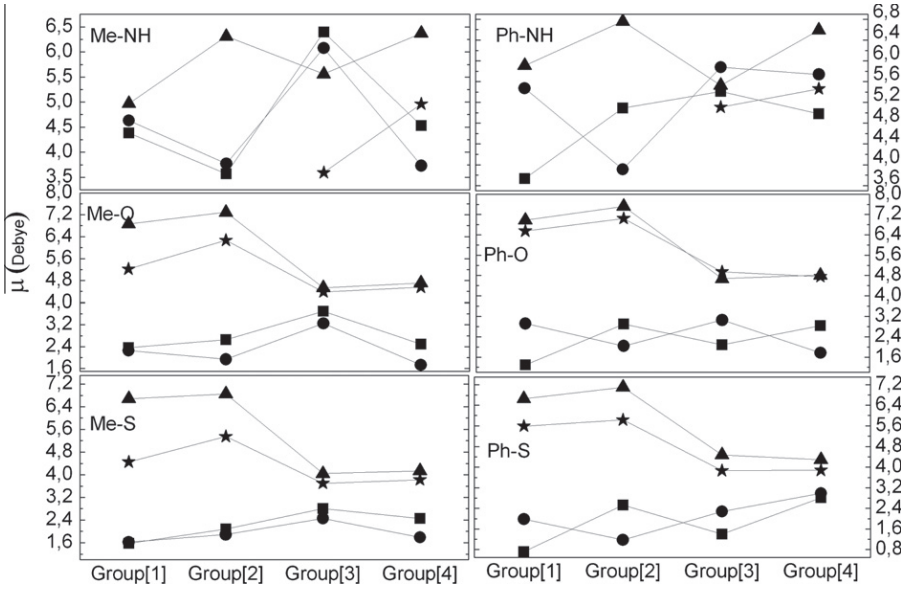

Fig. 7. Similar to Fig. 6, but for the PCM calculations.

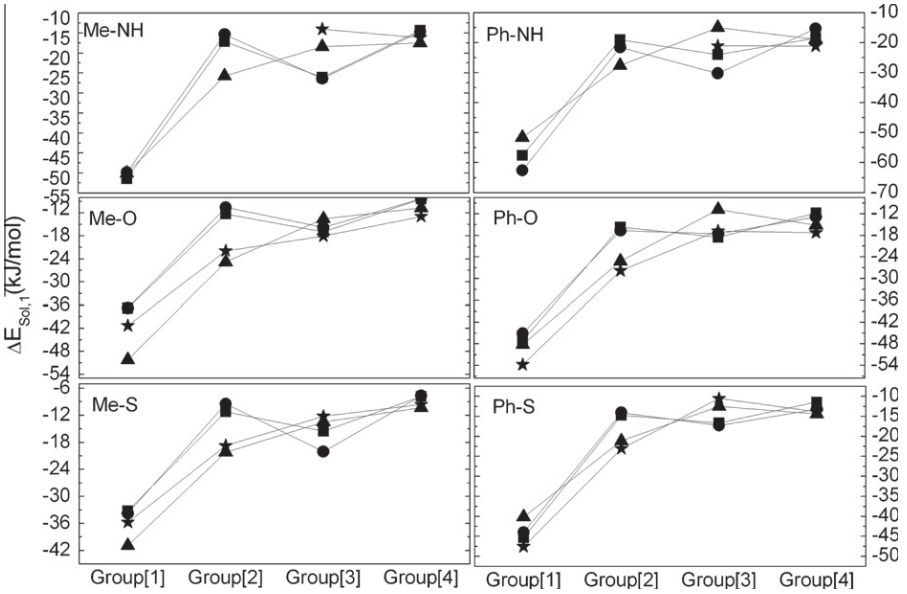

Fig. 8. Similar to Fig. 2, but for the free energy of solvation, $\Delta E_{sol,1}$.

explicitly, the dipole moment contains also contributions from those three water molecules. The results are shown in Fig. 7.

Without exception, the dipole moment for all molecules are increased when the molecule is being solvated, which can be explained as being due to the electrostatic interactions between the solvent and the solute. Such a behavior is common to PCM calculations and it is typically found that PCM calculations lead to an increase of the dipole moment of organic molecules relative to that of the gas phase by up to 30% [45]. In addition, the overall behavior of the dipole moment as a function of phosphorous substitution as found in the aqueous phase (Fig. 7) is very similar to what we found in the gas phase (Fig. 6), although details often differ between the two cases.

Finally, we observe here, what already was discussed above, that there is no simple relation between stability (i.e., relative total energy for the different structures) and dipole moment either in the gas phase nor in the PCM calculations. It is also not possible to identify a correlation between the most stable structures in the solution and the changes in the dipole moment upon solvation. Thus, the stability as found in the PCM calculations may depend also on properties related to the dipole moment, but not only.

3.3. Free energy of solvation

The free energy of solvation, $\Delta E_{sol,1}$, defined in Eq. (1), and $\Delta E_{sol,2}$, defined in Eq. (2), are shown in Figs. 8 and 9, respectively. According to their definitions, ΔE_{sol} is negative for systems that are found to be more stable in the solution than in the gas phase. This is seen to be the case for all systems according to the pure PCM calculations, whereas the inclusion of three explicit water molecules makes $\Delta E_{sol,2}$ positive in several cases.

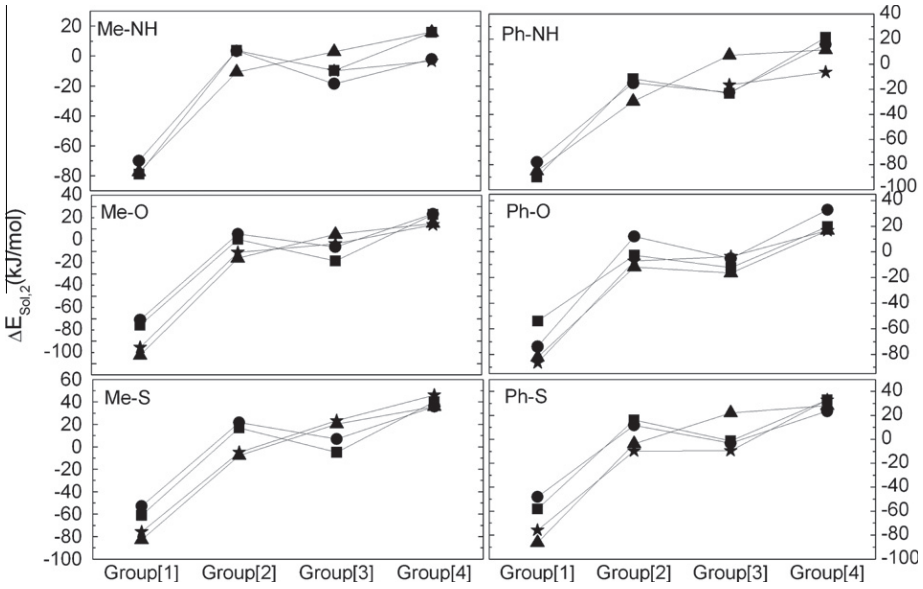

Fig. 9. Similar to Fig. 2, but for the free energy of solvation, $\Delta E_{sol,2}$.

For all systems of group [1], all isomers are well soluble in water. This is also the case for the N → P substituted systems according to the pure PCM calculations, but for several systems of group [2], group [3], and group [4], the calculations with three explicit water molecules find these to be not soluble in water. This tendency is, in general, largest for the compounds of group [4], and this can be attributed to less favorable hydrogen-bond formation between the phosphorous atoms at position 3 and 6 with the water molecules. However, the absolute values from this set of calculations may be taken with some caution, since they depend strongly on the number of water molecules around the solute [46,47] that can form strong hydrogen bonding. The fact that not all hydrogen bonds in the supermolecular contribute to the stability of the isomers maybe also attributed to the construction of the cavity, which may lead to inaccuracies when studying aggregation in solution [48].

Finally, we mention that there is a clear correlation between $\Delta E_{sol,1}$ and the dipole moment of the solute in the gas phase. Thus, a large dipole moment leads to a large, negative value of $\Delta E_{sol,1}$.

4. Conclusion

In this work, results of B3LYP/6-31G (d,p) calculations, both in gas phase and in aqueous phase, were reported with special emphasis on the changes in the properties when nitrogen atoms are replaced by phosphorous atoms. Thereby we focused on the relative energies of different tautomers and isomers, the dipole moment, the free energy of solvation, as well as the changes in the bonds lengths due to this substitution. For the study in the aqueous phase we considered both a pure continuum description of the complete solvent and a supermolecular/continuum model in which three water molecules were treated explicitly and the remaining parts of the solvent were treated as a continuum.

We found both in the gas phase and in the pure PCM calculations that intramolecular hydrogen bonds are responsible for the stability of the isomers. The formation of the hydrogen bonds were affected by the presence of phosphorous atoms, so that the compounds containing nitrogen atoms become more stable compared to their phosphorous analogs. The N → P substitution(s) affect also the relative stability (including their order) of the iso- and tautomers.

When including three water molecules in an explicit treatment, we find in particular for the only-nitrogen compounds strong hydrogen bonds between the solute and the water molecules, an effect that is much less pronounced for the phosphorous-containing compounds. In all cases we find that the inclusion of the explicit water molecules leads to much larger changes in the energetic ordering of the compounds than what is found with the pure continuum approach.

We also found that the changes due to the replacement of both N atoms with P atoms are not simply the superposition of the changes of the individual substitutions. This was exemplified through the dipole moment. The dipole moment itself showed also large changes (towards larger values) when the molecules are been solvated. Finally, the solvation energies suggested that the P-containing systems in some cases are not soluble in water.

Acknowledgment

We gratefully acknowledge the support from Deutscher Akademischer Austauschdienst (DAAD) for sponsoring the funding allocated to S.A.

References

[1] A.H. de Vries, P.Th. van Duijnen, Theoretical calculation of tautomer equilibria of 4-substituted imidazoles in the gas phase and in solution, Biophys. Chem. 43 (1992) 139–147.
[2] E.D. Raczynska, R.W. Taft, Prediction of tautomeric equilibrium constant in the gas phase for simple compounds containing the amidine group, Pol. J. Chem. 72 (1998) 1054–1067.
[3] R. Caminiti, A. Pieretti, L. Bencivenni, F. Ramondo, N. Sanna, Amidine N—C(N)—N skeleton: its structure in isolated and hydrogen-bonded guanidines from ab initio calculations, J. Phys. Chem. 100 (1996) 10928–10935.
[4] M. Remko, O.A. Walsh, W.G. Richards, Ab initio and DFT study of molecular structure and tautomerism of 2-amino-2-imidazoline, 2-amino-2-oxazoline and 2-amino-2-thiazoline, Chem. Phys. Lett. 336 (2001) 156–162.
[5] M. Remko, O.A. Walsh, W.G. Richards, Molecular structure and gas-phase reactivity of clonidine and rilmenidine: two-layered ONIOM calculations, Phys. Chem. Chem. Phys. 3 (2001) 901–907.
[6] N. Marchand-Geneste, A. Carpy, Ab initio calculations of tautomer equilibrium and protonation enthalpy of 2-amino-2-oxazoline in the gas phase: basis set and correlation effects, J. Mol. Struct. Theochem. 465 (1999) 209–217.
[7] M. Remko, O.A. Walsh, W.G. Richards, Theoretical study of molecular structure, tautomerism, and geometrical isomerism of moxonidine: two-layered ONIOM calculations, J. Phys. Chem. A 105 (2001) 6926–6931.

[8] M. Remko, P. Th. van Duijnen, M. Swart, Theoretical study of molecular structure, tautomerism, and geometrical isomerism of N-methyl- and N-phenyl-substituted cyclic imidazolines, oxazolines, and thiazolines, Struct. Chem. 14 (2003) 271–278.
[9] S. Abdalla, M. Springborg, Theoretical study of the effects of solvation, substitution, and structure on the properties of imidazolines, oxazolines, and thiazolines, J. Phys. Chem. A 114 (2010) 5823–5829.
[10] S. Abdalla, M. Springborg, Theoretical study of tautomerization and isomerization of methylamino and phenylamino substituted cyclic azaphospholines, oxaphospholines and thiaphospholines in gas and aqueous phases, J. Mol. Struct. Theochem. 962 (2010) 101–107.
[11] A.R. Katritzky, J.M. Lagowski, Advances in Heterocyclic Chemistry, vol. II, Academic Press, New York, 1963. pp. 1–81.
[12] M.M. Karelson, A.R. Katritzky, M. Szafran, M.C. Zerner, A theoretical treatment of solvent effects on the tautomeric equilibria of five-membered rings with two heteroatoms, J. Chem. Soc. Perkin Trans. 2 (1990) 195–201.
[13] S. Woodcock, D.V.S. Green, M.A. Vincent, I.H. Hillier, M.F. Guest, P. Sherwood, Tautomeric equilibria in 3-and 5-hydroxyisoxazole in the gas phase and in aqueuos solution: a test of molecular dynamics and continuum models of solvation, J. Am. Chem. Soc. Perkin Trans. 2 (1992) 2151–2154.
[14] F.J. Luque, J.M. López-Bes, J. Cemeli, M. Aroztegui, M. Orozco, Solvent effects on tautomerism equilibria in heterocycles, Theor. Chem. Acc. 96 (1997) 105–113.
[15] P.I. Nagy, F.R. Tejada, W.S. Messer Jr., Theoretical studies of the tautomeric equilibria for five-member N-heterocycles in the gas phase and in solution, J. Phys. Chem. B 109 (2005) 22588–22602.
[16] H.S. Rzepa, M.Y. Yi, M.M. Karelson, M.C. Zerner, Geometry optimisation at the semiempirical self-consistent-reaction-field level using the AMPAC and MOPAC programs, J. Chem. Soc. Perkin Trans. 2 (1991) 635–637.
[17] H.B. Schlegel, P. Gund, E.M. Fluder, Tautomerization of formamide, 2-pyridone and 4-pyridone. An ab initio study, J. Am. Chem. Soc. 104 (1982) 5347–5351.
[18] M.J. Scanlan, I.H. Hillier, A.A. MacDowell, Theoretical studies of the tautomeric equilibriums and isomer energetics of 2-, 3-, and 4-hydroxypyridine, J. Am. Chem. Soc. 105 (1983) 3568–3571.
[19] E.B. Fisher, J.R. Van Wazer, Phosphorus and its Compounds, Technology, Biological Functions, and Applications, vol. II, Interscience, Inc., New York, 1961. pp. 1897–1929.
[20] J.W. Bücher, R. Schiebs, G. Winter, K.H. Büchel, In Industrial Organic Chemistry, VCH, New York, 1989.
[21] F. Cramer, Neuere methoden der prparativen organischen chemie III 2. Darstellung von estern, amiden und anhydriden der phosphorsäure, Angew. Chem. 72 (1960) 236–249.
[22] M. Springborg, in: A. Hinchliffe (Ed.), Specialist Periodical Reports: Chemical Modelling, Applications and Theory, vol. 5, Royal Society of Chemistry, Cambridge, UK, 2008.
[23] J. Tomasi, B. Mennucci, R. Cammi, Quantum mechanical continuum solvation models, Chem. Rev. 105 (2005) 2999–3094.
[24] M.J. Huron, P. Claverie, Calculation of the interaction energy of one molecule with its whole surrounding. I. Method and application to pure nonpolar compounds, J. Phys. Chem. 76 (1972) 2123–2133.
[25] M.J. Huron, P. Claverie, Calculation of the interaction energy of one molecule with its whole surrounding. II. Method of calculating electrostatic energy, J. Phys. Chem. 78 (1974) 1853–1861.
[26] M.J. Huron, P. Claverie, Calculation of the interaction energy of one molecule with its whole surrounding. III. Application to pure polar compounds, J. Phys. Chem. 78 (1974) 1862–1867.
[27] G.W. Schnuelle, D.L. Beveridge, Statistical thermodynamic supermolecule-continuum study of ion hydration. I. Site method, J. Phys. Chem. 79 (1975) 2566–2573.
[28] J.H. McCreey, R.E. Christoffersen, G.G. Hall, On the development of quantum mechanical solvent effect models. Macroscopic electrostatic contributions, J. Am. Chem. Soc. 98 (1976) 7191–7197.
[29] P. Claverie, J.P. Daudey, J. Langlet, B. Pullman, D. Piazzola, M.J. Huron, Studies of solvent effects. 1. Discrete, continuum, and discrete-continuum models and their comparison for some simple cases: ammonium(1+) ion, methanol, and substituted ammonium(1+) ion, J. Phys. Chem. 82 (1978) 405–418.
[30] H.S. Rzepa, M.Y. Yi, An AM1 and PM3 molecular orbital and self-consistent reaction-field study of the aqueous solvation of glycine, alanine and proline in their neutral and zwitterionic forms, J. Chem. Soc. Perkin Trans. 2 (1991) 531–537.
[31] A.D. Becke, Density functional thermochemistry.III. The role of exact exchange, J. Chem. Phys. 98 (1993) 5648–5652.
[32] C. Lee, W. Yang, R.G. Parr, Development of the Colle–Salvetti correlation-energy formula into a functional of the electron density, Phys. Rev. B 37 (1988) 785–789.
[33] S.F. Soua, P.A. Fernandes, M.J. Ramos, General performance of density functionals, J. Phys. Chem. A 111 (2007) 10439–10452.
[34] M.J. Frisch, G.W. Trucks, H.B. Schlegel, G.E. Scuseria, M.A. Robb, J.R. Cheeseman, J.J.A. Montgomery, T. Vreven, K.N. Kudin, J.C. Burant, J.M. Millam, S.S. Iyengar, J. Tomasi, V. Barone, B. Mennucci, M. Cossi, G. Scalmani, N. Rega, G.A. Petersson, H. Nakatsuji, M. Hada, M. Ehara, K. Toyota, R. Fukuda, J. Hasegawa, M. Ishida, T. Nakajima, Y. Honda, O. Kitao, H. Nakai, M. Klene, X. Li, J.E. Knox, H.P. Hratchian, J.B. Cross, C. Adamo, J. Jaramillo, R. Gomperts, R.E. Stratmann, O. Yazyev, A.J. Austin, R. Cammi, C. Pomelli, J.W. Ochterski, P.Y. Ayala, K. Morokuma, G.A. Voth, P. Salvador, J.J. Dannenberg, V.G. Zakrzewski, S. Dapprich, A.D. Daniels, M.C. Strain, O. Farkas, D.K. Malick, A.D. Rabuck, K. Raghavachari, J.B. Foresman, J.V. Ortiz, Q. Cui, A.G. Baboul, S. Clifford, J. Cioslowski, B.B. Stefanov, G. Liu, A. Liashenko, P. Piskorz, I. Komaromi, R.L. Martin, D.J. Fox, T. Keith, M.A. Al-Laham, C.Y. Peng, A. Nanayakkara, M. Challacombe, P.M.W. Gill, B. Johnson, W. Chen, M.W. Wong, C. Gonzalez, J.A. Pople, Gaussian 03, Revision D.01, Gaussian, Inc., Wallingford, CT, 2004.
[35] J. Tomasi, M. Persico, Molecular interactions in solution: an overview of methods based on continuous distributions of the solvent, Chem. Rev. 94 (1994) 2027–2094.
[36] E. Cancês, B. Mennucci, J. Tomasi, A new integral equation formalism for the polarizable continuum model: theoretical background and applications to isotropic and anisotropic dielectrics, J. Chem. Phys. 107 (1997) 3032–3041.
[37] B. Mennucci, E. Cancês, J. Tomasi, Evaluation of solvent effects in isotropic and anisotropic dielectrics and in ionic solutions with a unified integral equation method: theoretical bases, computational implementation and numerical applications, J. Phys. Chem. B 101 (1997) 10506–10517.
[38] E. Cancês, B. Mennucci, New applications of integral equations methods for solvation continuum models: ionic solutions and liquid crystals, J. Math. Chem. 23 (1998) 309–326.
[39] S. Miertuš, E. Scrocco, J. Tomasi, Electrostatic interaction of a solute with a continuum. A direct utilizaion of ab initio molecular potentials for the prevision of solvent effects, Chem. Phys. 55 (1981) 117–129.
[40] R. Cammi, J. Tomasi, Remarks on the use of the apparent surface charges (ASC) methods in solvation problems: iterative versus matrix-inversion procedures and the renormalization of the apparent charges, J. Comput. Chem. 16 (1995) 1449–1458.
[41] J.L. Pascual-Ahuir, E. Silla, J. Tomasi, R. Bonaccorsi, Electrostatic interaction of a solute with a continuum. Improved description of the cavity and of the surface cavity bound charge distribution, J. Comput. Chem. 8 (1987) 778–787.
[42] A. Bondi, van der Waals volumes and radii, J. Phys. Chem. 68 (1964) 441–451.
[43] W.C. Topp, L.C. Allen, Structure and properties of hydrogen bonds between of electronegative atoms of the second and third rows, J. Am. Chem. Soc. 96 (1974) 5291–5293.
[44] V.K. Pogorelyi, Weak hydrogen bonds, Russ. Chem. Rev. 46 (1977) 316–337.
[45] G. Alagona, C. Ghio, P.I. Nagy, Int. theoretical studies on the effects of methods and parameterization on the calculated free energy of hydration for small molecules, J. Quantum. Chem. 99 (2004) 161–178.
[46] C. Alemân, S.E. Galembeck, Solvation of chromone using combined discrete/SCRF models, Chem. Phys. 232 (1998) 151–159.
[47] C. Alemân, Hydration of cytosine using combined discrete/SCRF models: influence of the number of discrete solvent molecules, Chem. Phys. 244 (1999) 151–162.
[48] J. Pitarch, V. Moliner, J.-L. Pascual-Ahuir, E. Silla, I. Tuñón, Can hydrophobic interactions be correctly reproduced by the continuum models?, J Phys. Chem. 100 (1996) 9955–9959.

Isolated and Deposited Potassium Clusters: Energetic and Structural Properties

Sahar Abdalla*, Michael Springborg†, and Yi Dong‡

Physical and Theoretical Chemistry,

University of Saarland, 66123 Saarbrücken, Germany

(Dated: June 26, 2012)

Abstract

We have studied the energetic and structural properties of isolated potassium clusters with up to 20 atoms as well as such clusters deposited on a potassium surface. The global total-energy-minima structures have been determined by using the Density Functional Tight Binding method (DFTB) combined with genetic algorithms. For the isolated clusters in the gas phase we analyze the binding energy as well as the stability function. Moreover, structural similarity is studied using so called similarity functions. Also the overall shape of the clusters and the radial distribution of the atoms are studied. Subsequently, we study the changes in the structure when these clusters are deposited on one out of two different surfaces. Also the energy related to the deposition is studied in detail.

PACS numbers: 61.46.Bc, 68.47.De, 73.22.-f

* Corresponding author; e-mail: s.abdalla@mx.uni-saarland.de

† e-mail: m.springborg@mx.uni-saarland.de

‡ e-mail: y.dong@mx.uni-saarland.de

1. Introduction

Whereas many — experimental and theoretical — studies on the properties of metal clusters in gas phase exist, much less studies have been performed for clusters that are deposited on some surface, although the properties of the clusters on surfaces are relevant, both because such systems provide one way of studying them experimentally and because of their importance for various chemical processes, including catalysis. Furthermore, the response of the clusters to being deposited on the surface can also provide relevant information on the clusters themselves.

Experimentally, there are various techniques for studying the behaviour of clusters deposited on a surface including scanning tunneling microscopy,[1–3] scanning transmission electron microscopy,[4] and field ion microscopy (FIM).[5] As a representative example we mention that Wang et al.[6] studied the properties of iridium clusters (with 2–13 atoms) on an Ir(111) surface by using FIM. They investigated the arrangement of the iridium atoms in the clusters in relation to the binding sites for a single atom on the Ir(111) surface.

Also theoretical studies have been used for clusters on surfaces. Among those, some have been based on semi-empirical methods like the Embedded Atom Method (EAM). These studies include some on Ni_N and Pt_N clusters on Ni(111) and Pt(111) surfaces.[7–10] Also Schwoebel et al.[11] used an EAM method but for studying the properties of small Pt clusters on the Pt(001) surface. The structures and the energies of Ni, Pd, and Pt clusters on the Pt(001) surface have also been studied theoretically.[12] The structural properties of Pd and Pt clusters on Ag(110) were studied by Roy et al.[13] Finally, using molecular-dynamics we have studied the depostion of Ni_{13} and Cu_{13} clusters on Ni(111) and Cu(111) surfaces.[14]

It has been found that the deposition of clusters on a surface influences both the energetic and the structural properties of the clusters so that the deposited clusters have properties different from those obtained in gas phase.

The purpose of the present work is to study in detail the effects of depositing potassium clusters on a potassium surface. To this end we, thus, need both the properties of the isolated clusters in the gas phase and those of the clusters on the surfaces. Therefore, the first part of this work presents results on the global total-energy-minima structures of isolated potassium clusters. In the second part, these optimized structures were deposited on two different potassium surfaces.

Over the years, several studies on the properties of potassium clusters in the gas phase have been presented. One of the simplest theoretical approaches treats the isolated potassium clusters within a spherical jellium model. With this model, discontinuities in the total energy as a function of cluster size are related to the existence of electronic shell structures,[15] similar to what has been reported for sodium clusters, with peaks or steps for those clusters which contain N = 2, 8, 20, 40, $\cdots$ atoms.[16,17] Early, this prediction was confirmed experimentally through mass spectra from potassium cluster beams.[18] Since then, potassium clusters in gas phase have been of considerable experimental interest.[19–26]

From the theoretical point of view, potassium clusters have been investigated with different theoretical methods, although most of these were limited to small sizes. Thus, potassium clusters with up to 8 atoms have been studied using the pseudopotential calculations.[27] An ab-initio study of both neutral and ionic structures of potassium clusters were carried through with configuration interaction (CI) methods.[28,29] The structures and the binding energies for clusters containing between four and six atoms were also investigated by using diatomics in molecules (DIM) approximation.[30] Valence-only self consistent field calculations was used to study neutral and singly ionized K clusters with up to four atoms.[31] K_9, K_{15}, and K_{27} have been studied using the SCF $X\alpha$ SW (local spin density-scattered wave) method.[32] Potassium clusters K_N ($N \leq 7$) were investigated using Hartree-Fock many-body perturbation calculations.[33] Florez and co-workers[34] investigated the properties of potassium clusters with up to eight atoms by applying two types of exchange-correlation functionals within a density-functional approach. Recently, Banerjee et al.[35] studied the properties of various isomers of potassium clusters containing even numbers of atoms up to 20 atoms by employing an all-electron density functional theory with a gradient corrected exchange-correlation functional. Their results include the binding energies, ionization potentials, and static polarizabilities as function of the cluster size. Thus, although potassium clusters have been the subject of several theoretical studies, it is surprising that there has been no attempt to identify the structures of the global total-energy-minima using unbiased structure-optimization methods in combination with electronic-structure calculations.

On the other hand, potassium clusters with up to 60 atoms were investigated using a Gupta potential for describing the interatomic interactions combined with both genetic and basin hopping algorithms[36] to search for the global minima. However, such a model does not include an explicit description of electronic effects, and may, in addition, tend to

overestimate the role of packing effects, so that the particularly stable clusters are those that are particularly closed packed and, hence, not in agreement with those obtained with the spherical jellium model and, it turns out, experiment.[15,18] This suggests that electronic effects are important for the properties of potassium clusters.

Accordingly, in the present study, we shall include electronic degrees of freedom explicitly for clusters with up to 20 atoms by utilizing the Density Functional Tight Binding (DFTB) method. To search for the global minima structures we use genetic algorithms. As we shall see, the sizes of the particularly stable clusters are found to be in agreement with those obtained experimentally. In order to obtain further information on the properties of the clusters, we shall use various descriptors for analyzing both energetic and structural properties as function of the cluster size.

To include the effect of surface on the properties of potassium clusters, we have considered the clusters when being deposited very softly on K(100) and K(110) surfaces. To our knowledge, this is the first study devoted to potassium clusters on a potassium surface. Thereby, we shall focus on the changes in the structures due to the adsorption as well as in the energetics related to the adsorption.

This paper is organized as follows: In section II our theoretical method is briefly described. Subsequently, in section III, we present and discuss our results for both isolated and deposited clusters. Finally, our results are summarized in section IV.

2. Theoretical Methods

Our theoretical method combines the Density Functional Tight Binding (DFTB) method for the calculation of the total energy for a given structure with genetic algorithms for the determination of the structure of the global total-energy minimum. The DFTB method is based on the density functional theory of Hohenberg and Kohn[37] in the formulation of Kohn and Sham[38] and was been developed by Seifert and coworkers.[39–41] Within the DFTB, the total energy of a given system relative to that of the isolated, non-interacting atoms is given as

$$E_{\rm tot} = \sum_{i}^{\rm occ} \varepsilon_i - \sum_{j} \sum_{m} \varepsilon_{jm} + \frac{1}{2} \sum_{j \neq j'} U_{jj'}(\mid R_j - R_{j'} \mid) \qquad (1)$$

where ε_i are the single particle energies of the system of interest, ε_{jm} are those of the isolated atoms (i.e., jth eigenvalue of the mth atom), and the last term is a pair potential, which

describes short-range interactions. In the DFTB, only the valance electrons are considered, whereas the other electrons are treated as a frozen core.

The orbital energies are calculated by expanding the orbital wavefunctions in a set of atom-centered basis functions, $\{\chi_{jm}\}$, where m marks the atom and j distinguishes between different functions centered at the same atom. Moreover, we assume that the potential experienced by the electrons can be written as a superposition of those of the isolated atoms,

$$V(\vec{r}) = \sum_m V_m(\vec{r} - \vec{R}_m). \tag{2}$$

Finally, we assume that $\langle \chi_{j_1 m_1} | V_m | \chi_{j_2 m_2} \rangle$ vanishes unless $m_1 = m$ and/or $m_2 = m$. Then, all information on the orbital energies can be extracted from accurate (parameter-free density-functional) calculations on two-atomic systems, i.e., in our case on the K_2 molecule, as a function of interatomic distance.

The last (repulsive) term in Eq. (1) is determined so that the total energy as a function of interatomic distance for the diatomics as obtained from the parameter-free density-functional calculations is reproduced accurately. Our approach is, accordingly, based on parametrizing results from the diatomic K_2 molecule and, subsequently, using those for larger K-based systems. In order to check whether this approach is reasonable, we calculated the lattice constant for crystalline K using the present approach. The optimized lattice constant was found to be $a = 5.29$ Å which compares well with the experimental value of $a = 5.33$ Å.

To determine the global minima structures, we have used genetic algorithms.[42–46] The main idea behind the genetic algorithms is to generate a larger number of structures (parent structures) and from those to generate a new set through cutting and pasting. From the total set of new and old structures, those with the lowest energy are kept (which then form the next so called generation) and this process is repeated until the lowest energy is unchanged for a larger number of generations. For the present work it is relevant to mention that the combination of DFTB and genetic algorithms have been used before to determine the global minima structures of sodium clusters.[47,48] Finally, we used our approach for K_N clusters for N up to 21, but shall here concentrate on the properties of the clusters with N up to 20.

For the calculations of the potassium clusters deposited on a surface, we considered two types of potassium surfaces, i.e., the (110) and (100) surface. We modeled the surface through a film with a thickness of three layers (i.e., $3a$) and with each layer containing 72

atoms. During the surface optimization, the structure of the bottom layers was kept fixed at the experimental crystal structure, whereas the first layer was allowed relax. Subsequently, a potassium cluster with the structure that was optimized in the gas phase was placed in the closest vicinity to the surface, and the resulting system was allowed to relax.

We emphasize that the goal of our work is to study what can happen when a cluster is deposited on a surface. Thus, we have not attempted to identify the optimal orientation and/or position of the cluster on the surface. Instead, the fact that we considered just a single deposition geometry will for sure influence our results. Moreover, by allowing only the top-most layer to relax, we make use of the near-sighted-ness of electronic interactions, although further relaxation effects may exist. Nevertheless, we believe that our study provides general information on the effects on structural and energetic properties when a cluster is deposited on a surface.

In order to analyze the changes due to the deposition of the cluster on the energy we at first define a deposition energy as

$$E_{\mathrm{D}} = E_{\mathrm{tot}} - E_{\mathrm{IS}} - E_{\mathrm{IC}} \tag{3}$$

where E_{tot} is the total energy of the complete system (cluster+surface), E_{IS} is that of the isolated surface, and E_{IC} is that of the isolated cluster. E_{D} can be considered as consisting of three contributions, i.e., an energy related to changing the structure of the surface from that of the isolated system to that of the cluster+surface system, a similar energy for the cluster, and an interaction energy between the two. Whereas the first two per construction are positive (see, however, later), the latter should be negative so that E_{D} becomes negative.

In detail, the interaction energy between the surface and the cluster can be defined as

$$E_{\mathrm{int}} = E_{\mathrm{tot}} - E_{\mathrm{DS}} - E_{\mathrm{DC}}. \tag{4}$$

here, E_{DS} is the energy of the surface in the structure it has after the deposition, and E_{DC} is, equivalently, the energy of the cluster in the structure after the deposition. The energy costs related to restructuring the surface and the cluster, respectively, are then given as

$$E_{\mathrm{RC}} = E_{\mathrm{DC}} - E_{\mathrm{IC}} \tag{5}$$

and

$$E_{\mathrm{RS}} = E_{\mathrm{DS}} - E_{\mathrm{IS}}. \tag{6}$$

3. Results and Discussion

3.1. Isolated Potassium Clusters

At first, we shall discuss the properties of isolated K_N clusters with N up to 20. We shall discuss their energetic and structural properties and also compare with those of Na_N clusters, as the two types of systems often are considered as being very similar.

3.1.1. Energetic Properties

The binding energy per atom, i.e., $-E_{\rm tot}(N)/N$ with $E_{\rm tot}(N)$ being the total energy of Eq. (1) for the cluster with N atoms, is an overall increasing function of N, as can be seen in the upper part of Fig. 1. However, as always found for such small systems, additional size-dependent features are seen in the figure, suggesting that certain cluster sizes are more stable than the neighbouring sizes.

The stability of the clusters can at best be quantified through the stability function,

$$S(N) = E_{\rm tot}(N+1) + E_{\rm tot}(N-1) - 2E_{\rm tot}(N). \quad (7)$$

This function has maxima for particularly stable clusters and is shown in the lower panel in Fig. 1. At first, a clear even-odd oscillatory pattern is identified, which can be related to electronic shell-filling effects, but, in addition, more pronounced peaks are found for $N = 8$, 18, and 20. That these cluster sizes should be particularly stable is in agreement with what is obtained from the simplest spherical jellium model as well as mass spectra of potassium cluster beams.[15,18]

When comparing with our earlier results for Na_N clusters using the same theoretical approach[47,48] we see a very close similarity. Thus, both the even-odd oscillations and the peaks at 8, 18, and 20 are found for both systems. At first, together with the results for the spherical jellium model this suggests that both systems can be considered as roughly spherical clusters for which electronic-shell effects are the dominating ones. However, as we shall see below, this is not the case and, indeed, K_N and Na_N clusters are less similar than what could be suggested based on their energetic properties.

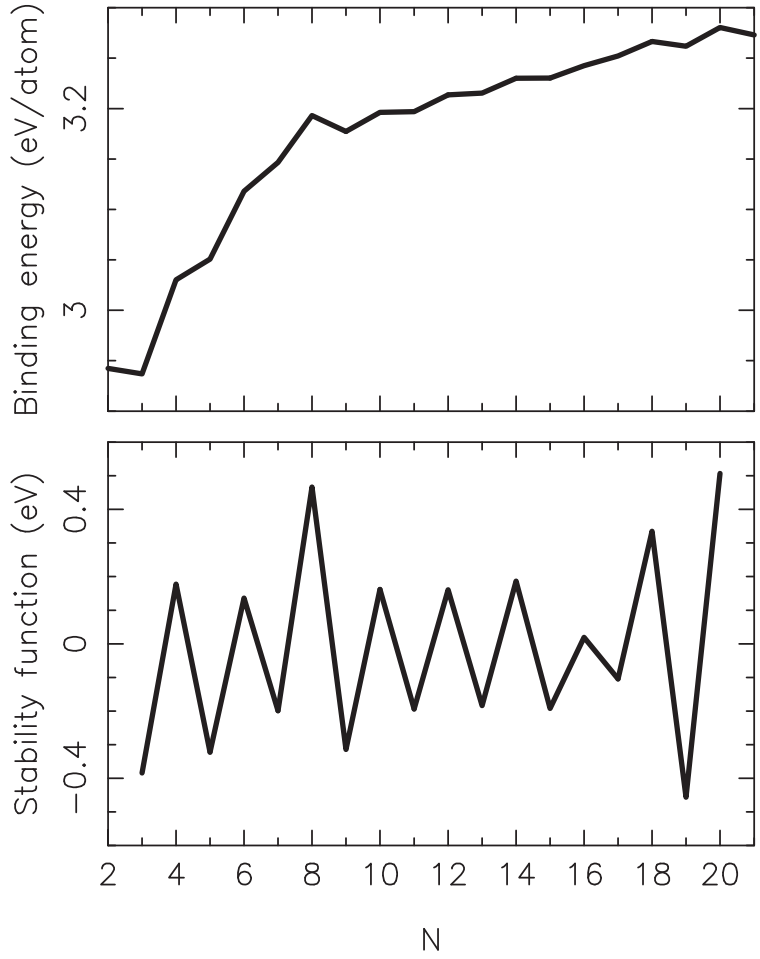

FIG. 1: The upper panel shows the binding energy per atom for potassium clusters with up to 20 as function of the size of the clusters, whereas the lower panel shows the stability function for the same clusters.

3.1.2. Structural Properties

The global minima structures of the potassium cluster with up to 20 atoms are shown in 2. We see that up to $N = 5$, the structures are planar. In the figure, also the point group symmetries of the individual clusters are given. Comparing those with the similar results for Na_N clusters, about half-part of the clusters have the same symmetries for the two systems, although this similarity in most cases results from a particularly low symmetry (C_1 or C_s).

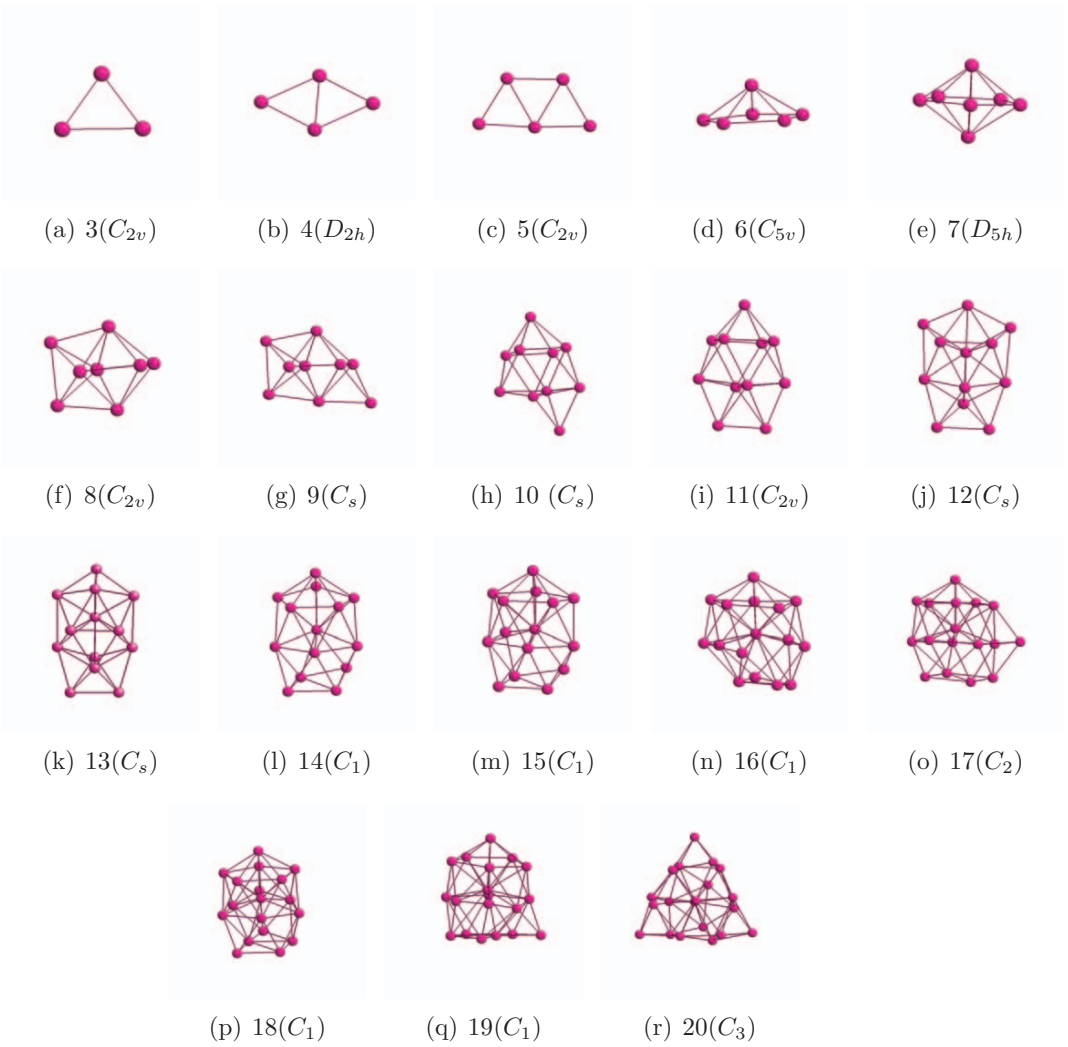

(a) 3(C_{2v}) (b) 4(D_{2h}) (c) 5(C_{2v}) (d) 6(C_{5v}) (e) 7(D_{5h})

(f) 8(C_{2v}) (g) 9(C_s) (h) 10 (C_s) (i) 11(C_{2v}) (j) 12(C_s)

(k) 13(C_s) (l) 14(C_1) (m) 15(C_1) (n) 16(C_1) (o) 17(C_2)

(p) 18(C_1) (q) 19(C_1) (r) 20(C_3)

FIG. 2: The structures of the global total-energy minima of K_N ($2 \leq N \leq 20$) clusters obtained with DFTB. Below each structure, both N and the corresponding point group are given.

In order to compare our results with those of other, previous studies, we tabulate the structures of K_N for $N \leq 8$ and their corresponding point groups in Table I. There we have also listed the results of previous theoretical studies.[26,29–31,33–35,49] It is seen that our results are in good agreement with what has been found in most other studies. There are also deviations, although in no case our results differ from those of all other theoretical studies. We interpret this as being in support of our theoretical approach.

For the triangular structure for K_3 we find indications of a weak Jahn-Teller distortion.

TABLE I: Comparison of the structures for K_N for $N \leq 8$.

K_N	Structure	Point group	References
K_3	isoceles triagle	C_{2v}	present, ref. [26,29,31,33]
	linear	$D_{\infty h}$	ref. [34
K_4	rhombus	D_{2h}	present, ref.[29,31,35,49]]
K_5	trapezoidal	C_{2v}	present, ref. [29,34]
	trigonal pyramidal	D_{3h}	ref. [30]
	deformed tetrahedral		ref. [33]
K_6	pentagonal pyramidal	C_{5v}	present, ref. [29,35]
	planar	C_{2v}	ref. [34]
	octahedral		ref. [30]
K_7	pentagonal bipyramid	D_{5h}	present, in ref. [34]
K_8	compact structure	C_{2v}	present, in ref. [34]

(a)K_4 (b)K_6

FIG. 3: The structures of K_4 and K_6 showing the definition of the lengths a and b.

For K_4 we obtained a rhombus structure with D_{2h} symmetry. The rhombus sides have all the same length, a, which is longer than that of the diagonal, b (see Fig. 3). We find $a = 4.45$ Å

and b being 4.16 Å. A similar difference has also been reported in some earlier studies,[31,35,49] whereas others studies have found $a = b$.[28,29,33]

The transition from 2D to 3D occur at K_6, which is predicted to have pentagonal pyramidal structure with C_{5v} symmetry in agreement with the result obtained by Banerjeeet al.[35] and in contrast with that obtained from Florez et al.[34] and Richtsmeier et al.[30] These found planar and octahedral structures, respectively. For K_6, the length a and b (see Fig. 3) are found to be $a = 4.48$Å and $b = 4.41$Å. A similar difference in the lengths has been also been found in some previous studies,[31,35,49] where in other studies[28,29,33] $a = b$ was found. It is worth noting that the transition from 2D to 3D has been also predicted for sodium clusters to occur at Na_6.[50]

Low symmetric structures are found for the clusters in the size range $9 \leq N \leq 20$, where the most dominant point groups are C_1, C_2, and C_s. The structures of K_9 and K_{10} are characterized by a C_s symmetry similar to that obtained for sodium clusters.[47,48] The structure of K_{11} has C_{2v} symmetry. For the magic clusters with $N = 18$ and 20, the corresponding point groups are C_1 and C_3, i.e., these structures are not of particularly high symmetry. Our finding for K_{18} is in contrast to the C_{2v} symmetry obtained for Na_{18},[47] although both studies agree that the structure for this size is of relatively low symmetry and far from the roughly spherical symmetry assumed by the spherical jellium model.

To identify how the clusters grow and to quantify whether the cluster with N atoms can be derive from the cluster with $N-1$ atoms by simply adding one atom, we have used two different theoretical approaches. In the first case, we have used a so called similarity that we have found to be useful, at least for relatively compact systems.[51,52] For the comparison of two systems with P atoms, we calculate and sort the interatomic distances of the two systems, $\{d_i\}$ and $\{d'_i\}$, respectively. Subsequently we calculate

$$q = \left[\frac{2}{P(P-1)} \sum_{i=1}^{P(P-1)/2} (d_i - d'_i) \right]^{\frac{1}{2}} . \tag{8}$$

When comparing clusters with N and $N-1$ atoms, we consider all those N structures that can be obtained from the N-atomic cluster by removing a single atom. For each of those, the resulting structure is compared with the $(N-1)$-atomic cluster, and out of all the N different values of q, the lowest one, $q_{\min}$, is chosen to define a similarity function

$$S = \frac{1}{1 + q_{\min}/u_l} \tag{9}$$

where u_l is a length unit.

This approach is not easily applied for comparing structures with very different sizes or that are open. We have therefore developed a new approach for the comparison of two systems A_N and B_M for which we will assume that $M \geq N$.[53] At first, the two structures are scaled, and subsequently the two resulting structures are placed upon each other so that

$$Q = \sum_{i=1}^{N} \left| \frac{1}{d_A} \vec{R}_{A,i} - \frac{1}{d_B} \vec{R}_{B,i} \right|^2 \tag{10}$$

is minimized. Here, d_A and d_B are the two scaling factors for the two systems, $\vec{R}_{A,i}$ is the position of the ith atom of the A cluster, and $\vec{R}_{B,i}$ is the position of that atom of the B cluster that (after scaling) is closest to the ith atom of the A cluster (also after scaling). From the minimum value of Q we define a similarity function similar to Eq. (9),

$$S = \frac{1}{1 + (Q/N)^{1/2}}. \tag{11}$$

At first, we compare the clusters with K_N and K_{N-1} atoms. The results are shown in Fig. 4(a), where we compare the two approaches of Eqs. (9) and (11). In the former, we have used $u_l = 1$Å, and in the latter we have scaled all atomic coordinates by a factor of 4.97 Å (which is the average of the nearest and next-nearest neighbour distance in the crystal structure). The shapes of the two curves are very similar, although the differences in the scaling factors result in differences in the absolute values. That the two approaches give similar results can be explained from the fact that the present clusters are fairly closed packed. It is interesting to observe the even-odd oscillatory pattern in particular for the smallest clusters. This suggests that the cluster with, e.g., 5 atoms has a structure very similar to that of the 4-atomic cluster, although a new electronic orbital is being occupied. For the 6-atomic cluster, a new structure is found, which, to a large extend, is found for the 7-atomic cluster, too. This trend continues up to N around 16, although it becomes less pronounced for the larger values of N. The fact that the structure changes whenever two atoms are added can be seen in Fig. 4(b) where we compare the structure of K_N with that of K_{N-2}. Finally, a similar oscillatory pattern was also found for the Na_N clusters.[48]

Since simple chemical reasoning may suggest that Na_N and K_N clusters have very similar properties, we also applied the similarity function of Eq. (11) to compare the structures of

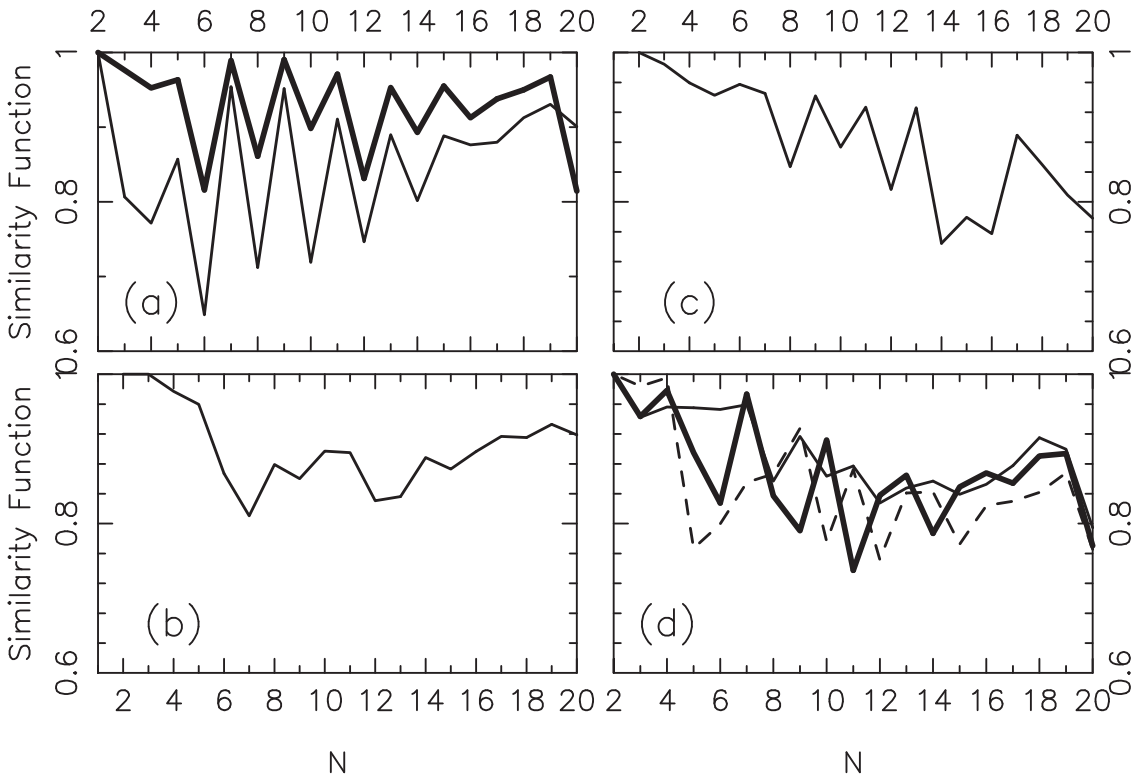

FIG. 4: Different similarity functions used in quantifying the similarity between different objects. In (a), K_N and K_{N-1} clusters are compared with the thin curve showing the results using Eq. (9) and the thick curve showing those for Eq. (11). In (b), K_N and K_{N-2} clusters are compared, and in (c), K_N and Na_N clusters are compared. Finally, in (d) the K_N clusters after deposition on the surfaces are compared with those in the gas phase. In this case, the thick line represents the similarity function for the clusters on the K(100) surface, the thin line represents the similarity function for the clusters on the K(110) surface, and the dashed-line compares the structures of the K_N clusters on the two surface. In (b), (c), and (d), only the similarity function according to Eq. (11) is used.

the two sets of systems. For each of the two systems, we used a scaling factor being equal to the average of the nearest and next-nearest neighbour distance in the crystal structure. The resulting similarity function is shown in Fig. 4(c), where it can be seen that the clusters become increasingly different as N grows. Thus, the two systems are not completely

analogous to each other.

In order to get further information on the structure, we study the so called radial distances. For each K_N cluster we first define its center,

$$\vec{R}_0 = \frac{1}{N}\sum_{i=1}^{N}\vec{R}_i \tag{12}$$

and subsequently for each atom its radial distance,

$$r_i = |\vec{r}_i| = |\vec{R}_i - \vec{R}_0|. \tag{13}$$

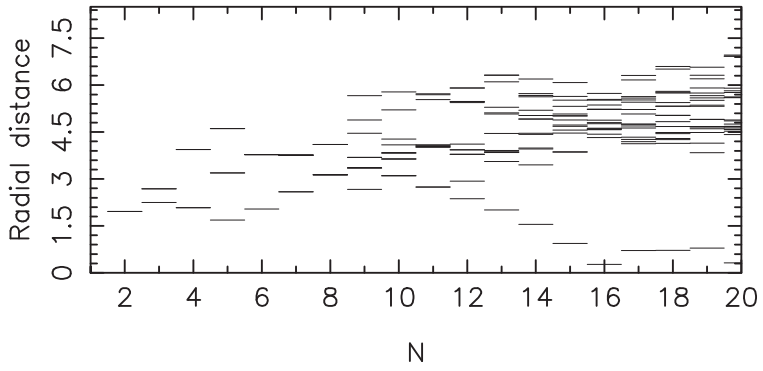

FIG. 5: The distribution of radial distances (in Å) for K_N clusters as function of clusters size. For each value of N, each small line represents at least one atom that has that radial distance.

The radial distances themselves are shown in Fig. 5. For some of the smallest clusters ($N = 6$, 7, 8, and 11, for instance), we have only few different values of the radial distances, which is a consequence of the high symmetry of these clusters. This is, on the other hand, not the case for the larger clusters. Here, instead there is a tendency for developing structures with a small core (with corresponding small values of radial distances) covered by a shell of atoms (with larger radial distances). This tendency is most pronounced for the largest cluster with $N \geq 15$.

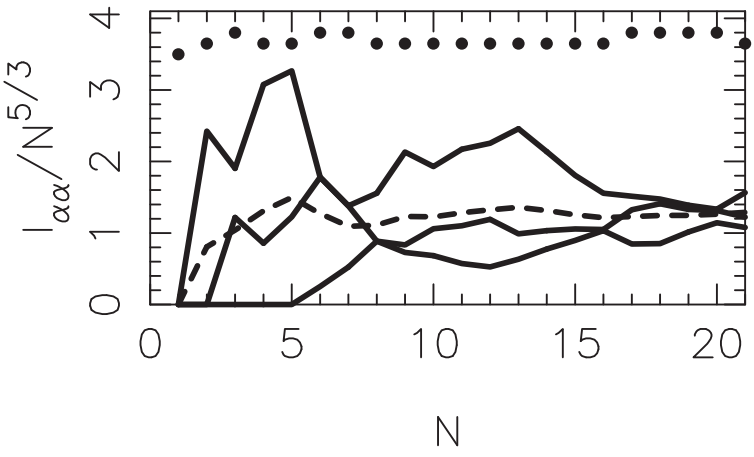

FIG. 6: Properties related to the eigenvalues $I_{\alpha\alpha}/N^{5/3}$. The solid line lines show the eigenvalues themselves, whereas the dashed line shows their average. In the upper part we mark whether the clusters have an overall spherical shape (lowest row), a lens-like shape (middle row), or cigar-like shape (upper row).

Fig. 5 gives also some information on the overall shape of the clusters. Thus, the clusters with $6 \leq N \leq 8$ appear to be more compact than those of the neighbouring sizes. Further information on the shape can be obtained as follows. For each cluster size we first define the 3×3 matrix containing the elements

$$I_{st} = \frac{1}{u_l^2} \sum_{i=1}^{N} s_i t_i \tag{14}$$

with u_l being a length unit, and s and t being x, y, or z. The three eigenvalues of this matrix, $I_{\alpha\alpha}$, can be used in separating the clusters into being overall spherical (if all eigenvalues are identical), cigar-shaped (if one of the eigenvalues is large compared to the other two), or lens-shaped (if we have two large and one small eigenvalue). Since the eigenvalues for a spherical jellium will scale as $N^{5/3}$, we show in Fig 6 the three eigenvalues, $I_{\alpha\alpha}$, and their average scaled by $N^{-5/3}$. The fact that no cluster has three identical values of $I_{\alpha\alpha}$ implies that no cluster has an overall spherical shape, which in turn suggests that the spherical jellium model at most can be of limited success for these systems. Instead in particularly

the clusters for $N < 15$ have markedly different values for $I_{\alpha\alpha}$ so that their structure is significantly different from spherical, and first for $N > 15$ the three eigenvalues approach each other. The fact that the smallest clusters are planar manifests itself here in that the smallest value of $I_{\alpha\alpha}$ equals 0.

3.2. Deposited Potassium Clusters

Next, we shall discuss the changes in the properties of the potassium clusters after they have been deposited softly on a (100) or (110) surface of a potassium crystal.

3.2.1. Energetic properties

When the cluster is deposited on the surface, the total energy of the cluster+surface system is lowered, and the system is stabilized, which can be seen from the negative deposition energies in Fig. 7(b). In that figure it is also seen that the deposition energy is largely independent of the crystal surface. The deposition energy per cluster atom [shown in Fig. 7(a)] is an overall increasing function of N since the fraction of the cluster atoms that is in contact with the surface is an overall decreasing function of N. There are, however, certain extra features in Fig. 7(a) of which the maximum for $N = 8$ and the minimum for $N = 5$ are the most pronounced ones. For $N \leq 5$ the gas-phase clusters are planar and can, thus, be placed on the surface so that all cluster atoms experience (attractive) interactions. This result in the particularly low values for the deposition energies in this size range. The maxima for $N = 8$ in Fig. 7(a) might be due to the high stability of this cluster size in the gas phase, suggesting that this cluster will not benefit much from interactions with the surface.

The fact that the deposition energy becomes increasingly negative as a function of cluster size is consistent with the results for the energetic properties of the gas-phase clusters, Fig. 1. Thus, the K systems are increasingly more stable, the larger the systems are.

As described in Sec. , it can be useful to split the deposition energy into three different contributions: a restructuring energy of the cluster describing the energy costs for the cluster to change the structure from that of the gas phase to the one it has on the surface, a similar

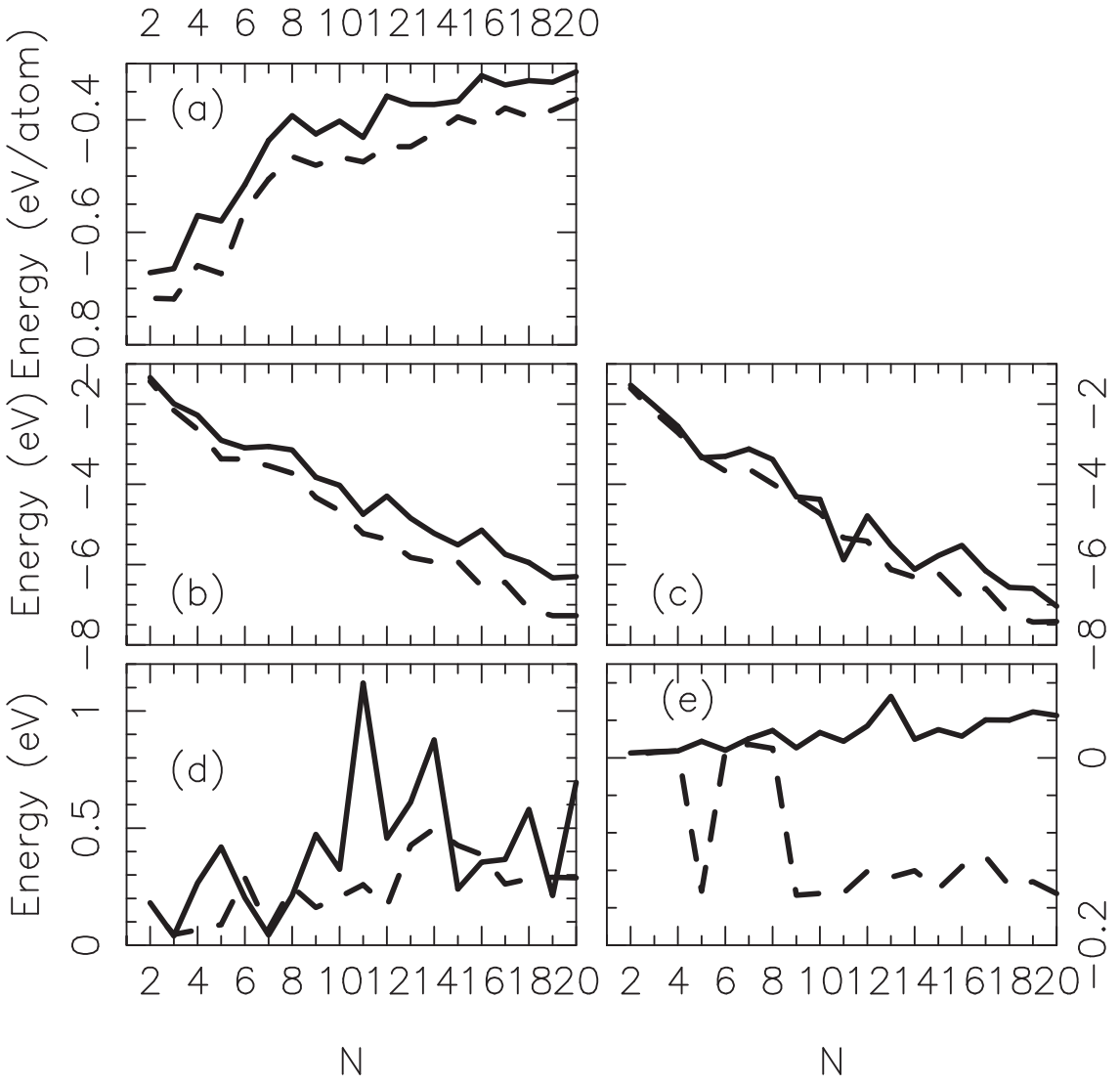

FIG. 7: Various energetic properties related to the deposition of the K_N clusters on a K surface as function of clusters size, N. The solid curves represent results for the K(100) surface and the dashed curves represent those for the K(110) surface. (b) shows the deposition energy, $E_{\rm D}$, that is split into the interaction energy, $E_{\rm int}$ [shown in (c)], and the restructuring energy of the cluster, $E_{\rm RC}$ [shown in (d)], and of the surface, $E_{\rm RS}$ [shown in (e)]. (a) shows the deposition energy per cluster atom.

energy for the surface, and the remaining part that then describes the interaction between the cluster and the substrate. These three contributions are shown in Figs. 7(d), (e), and (c), respectively.

At first, it is seen that the restructuring energy of the surface, Fig. 7(e), is essentially vanishing. In some of the calculations it takes even negative values, which we shall explain below. The small values of the restructuring energy of the surface suggest that the changes in the surface structures indeed are small, so that our approach based on letting only the top-most layer relax is justified.

On the other hand, the restructuring energy of the cluster, Fig. 7(d), is clearly non-zero and positive, although also here there are cases where it is fairly small. The largest value is found for K_{11} deposited on the (100) surface, but since a smaller value is found for the same cluster on the (110) surface, we suggest that this large value is biased by our more or less arbitrary choice of the deposition geometry.

Compared to the total deposition energy, the two restructuring energies are accordingly the smaller parts and, instead, the dominating part is the interaction energy between cluster and surface. Thus, this energy, Fig. 7(c), follows close the deposition energy.

3.2.2. Structural Properties

We shall now discuss the structures that result from the deposition of the clusters on the two surfaces. At first, we shall compare the structure of the clusters before and after deposition as well as the structures of the clusters on the two different surfaces. To this end we use the similarity function of Eq. (11). The results are shown in Fig. 4(d). Compared to the other panels in that figure, the values of Fig. 4(d) are in general lower, implying that the changes in the cluster structures are significant. Moreover, the structures on the two different surfaces are clearly different, suggesting that deposited clusters of the same size may not take only one structure but the resulting structure depends also on the orientation and position of the cluster on the surface.

That the structures of the clusters change upon deposition on the surfaces can also be recognized in Figs. 8 and 9, where we show these. It is clear that the structures differ from those of Fig. 2, and a careful examination of the structures on the surfaces suggests that the

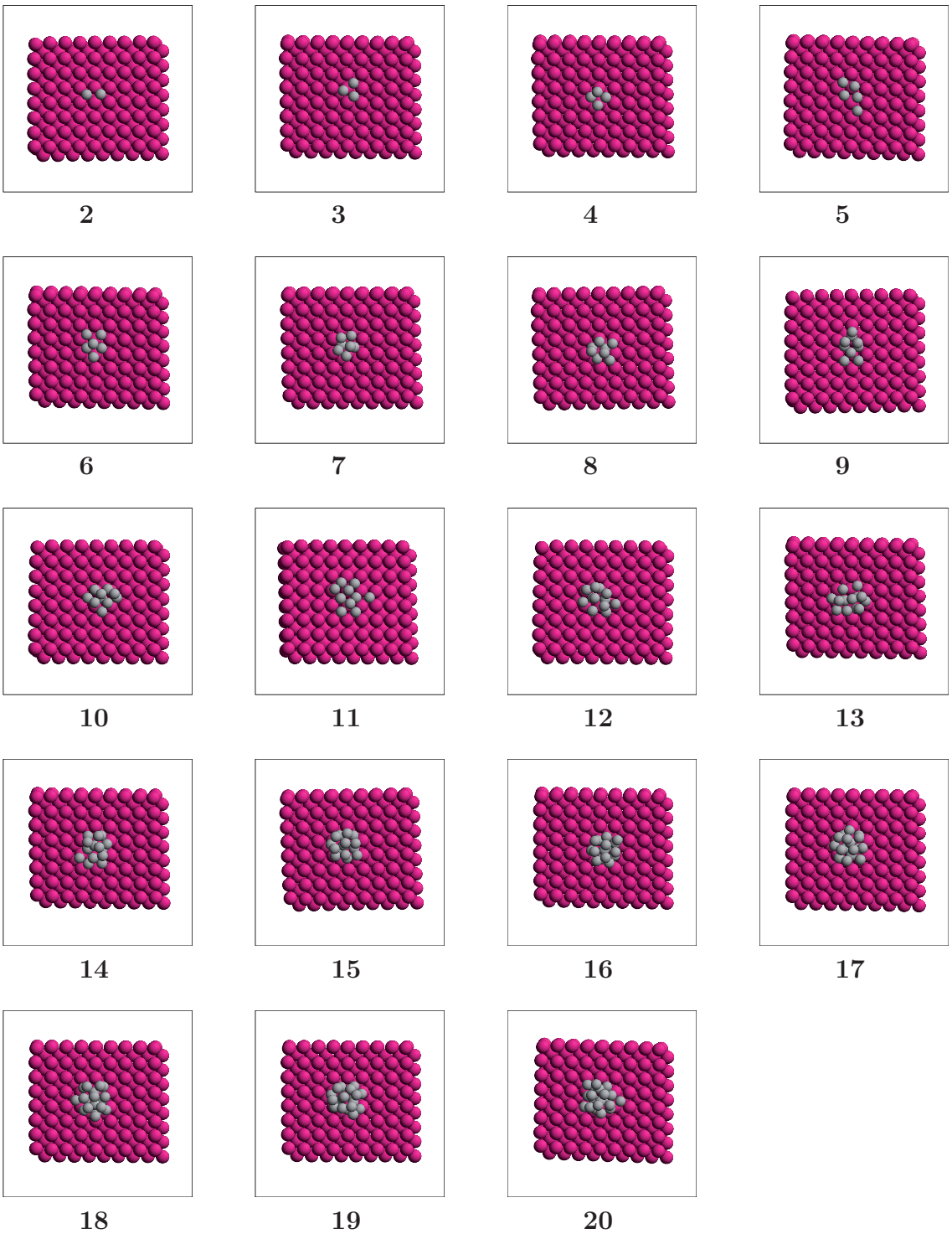

FIG. 8: A top view of the structures of the K_N clusters on the K(100) surface. The cluster and the surface atoms have been given different colours.

clusters there have a structure that is partly dictated by a tendency of the cluster atoms to

FIG. 9: A top view of the structures of the K_N clusters on the K(100) surface. The cluster and the surface atoms have been given different colours.

sit on positions on the surface where they have a large number of surface-neighbours. This

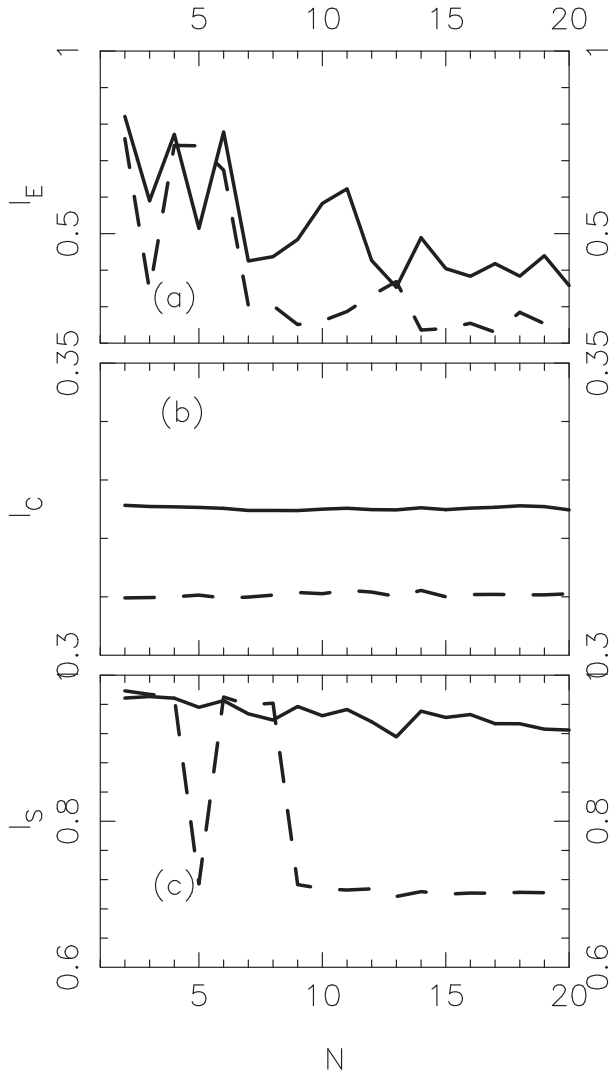

FIG. 10: Various quantities describing the structural properties of the cluster+surface system. The full and the dashed curve shows the results for the (100) and (110) surface, respectively. For further details, see the text.

is the case for bridged and hole positions on the surface. One may thus suggest that there is a certain tendency for the cluster atoms to place themselves epitaxially on the surface.

In order to quantify to which extend the surface changes structure upon the deposition and to which extend the cluster atoms are placed epitaxially on the surface, we apply certain so called indices that are defined as follows. At first we define an index of epitaxy, I_E. Taking the positions of the two bottom layers of atoms for the slab model that is used for the surface, we imagine the positions of these atoms being continued virtually into those parts of space

where the uppermost surface layer and the cluster are placed. Subsequently, we define

$$q_E^2 = \frac{1}{N}\sum_{i=1}^{N} |\vec{R}_i - \vec{R}_{iX0}|^2, \tag{15}$$

where $\vec{R}_i$ is the position of the ith atom of the cluster that has N atoms. Moreover, $\vec{R}_{iX0}$ is the position of that atom of the virtual continuation of the crystal that is closest to $\vec{R}_i$. Subsequently, we define

$$I_E = \frac{1}{1 + q_E/u_l}. \tag{16}$$

In a similar way we define an index, I_C, for the surface describing whether the positions of the atoms of the uppermost surface layer in the presence of the cluster are close to those of the virtual continuation of the crystal. The only difference is that the summation in Eq. (15) then runs over the 72 atoms of the upper surface layer. Finally, we compare the structure of the surface layer without and with the cluster through a further index, I_S, defined as

$$I_S = \frac{1}{1 + q_S/u_l} \tag{17}$$

with

$$q_S^2 = \frac{1}{72}\sum_{i=1}^{72} |\vec{R}_{iS0} - \vec{R}_{iS}|^2, \tag{18}$$

where $\vec{R}_{iS0}$ and $\vec{R}_{iS}$ is the position of the ith atom of the upper surface layer in the absence and in the presence of the cluster, respectively.

These three indices are shown in Fig. 10. At first it is seen that I_E takes fairly low values, implying that the cluster atoms are not placed at positions close to those of the crystal. However, I_C is even smaller, giving that the outermost surface layer experiences strong structural relaxations compared to the crystal. As suggested already by the results of Fig. 7(e), the structural relaxation of the surface upon deposition of the cluster is small with some exceptions. In fact, these exceptions are closely related to those for which the restructuring energy of the surface was particularly low. A careful inspection of the structural changes in those case reveals that the changes are related to a single atom at the boundary of the finite surface model. This atom changes in some cases place and lowers thereby the total energy of the complete surface. That this is possible is not surprising: after all, the structure of the surface model was not determined as that of the lowest total energy for the system of 216 K atoms, but rather a local total-energy minimum. Thus, a small perturbation, for instance the presence of a cluster, may change this structure.

4. Conclusions

In summery, we have presented results for the structural and energetic properties of potassium clusters with up to 20 atoms that are either isolated or deposited on a surface of a potassium crystal. The structure optimization was performed by using a combination of DFTB calculations for the determination of the total energy for a given structure and genetic algorithms for the determination of the global total-energy-minima structures. From the stability function it is clearly seen that the K_N clusters show an even-odd oscillatory pattern and that more pronounced peaks are found for the sizes 8, 18, and 20, which is in agreement with the results obtained from the spherical jellium model and mass spectra of potassium cluster beams. However, the structural analysis showed that these clusters are not even approximately spherical. Moreover, the similarity function demonstrated that there is a tendency for the smaller clusters to pairwise possess similar structures. This is the case for the clusters with 4 and 5 atoms, with 6 and 7 atoms, with 8 and 9 atoms, etc.

When the potassium clusters are deposited softly on a potassium surface, both the energetic and the structural properties change. By separating the deposition energy into two structural reorganization energies (for the surface and the cluster, respectively) and an interaction energies, we found that the interaction energy is the dominating one, although the restructuring energy of the clusters occasionally is fairly large. Although the deposition energy in general becomes increasingly negative with cluster size, the deposition energy per cluster atom is most negative for the smallest clusters. By analyzing the structures of the clusters on the surfaces we found that these are significantly different from those of the clusters in the gas phase. Moreover, the structure of the surface relaxes significantly compared to the crystal structure, but only little upon deposition of the clusters. The cluster atoms did not show any tendency toward an epitaxial growth of the crystal.

Acknowledgement

One of the authors (SA) would like to thank Deutscher Akademischer Austauschdienst (DAAD) for the financial support.

REFERENCES

[1] Golovchenko J A 1986 *Science* 232 48

[2] Hamers R J 1989 *Annu. Rev. Phys. Chem.* 40 531

[3] Tromp R M 1989 *J. Phys. Condens. Matter* 1 10211

[4] Crewe A V 1983 *Science* 221 325.

[5] Panitz J A 1982 *J. Phys. E Sci. Instrum.* 15 1281

[6] Wang S C and Ehrlich G 1990 *Surf. Sci.* 239 301

[7] Fallis M C, Daw M S and Fong, C Y 1995 *Phys. Rev. B* 51 7817

[8] Longo R C, Rey C and Gallego L J 1999 *Surf. Sci.* 424 311

[9] Breeman M, Barkema G T and Boerma D O 1995 *Surf. Sci.* 323 71

[10] Liu C-L and Adams J B 1992 *Surf. Sci.* 268 73

[11] Schwoebel P R, Foiles S M, Bisson C L and Kellogg G L 1989 *Phys. Rev. B* 40 10639

[12] Wright A F, Daw M S and Fong C Y 1990 *Phys. Rev. B* 42 9409

[13] Roy H-V, Fayet P, Patthey F, Schneider W-D, Delley B and Massorbrio C 1994 *Phys. Rev. B* 49 5611

[14] Kasabova E, Alamanova D, Springborg M and Grigoryan V G 2007 *Eur. Phys. J. D* 45 425

[15] Chou M Y, Cleland A and Cohen M L 1984 *Solid State Commun.* 52 645

[16] Knight W D, Clemenger K, de Heer W A, Saunders W A, Chou M Y and Cohen M L 1984 *Phys. Rev. Lett.* 52 2141

[17] Knight W D, Clemenger K, de Heer W A and Saunders W A 1985 *Phys. Rev. B* 31 2539

[18] Knight W D, de Heer W A, Clemenger K and Saunders W A 1985 *Solid State Commun.* 53 445

[19] Thompson G A and Lindsay D M 1981 *J. Chem. Phys.* 74 959.

[20] Saunders W A, Clemenger K, de Heer W A and Knight W D 1985 *Phys. Rev. B* 32 1366

[21] Knight W D, de Heer W A and Saunders W A 1986 *Z. Phys. D* 3 109

[22] Brèchignac C and Cahuzac Ph 1985 *Chem. Phys. Lett.* 117 365

[23] Brèchignac C and Cahuzac Ph 1986 *Z. Phys. D* 3 121

[24] Kappes M M, Schär M, Radi P and Schumacher E 1986 *J. Chem. Phys.* 84 1863

[25] Kappes M M, Radi P, Schär M and Schumacher E 1985 *Chem. Phys. Lett.* 113 243

[26] Kornath A, Ludwig R and Zoermer A 1998 *Angew. Chem. Int. Ed.* 37 1575

[27] Soll H, Flad J, Golka E and Krüger Th 1981 *Surf. Sci.* 106 251

[28] Pacchioni G, Beckmann H O and Koutecký J 1982 *Chem. Phys. Lett.* 87 151

[29] Spiegelmann F and Pavolini D J 1988 *Chem. Phys.* 89 4954

[30] Richtsmeier S C, Dixon D A and Gole J L 1982 *J. Phys. Chem.* 86 3942

[31] Flad J, Igel G, Dolg M, Stoll H and Preuss H 1983 *Chem. Phys.* 75 331

[32] Pellegatti A, McMaster B N and Salahub D R 1983 *Chem. Phys.* 75 83

[33] Ray A K and Altekar S D 1990 *Phys. Rev. B* 42 1444

[34] Florez E and Fuentealba P 2009 *Int. J. Quant. Chem.* 109 1080

[35] Banerjee A, Ghanty T K and Chakrabarti A 2008 *J. Phys. Chem. A* 112 12303

[36] Lai S K, Hsu P J, Wu K L, Liu W K and Iwamatsu M 2002 *J. Chem. Phys.* 117 10715

[37] Hohenberg P and Kohn W 1964 *Phys. Rev.* 136 B864

[38] Kohn W and Sham L J 1965 *Phys. Rev.* 140 A1133

[39] Seifert G and Schmidt R 1992 *New J. Chem.* 16 1145

[40] Porezag D, Frauenheim Th., Köhler Th, Seifert G and Kaschner R 1995 *Phys. Rev. B* 51 12947

[41] Seifert G, Porezag D and Frauenheim Th 1996 *Int. J. Quant. Chem.* 58 185

[42] Deaven D M and Ho K M 1995 *Phys. Rev. Lett.* 75 288

[43] Morris J R, Deaven D M and Ho K M 1996 *Phys. Rev. B* 53 R1740

[44] Niesse J A and Mayne H R 1996 *Chem. Phys. Lett.* 261 576

[45] Roberts C, Johnston R L and Wilson N T 2000 *Theor. Chem. Acc.* 104 123

[46] Hartke B 1995 *Chem. Phys. Lett.* 240 560

[47] Tevekeliyska V, Dong Y, Springborg M and Grigoryan V G 2007 *Eur. Phys. J. D* 43 19

[48] Tevekeliyska V, Dong Y, Springborg M and Grigoryan V G 2011 in *Aromaticity and Metal Clusters*. Ed. Chattaraj, P. K. Taylor & Francis 161

[49] Jiemchooroj A, Sernelius B E and Norman P 2007 *J. Comput. Method Sci. Eng.* 7 475

[50] Poteau R and Spiegelmann F 1992 *Phys. Rev. B* 45 1878

[51] Grigoryan V G and Springborg M 2004 *Phys. Rev. B* 70 205415

[52] Springborg M 2012 in *Handbook of Computational Chemistry*. Ed. Leszczynski, J. Springer Verlag. 955

[53] Dong Y, Springborg M, Pang Y, Morillon F M *in preparation*